Degradation of TBC Systems in Environments Relevant to Advanced Gas Turbines for IGCC Systems

Principal Investigators: **Brian Gleeson, Frederick S. Pettit and Gerald H. Meier**

Graduate Student: **Nate Bohna**
Postdoc: **Thomas Gheno**

DOE PROGRAM: DE-FOA-0000459

Seth Lawson, Program Manager, DOE/NETL

Project Awarded 10/01/2011 (36 months duration)

Integrated Gasification Combined Cycle

IGCC Process

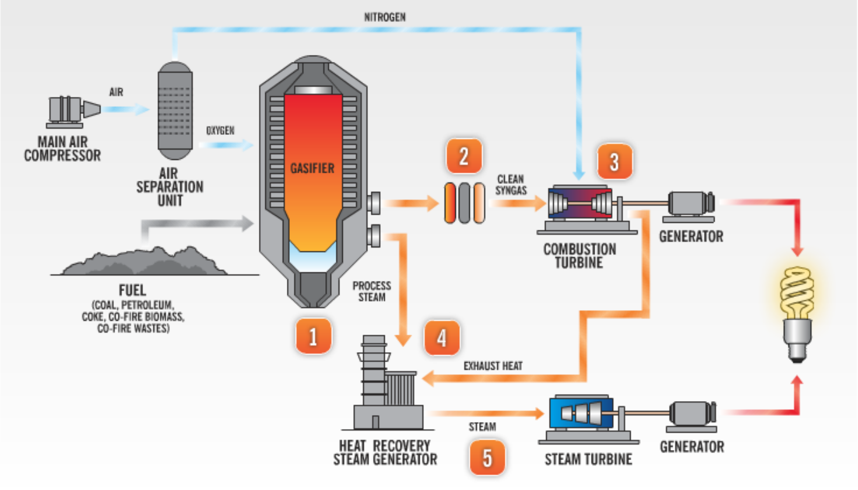

Sources of Deposits:

- Ambient air passing through turbine
- Upstream components
- Fuel source (coal)

Thermal Barrier Coatings used in **hottest sections** of turbines

TBCs subjected to **deposits** and multi-oxidant **gas environments**

O_2+CO_2+H_2O+SO_2 …

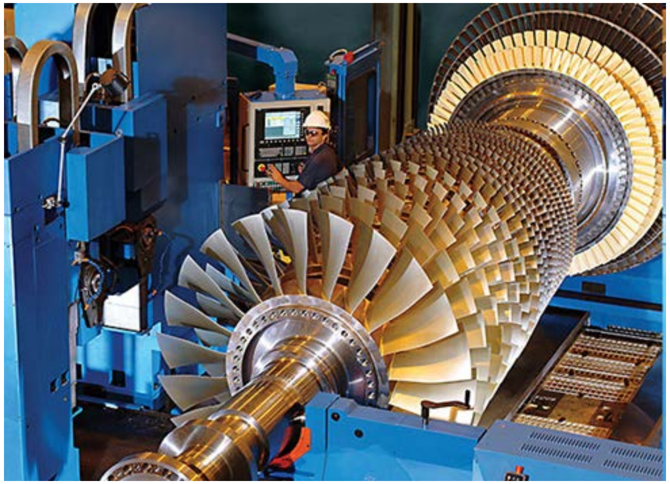

Font et al., *Fuel*, **89** (2010) pp. 3250-3261

Comparison of Typical Deposits

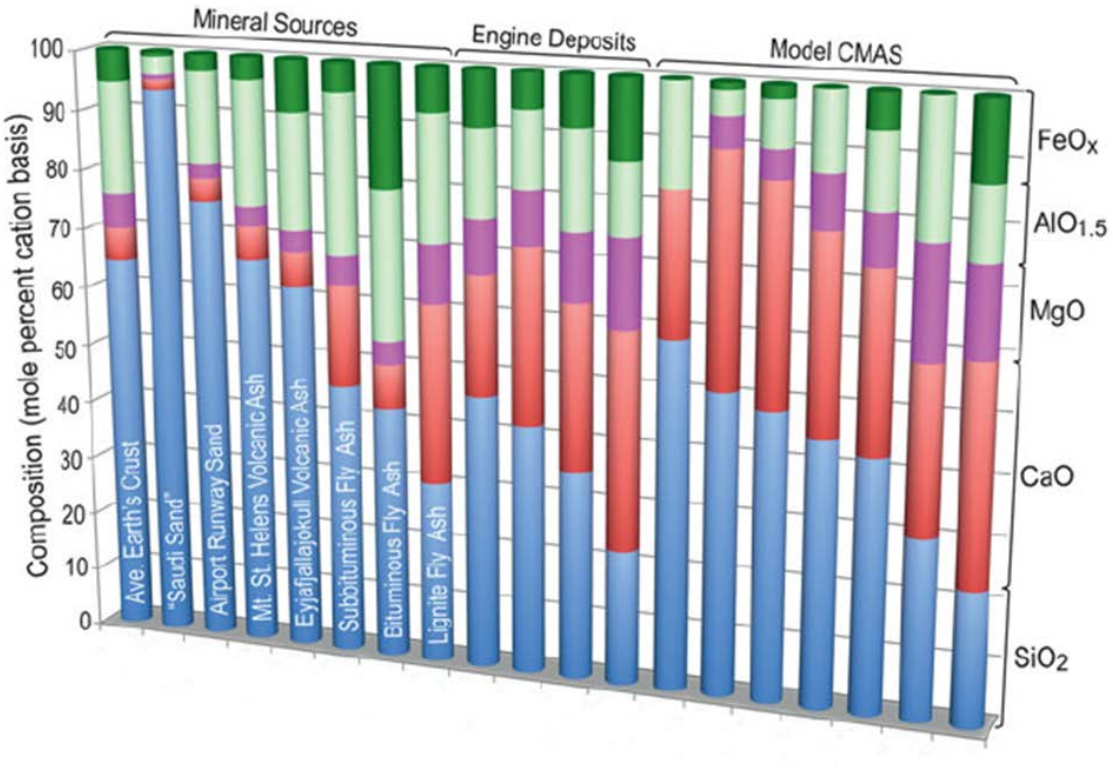

- Engine deposits in combustion turbines contain oxides **similar to CMAS**
- **Variability** due to location and fuel source (coal, syngas, ng)
- Coal and IGCC ash also contain sulfates that will be **liquid**

Typical IGCC Fly-Ash

	SiO_2	Al_2O_3	CaO	Fe_2O_3	MgO	MnO	P_2O_5	TiO_2	K_2O	Na_2O	SO_3	C
Wt%	56	19	3.2	5	0.7	0.04	0.7	0.6	4.1	0.6	3.3	2.8

Levi, Hutchinson, Vidal-Sétif, Johnson, MRS BULLETIN, 37 (2012).

Example of Commercial Fly Ash

Class C Fly ash

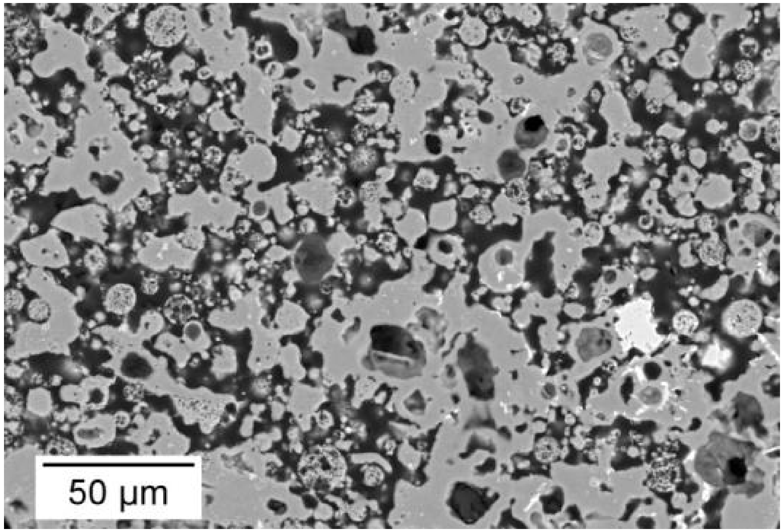

From Boral Material Technologies
Source: Plant Scherer, GA (pulverized coal)

Composition (wt. %)

As reported:

SiO_2	26.4
Al_2O_3	20.0
Fe_2O_3	6.1
CaO	33.4
MgO	8.0
SO_3	3.4
Na_2O	2.3
K_2O	0.4

→

SiO_2	26.4
Al_2O_3	20.1
Fe_2O_3	6.1
CaO	33.4
MgO	8.0
Na_2SO_4	5.2
K_2SO_4	0.7

Reactions of Fly Ash with YSZ

YSZ isothermal exposure to “class C” ash in dry air.

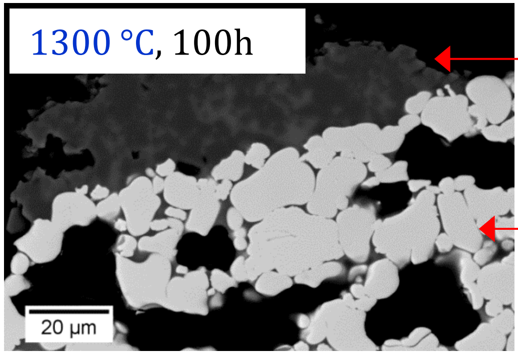

Ash

Melted ash has severely degraded the YSZ

“T_m”

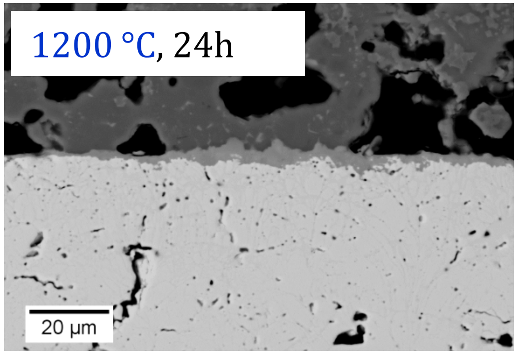

Ash

Complex Reaction Layer

Composition (wt. %)

SiO_2	26
Al_2O_3	20
Fe_2O_3	6
CaO	33
MgO	8
Na_2SO_4	5
K_2SO_4	1

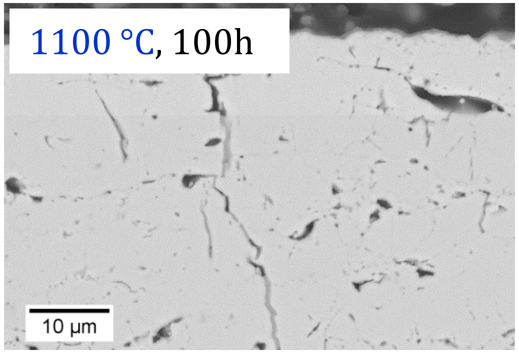

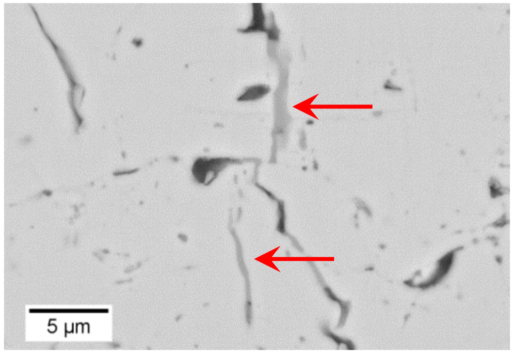

Some infiltration of ash constituents, partial melting

Main Aims of Present Study

- Determine the effects of fly-ash deposits at temperatures below ash liquidus.
- Systematically assess the interplay between prototypical deposit chemistries (*i.e.*, ash oxide and sulfate constituents) and environmental oxidants (*i.e.*, O_2, H_2O and CO_2) on the high-temperature degradation behavior of advanced TBC systems.
- Determine the combined effects of deposit-induced attack at relatively low temperatures on TBC performance.
- Establish reliable test procedures for assessing deposit-induced degradation of TBCs in different gas atmospheres.

Two TBC Systems Studied

Provided by **Praxair Surface Technologies**, a collaborator on this project

Low Density (HP-LD)   Dense Vertically Cracked (DVC)

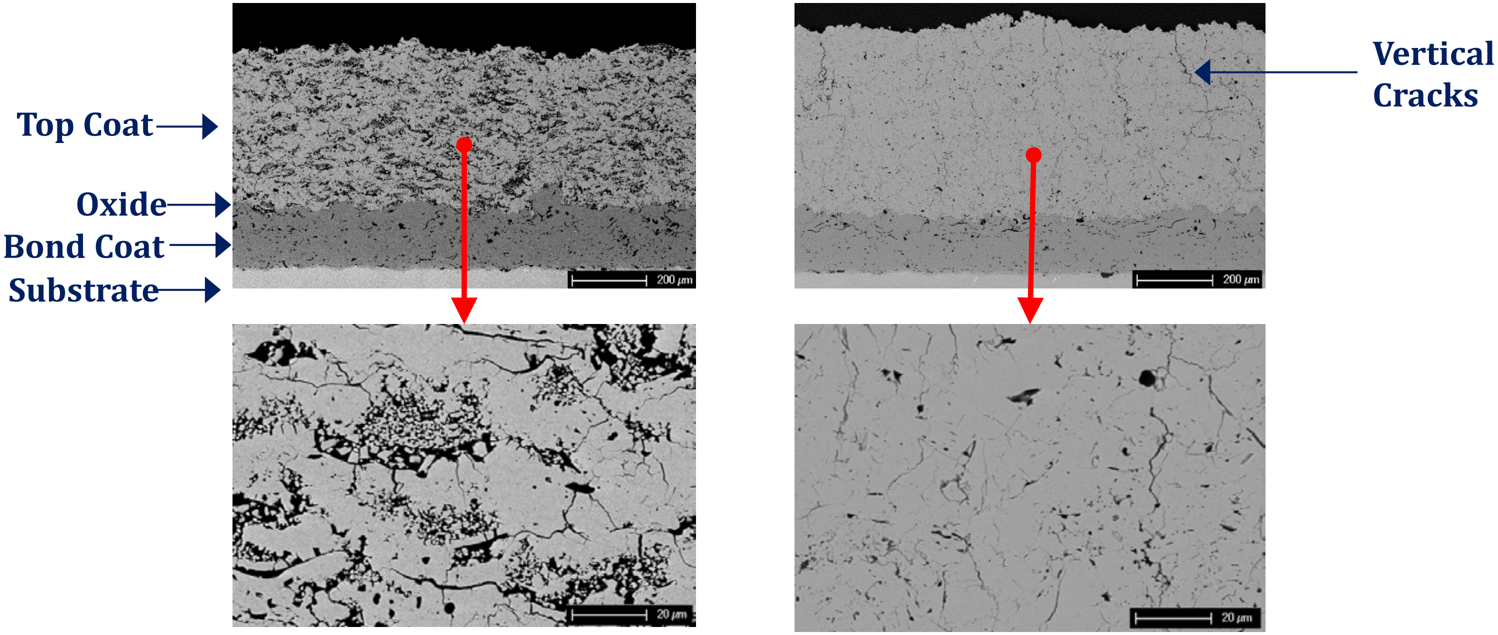

Density 85% T.D.   Density 92% T.D.

Substrate: *2nd generation Ni-base single crystal superalloy (René N5 or PWA 1484)*

Bond Coat: *NiCoCrAlY (Ni-22Co-16Cr-13Al-0.5Y wt.%) applied by Ar-shrouded plasma spraying at PST*

TBC: *Standard YSZ composition – 7wt.%*Y_2O_3 *– deposited by APS at thickness of ~380 µm*

Experimental Setup

Thermal Cycling Experimental Setup

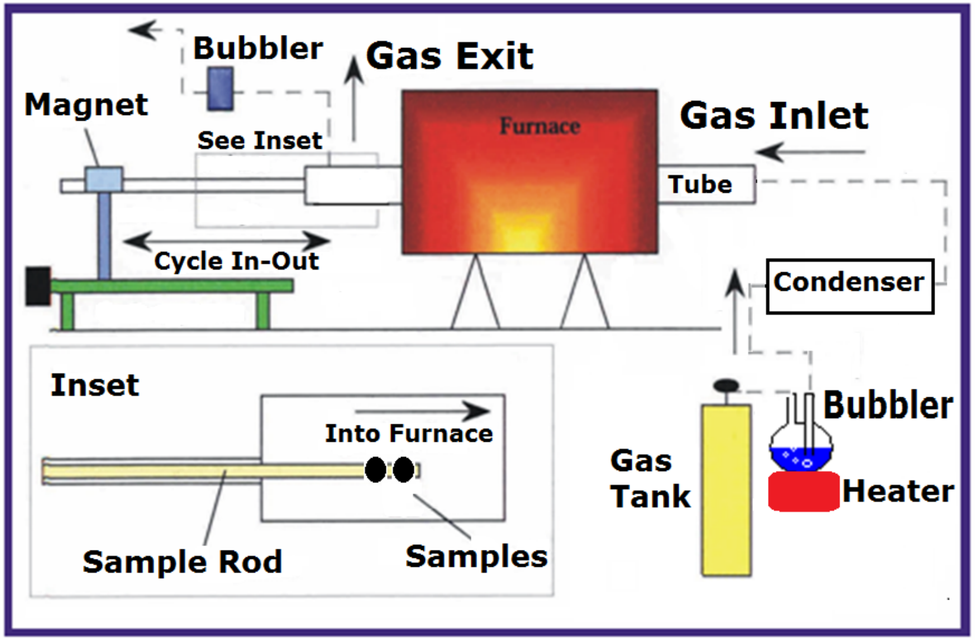

<u>Isothermal Testing at 1100°C</u>: *Free-standing YSZ*

- Reactions between YSZ/deposit
- Phase transformation in YSZ

<u>Cyclic Testing between 1100°C/160°C</u>: *DVF and HPLD TBCs*

- Early failure from fly-ash
- Atmospheric Effects

<u>Gas Atmospheres:</u>

- Dry Air
- Air+steam

Testing of 7YSZ top coat

High-CaO Ash

- Reaction with YSZ
- Additions of sulfate
- Cyclic failure of TBCs

High SiO_2-Ash

YSZ Reaction with Synthetic Ash

Dry Air exposures at 1100°C, 72h

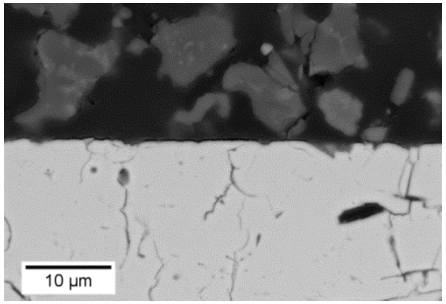

10% CaO

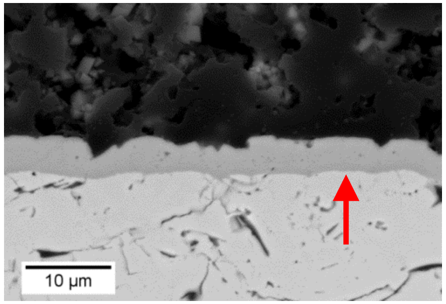

82% CaO

Increasing CaO →

Oxide	Wt%
SiO_2	50
Al_2O_3	25
Fe_2O_3	10
MgO	5
CaO	**10**

Oxide	Wt%
SiO_2	10
Al_2O_3	5
Fe_2O_3	2
MgO	1
CaO	**82**

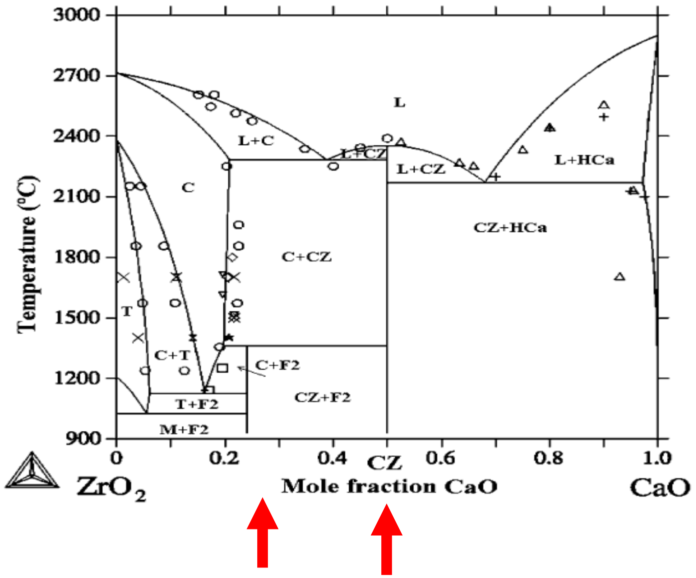

$CaZr_4O_9$ $CaZrO_3$

Reaction product predominantly **$CaZrO_3$**

Same reaction with pure CaO and high-CaO ash

Consequences of $CaZrO_3$

Thermal Cycling in lab air with $CaZrO_3$ layer

200 Cycles: 45min hold at 1100°C, 10min cool to 45°C

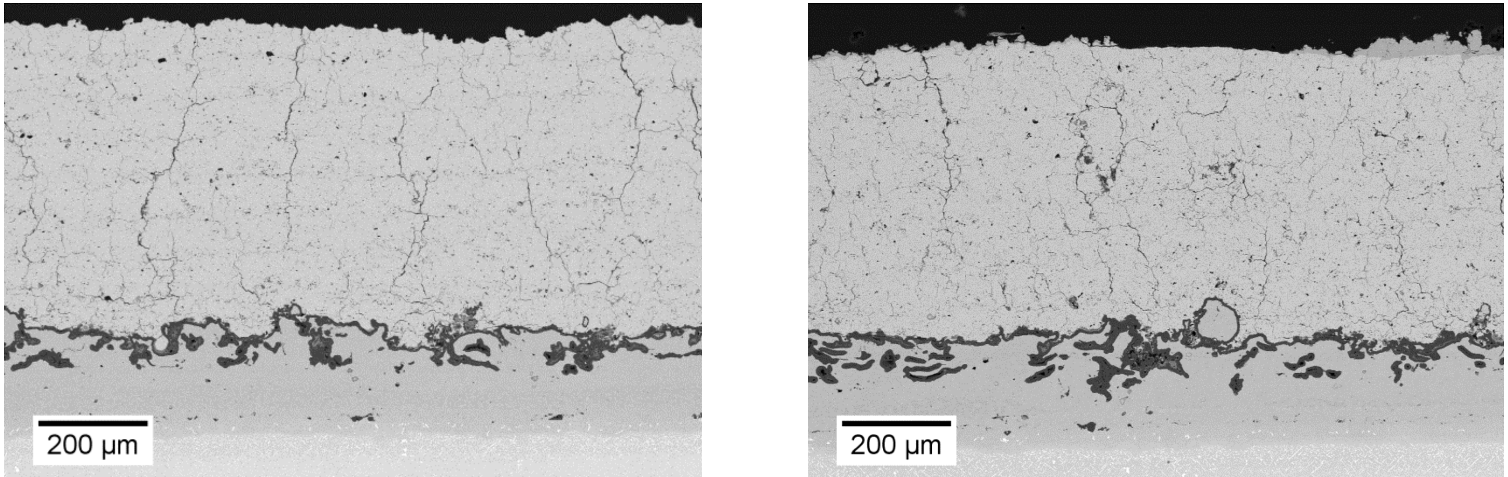

Cycling without reaction layer

Cycling after pre-formed $CaZrO_3$

- TBC reacted with CaO isothermally for 72h, then tested in cyclic furnace
- Very little spallation of $CaZrO_3$ layer at YSZ surface
- No significant overall affect on TBC performance

Testing of 7YSZ top coat

High-CaO Ash

- Reaction with YSZ
- Additions of sulfate
- Cyclic failure of TBCs

High SiO_2-Ash

Synthetic Ash with/without Addition

- Found that it is mainly CaO from fly-ash that reacts directly with YSZ
- Fly ash typically contains **sulfates**

Reactions in dry air at 1100°C, 72h

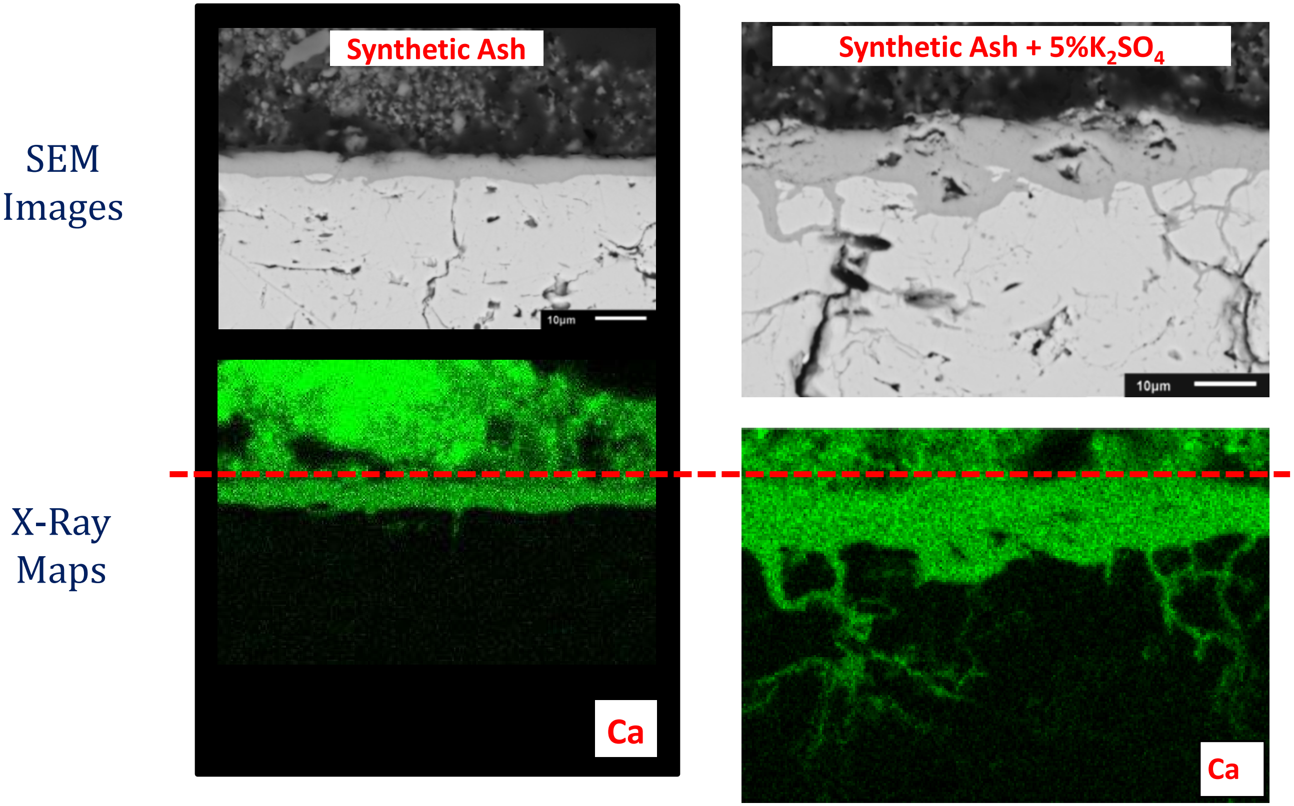

Addition of K_2SO_4 to synthetic ash causes infiltration of Ca into YSZ

Synthetic Ash + K_2SO_4 Addition

Free-standing DVC YSZ, reacted for 72h, 1100°C in dry air

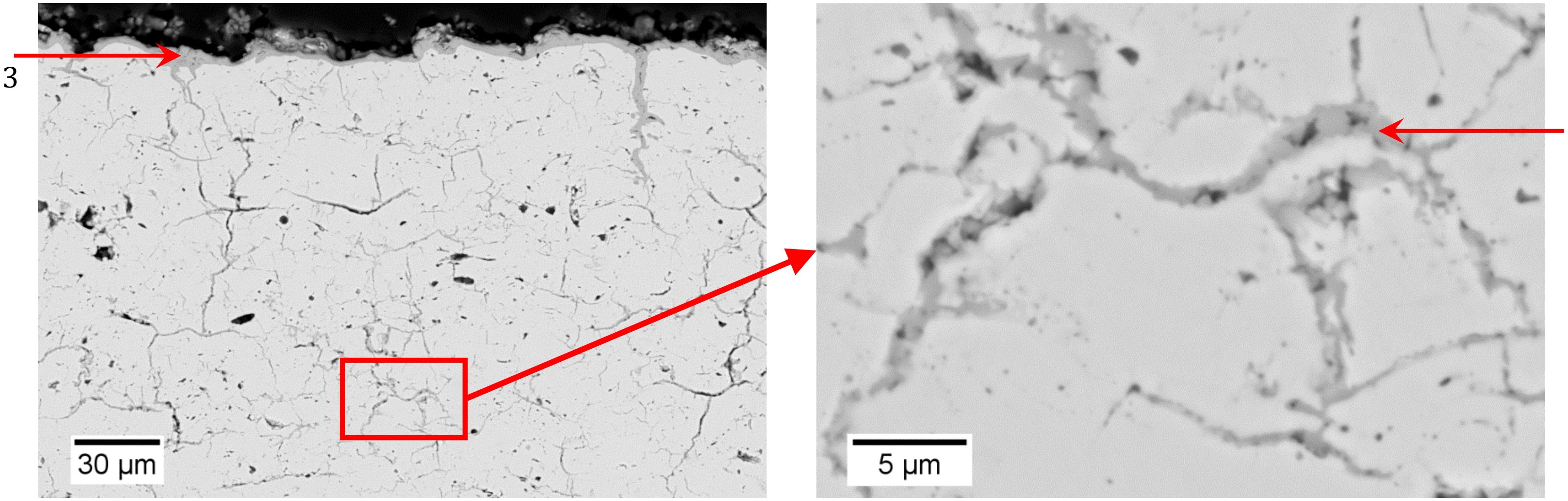

$CaZrO_3$

$CaZrO_3$

Ash Composition

	CaO	SiO_2	Al_2O_3	Fe_2O_3	MgO	K_2SO_4
Wt%	63	16.2	8.1	1.8	0.9	10

Consequence of Infiltration

Thermal Cycling in Lab Air

140 Cycles: 45min hold at 1100°C, 10min cool to 45°C

High-CaO Deposit <u>without</u> K_2SO_4

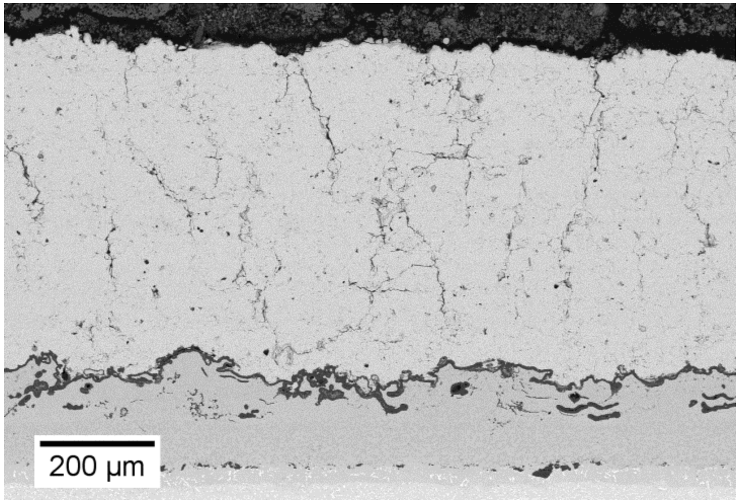

High-CaO Deposit <u>with</u> K_2SO_4

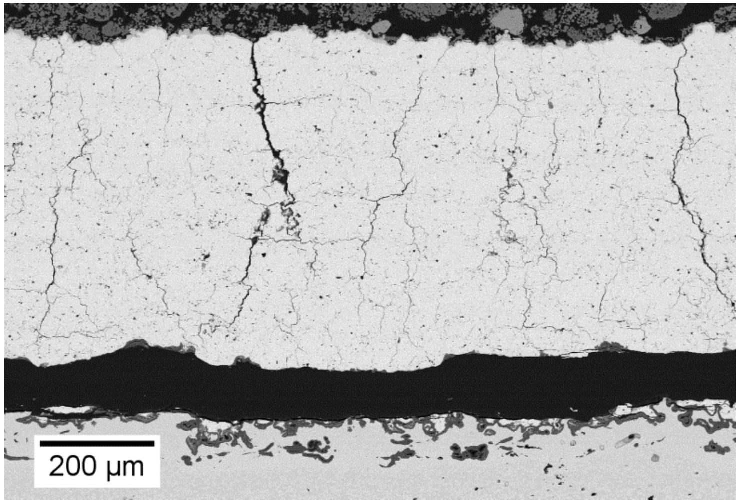

Early failure of DVC TBC caused by infiltration of top coat

Reaction with CaO+K_2SO_4

Free-standing DVC YSZ reacted with CaO+50wt%K_2SO_4, 1100°C, in dry air

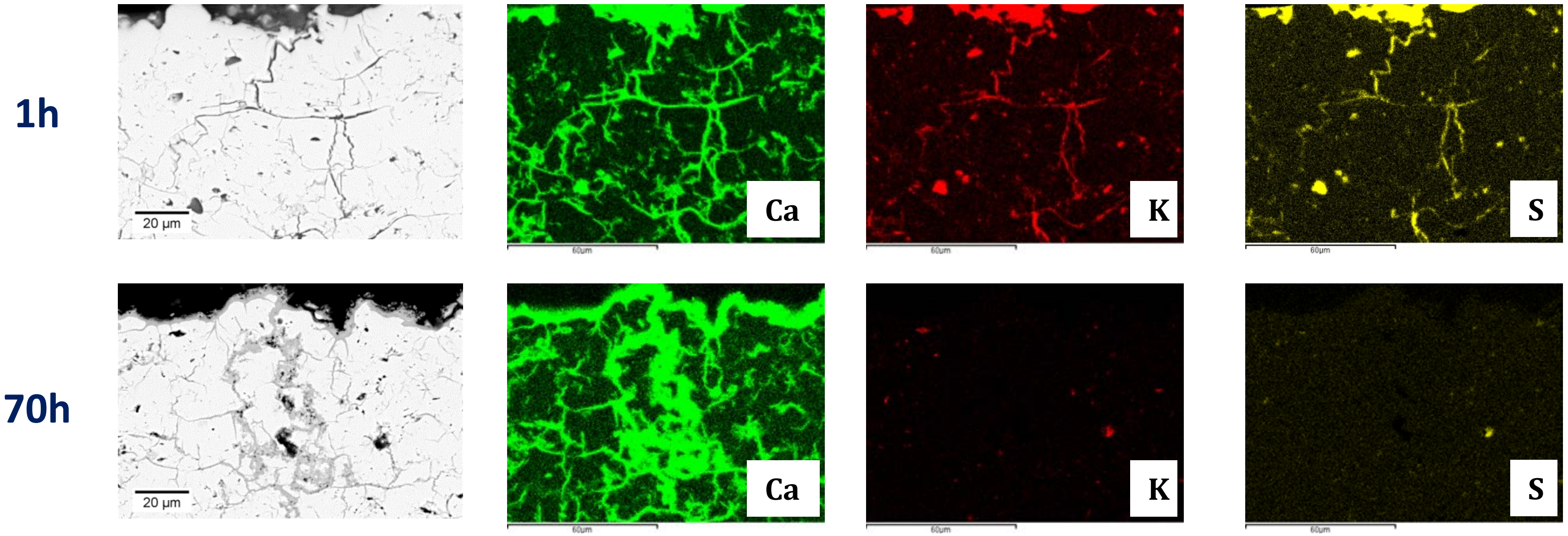

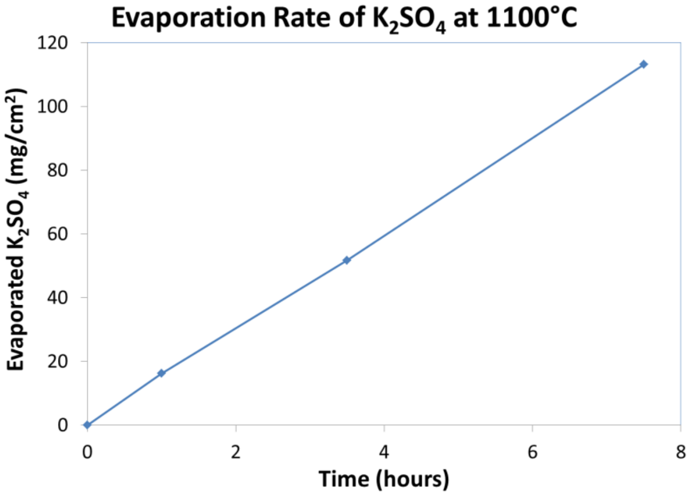

- Short times: CaO and K_2SO_4 both infiltrate
- Longer times: Loss of K_2SO_4, CaO reacts with YSZ

Reaction with CaO+K_2SO_4

70h Dry Air Exposures at 1100°C

0.1CaO-0.90K_2SO_4

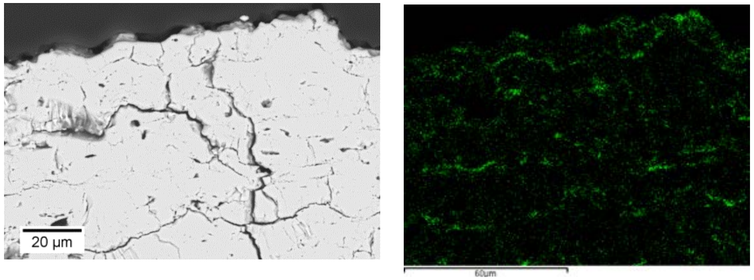

0.5CaO-0.5K_2SO_4

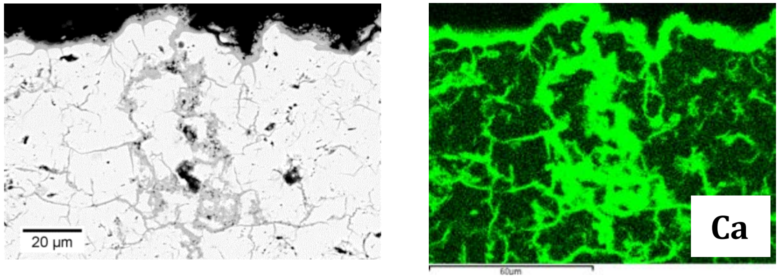

- Very low solubility of CaO in liquid K_2SO_4
- Increased CaO in deposit correlates with increased $CaZrO_3$ penetration
- Suggests CaO carried in suspension with liquid K_2SO_4

Testing of 7YSZ top coat

High-CaO Ash

- Reaction with YSZ
- Additions of sulfate
- Cyclic failure of TBCs

High SiO_2-Ash

TBC Failure after Cyclic Exposure

How does infiltration of $CaZrO_3$ affect **TBC performance**?

Thermal Cycling in dry air: 45min at 1100°C/ 15min at 160°C

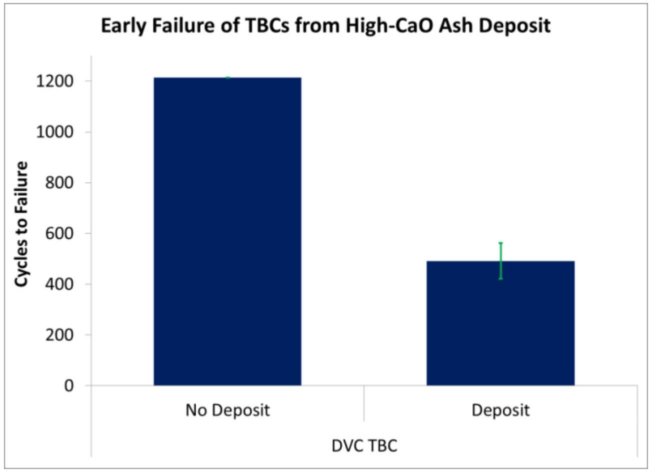

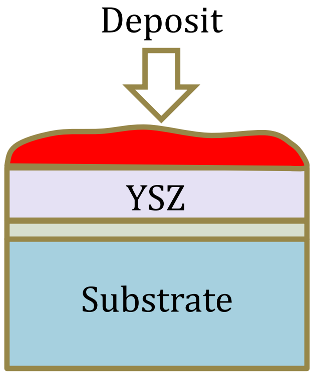

"High-CaO" Ash+$.05K_2SO_4$+.05FeS

	Wt%
CaO	63
SiO_2	16.2
Al_2O_3	8.1
Fe_2O_3	1.8
MgO	.9
K_2SO_4	5
FeS	5

DVC TBC Failure with deposit

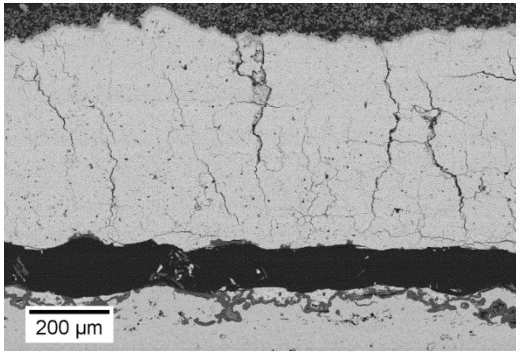

DVC TBC Failure without deposit

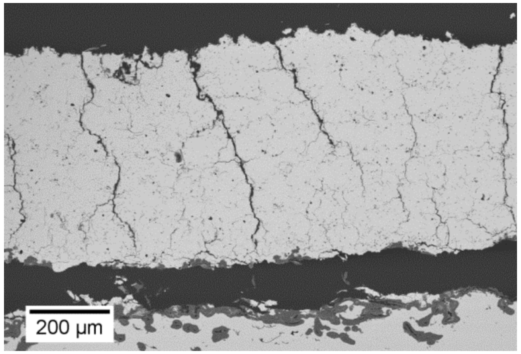

TBC Failure after Cyclic Exposure

Stress in TBC from CTE mismatch

$$\boxed{\sigma_o = E_{tbc}\frac{\Delta\alpha\Delta T}{1-\upsilon}}$$

Typical Values

	E (Gpa)	α (x10^{-6} C^{-1}ppm)
YSZ	30-50	11-13
Metal	200	17.1

Key parameters affecting stress in top coat: E, α, ΔT

Free-standing YSZ heat treated 72h: 3-Pt Bend Test

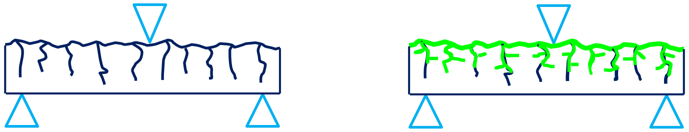

No Deposit

With Deposit

E = **30** ±3 GPa

E = **132** ±19 GPa

Significant increase in elastic modulus
Contributes to overall increased stress

Choi; Hutchinson; Evans, *Mechanics of Materials* **31** (1999), 431-447.

TBC Failure after Cyclic Exposure

TBC Degradation in HPLD Top Coat

Thermal Cycling in dry air: 45min at 1100°C/ 15min at 160°C

Failure Without Deposit

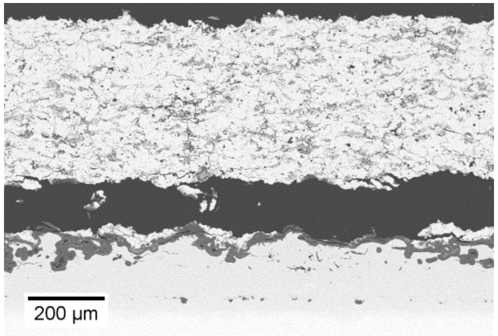

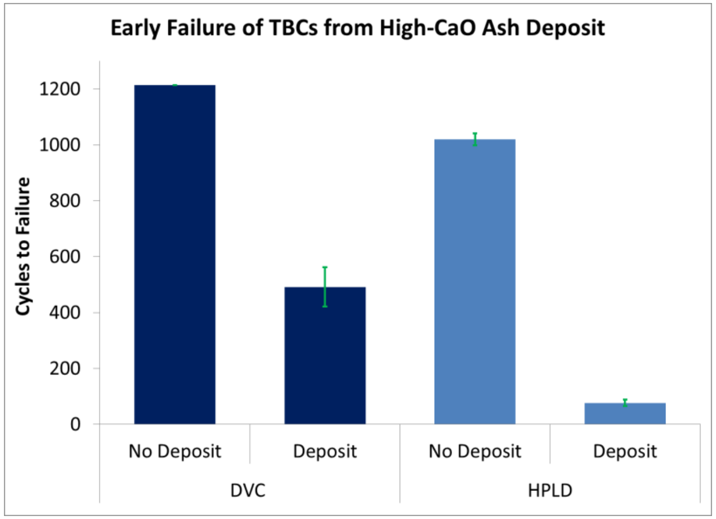

Failure With Deposit

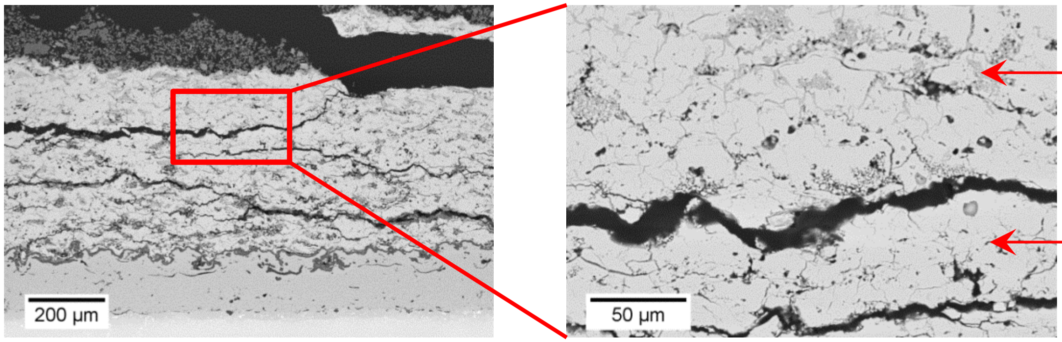

$CaZrO_3$ Infiltration

Very Little $CaZrO_3$

Testing of 7YSZ top coat

High-CaO Ash

- Reaction with YSZ
- Additions of sulfate
- Cyclic failure of TBCs

High SiO_2-Ash

High-SiO_2 Ash Exposed to YSZ

- Effects of lower-CaO ash that should **not** form $CaZrO_3$?
- Infiltrated cracks at YSZ surface contain ash constituents
- Some liquid infiltration likely

Synthetic Ash+.1K_2SO_4

	Wt%
SiO_2	45
Al_2O_3	22.5
CaO	9
Fe_2O_3	9
MgO	4.5
K_2SO_4	10

72h Exposure in Dry Air, 1100°C

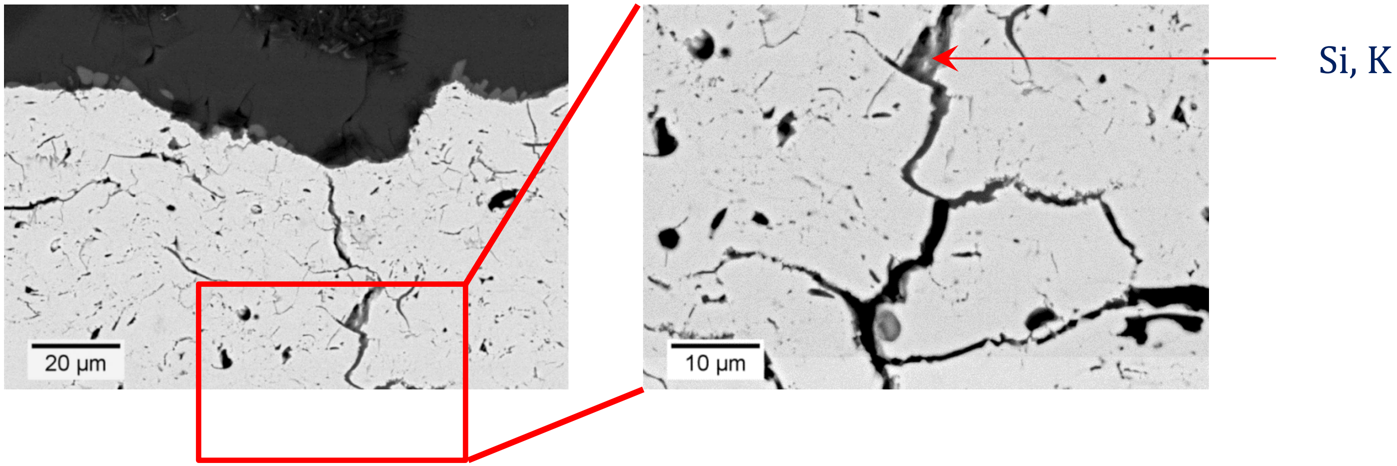

Cyclic TBC Exposure to High-SiO$_2$ Ash

Early Failure of HPLD TBCs with **“high-SiO$_2$”** ash with K$_2$SO$_4$

Thermal Cycling in dry air: 45min at 1100°C/ 15min at 160°C

Failure Without Deposit

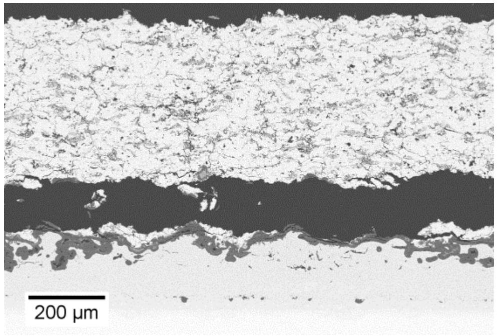

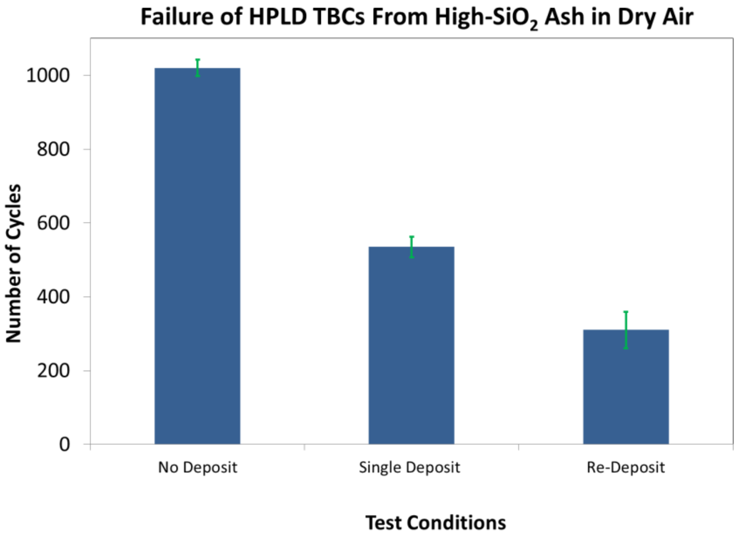

“High-SiO$_2$”
Ash+.1K$_2$SO$_4$

	Wt%
SiO$_2$	**45**
Al$_2$O$_3$	22.5
CaO	9
Fe$_2$O$_3$	9
MgO	4.5
K$_2$SO$_4$	10

With Deposit

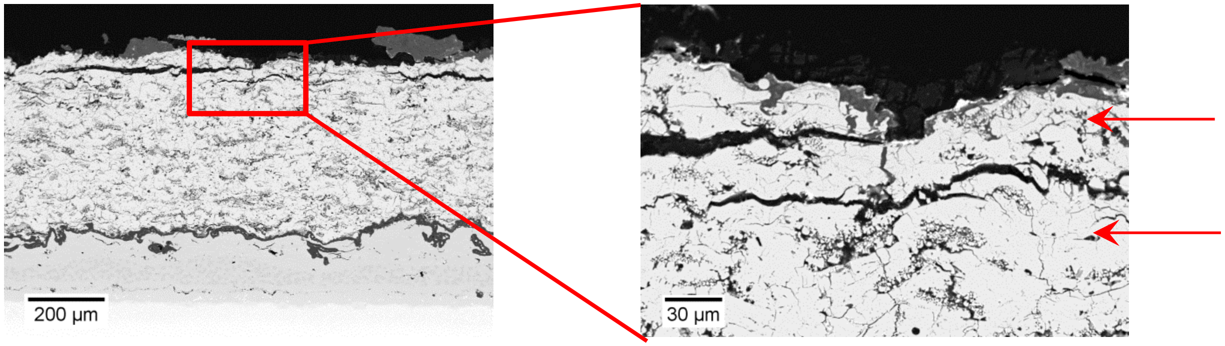

Summary of Top Coat Results

- Infiltration into YSZ when K_2SO_4 is present
- TBC degradation at temperatures below overall ash melting temperature
- Different modes of failure for DVC and HPLD top coats

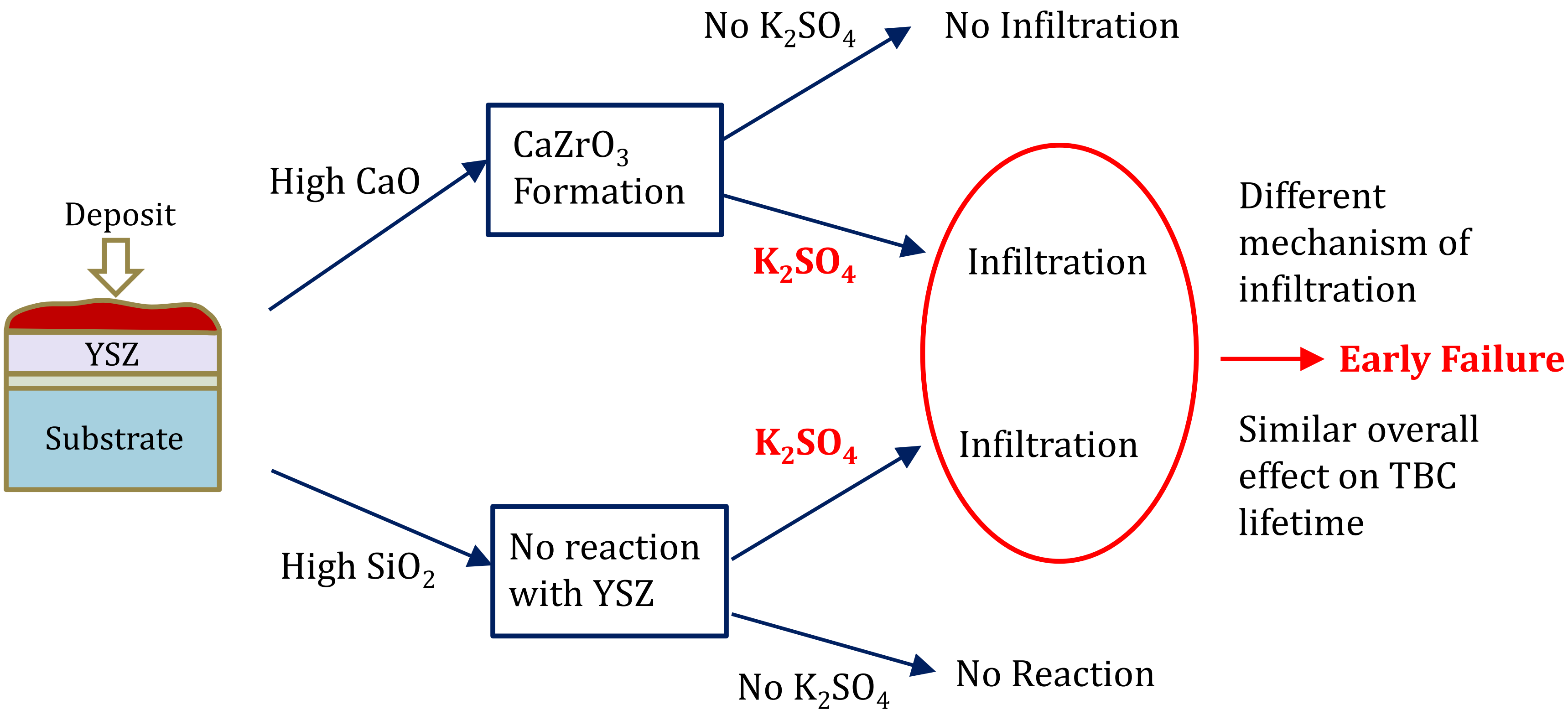

Deposit

YSZ

Substrate

High CaO

$CaZrO_3$ Formation

No K_2SO_4

No Infiltration

$\mathbf{K_2SO_4}$

Infiltration

Different mechanism of infiltration

Early Failure

High SiO_2

No reaction with YSZ

$\mathbf{K_2SO_4}$

Infiltration

Similar overall effect on TBC lifetime

No K_2SO_4

No Reaction

MCrAlY Bondcoats – Background

Bondcoats: corrosion-resistant metallic coatings

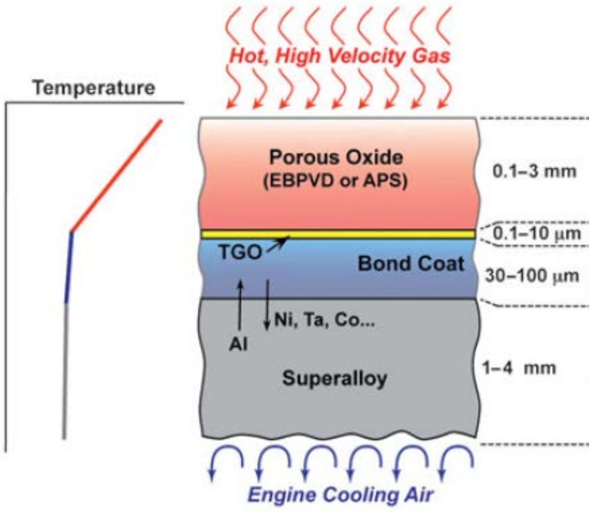

in Clarke et al, MRS Bulletin 37 (2012)

Overlay: MCrAlY (M=Ni,Co)

- Two-phase β-γ structure
- Commonly used in land-based turbines for power generation

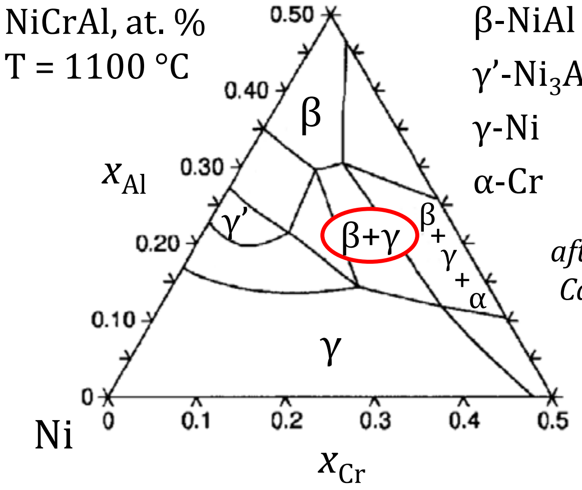

β-NiAl
γ'-Ni_3Al
γ-Ni
α-Cr

after N. Dupin et al, Calphad 25 (2001)

Top Coat

Bond Coat

Substrate

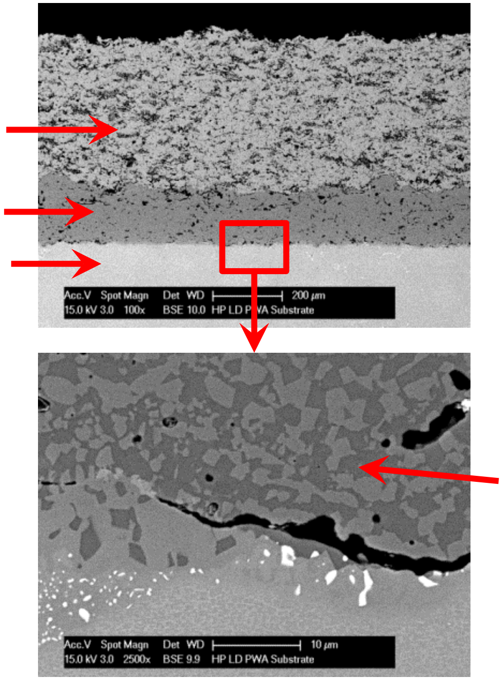

Al-rich β-phase, source of Al to form Al_2O_3 TGO

MCrAlY Bondcoats – Background

Bondcoats: corrosion resistant metal coatings

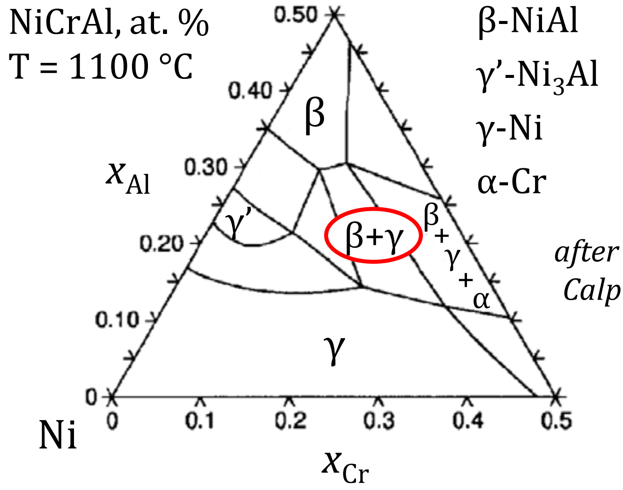

after N. Dupin et al, Calphad 25 (2001)

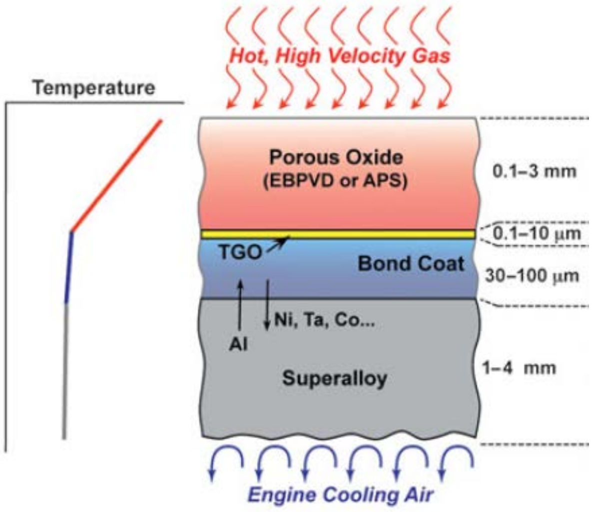

in Clarke et al, MRS Bulletin 37 (2012)

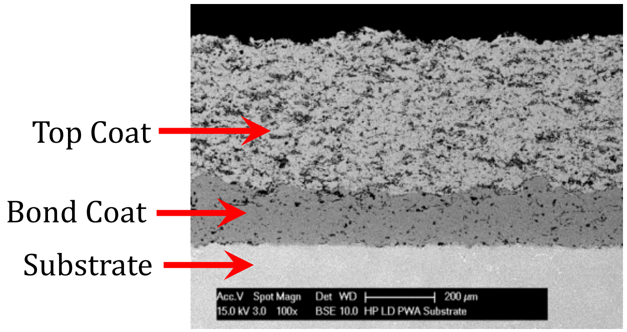

Identified modes of degradation:

- air oxidation; thermal cycling
- sulfate-induced accelerated attack: type I and type II hot corrosion

Fly ash-induced corrosion ?

Fly Ash Corrosion

Fly ash oxide-sulfate mixtures found to cause degradation of NiCoCrAlY alloys at intermediate temperatures (900-1100 °C)

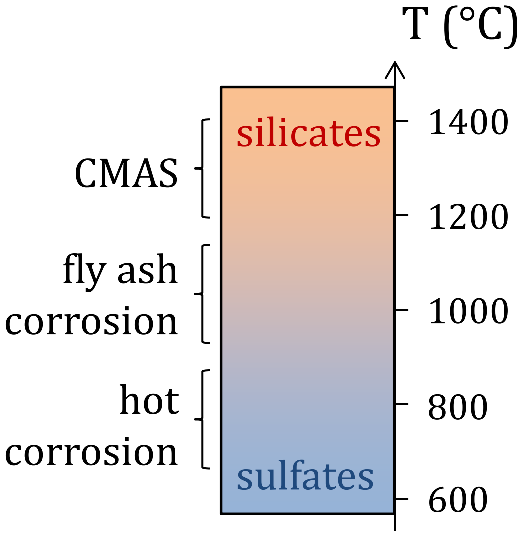

Ni-30Co-30Cr-12Al-0.1Y,
50 h at 1100 °C
CO_2-$20H_2O$

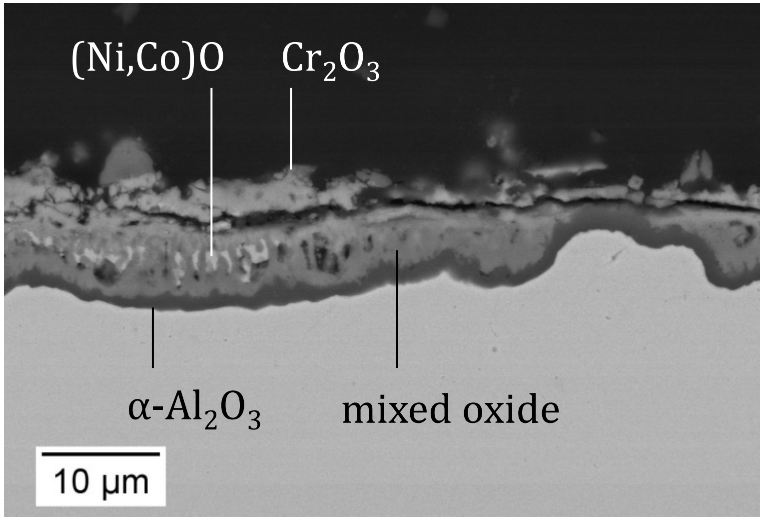

Class C ash (wt. %)

SiO_2	26
Al_2O_3	20
CaO	33
Fe_2O_3	6
MgO	8
Na_2SO_4	5
K_2SO_4	1

Factors Considered in the “Bondcoat” Study

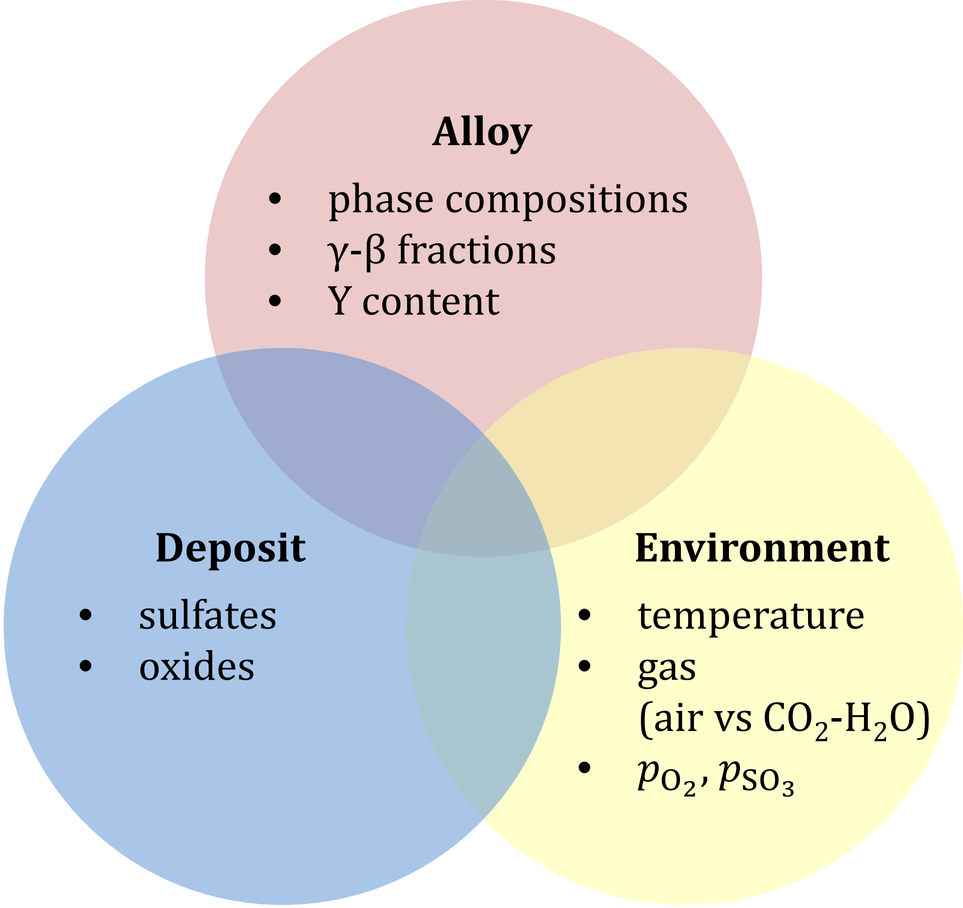

Alloy

- phase compositions
- γ-β fractions
- Y content

Deposit

- sulfates
- oxides

Environment

- temperature
- gas (air vs CO_2-H_2O)
- p_{O_2}, p_{SO_3}

Factors affecting fly-ash corrosion

1. Experimental protocol
2. Reactivity of class C ash, effect of alloy composition
3. Reactivity of individual oxides: *CaO in this presentaion*
4. Interactions between oxide and sulfate constituents, and gas p_{SO_3} and temperature

Experimental Protocol

Experimental conditions:

- Cast NiCoCrAlY alloys used in place of thermally sprayed coatings
- 50 h exposures at 900 °C and 1100 °C

Deposits:

- Class C fly ash
- Individual oxides, sulfates
- Synthetic mixtures:

Acidic oxide	+	Basic oxide	+	Sulfate
Al_2O_3		CaO		Na_2SO_4
SiO_2		MgO		

Gas mixtures:

- dry air
- CO_2-$20H_2O$
- CO_2-$20H_2O$-$1.6O_2$
- O_2-$0.1SO_2$

Mode of Reaction with Class C Ash

1100 °C

Ni-30Co-27Cr-12Al-0.1Y

Class C ash

CO_2-20%H_2O

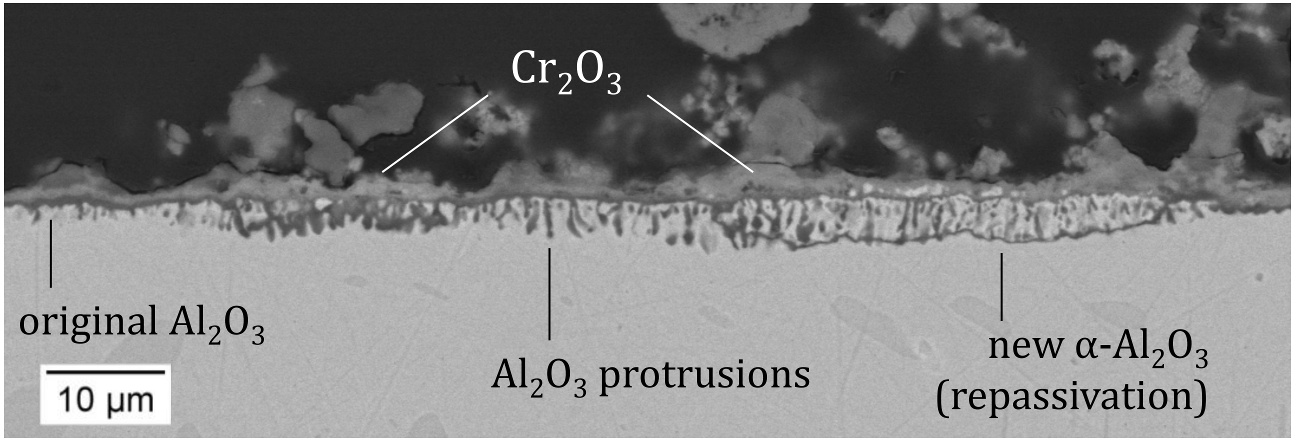

1 h

↓

50 h

CO_2-20%H_2O, no deposit, 50 h

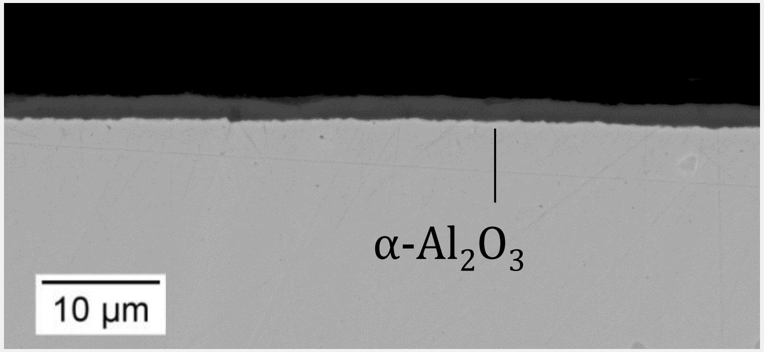

With no deposit, all alloys studied formed external Al_2O_3 scales in all atmospheres

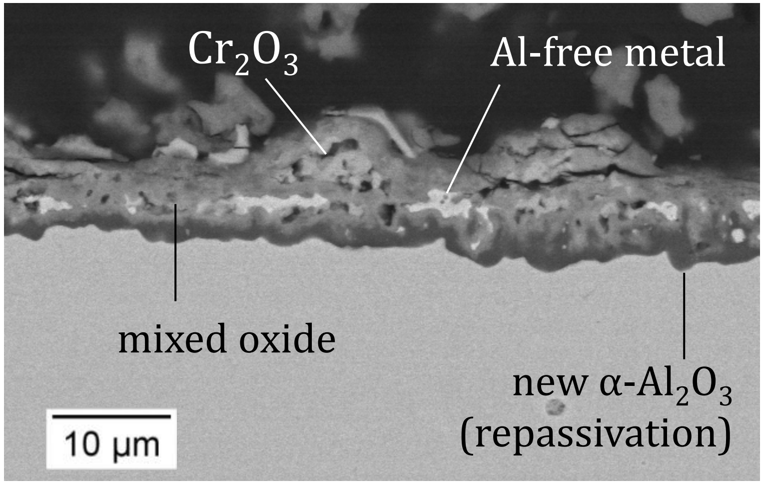

Effect of Alloy Composition

1100 °C, 50 h
CO_2-20%H_2O

NiCoCrAl
Pseudo-ternary diagram
$x_{Co} = 0.3$
T = 1100 °C

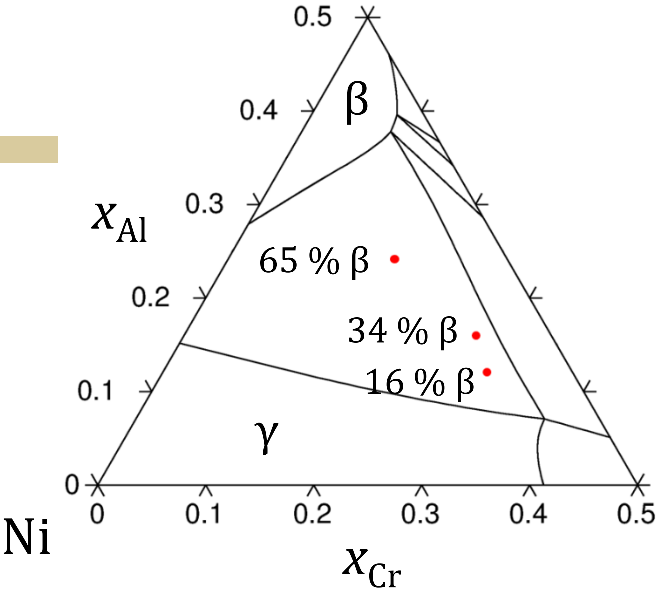

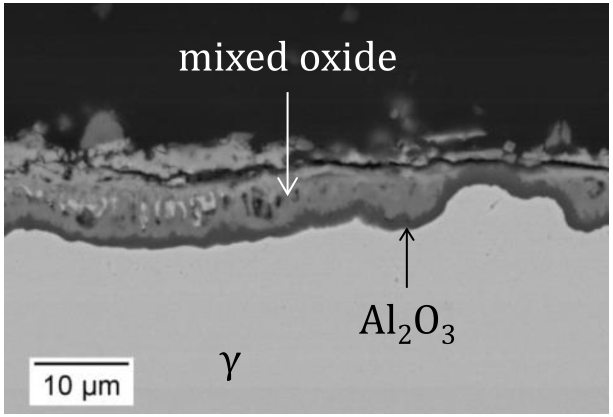
Ni-30Co-30Cr-12Al-0.1Y
(γ-16β)

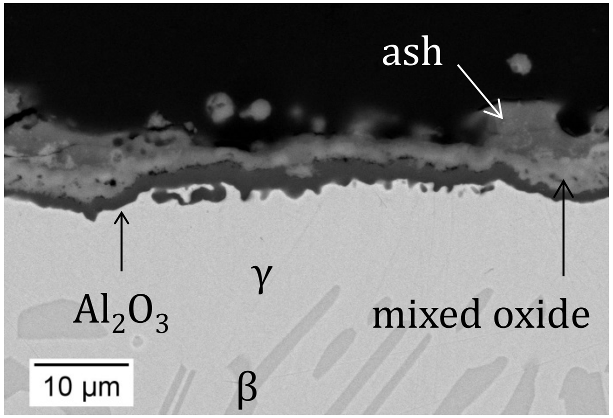
Ni-30Co-27Cr-16Al-0.1Y
(γ-34β)

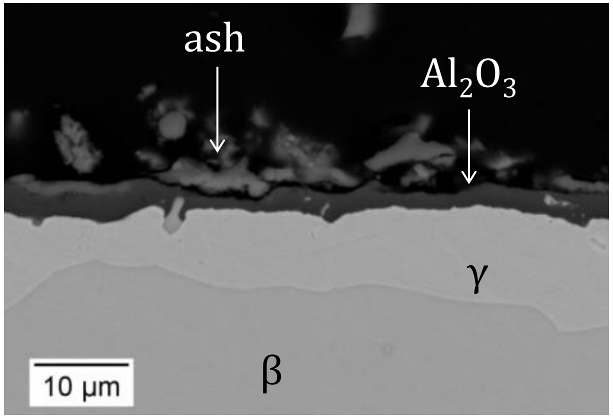
Ni-19Co-15Cr-24Al-0.1Y
(γ-65β)

Extent of degradation decreases with increasing β fraction.

Effect of Y Content

1100 °C, 50 h
Ni-19Co-15Cr-24Al

0.1Y

0.3Y

Dry air,
No deposit

CO_2-20%H_2O,
class C ash

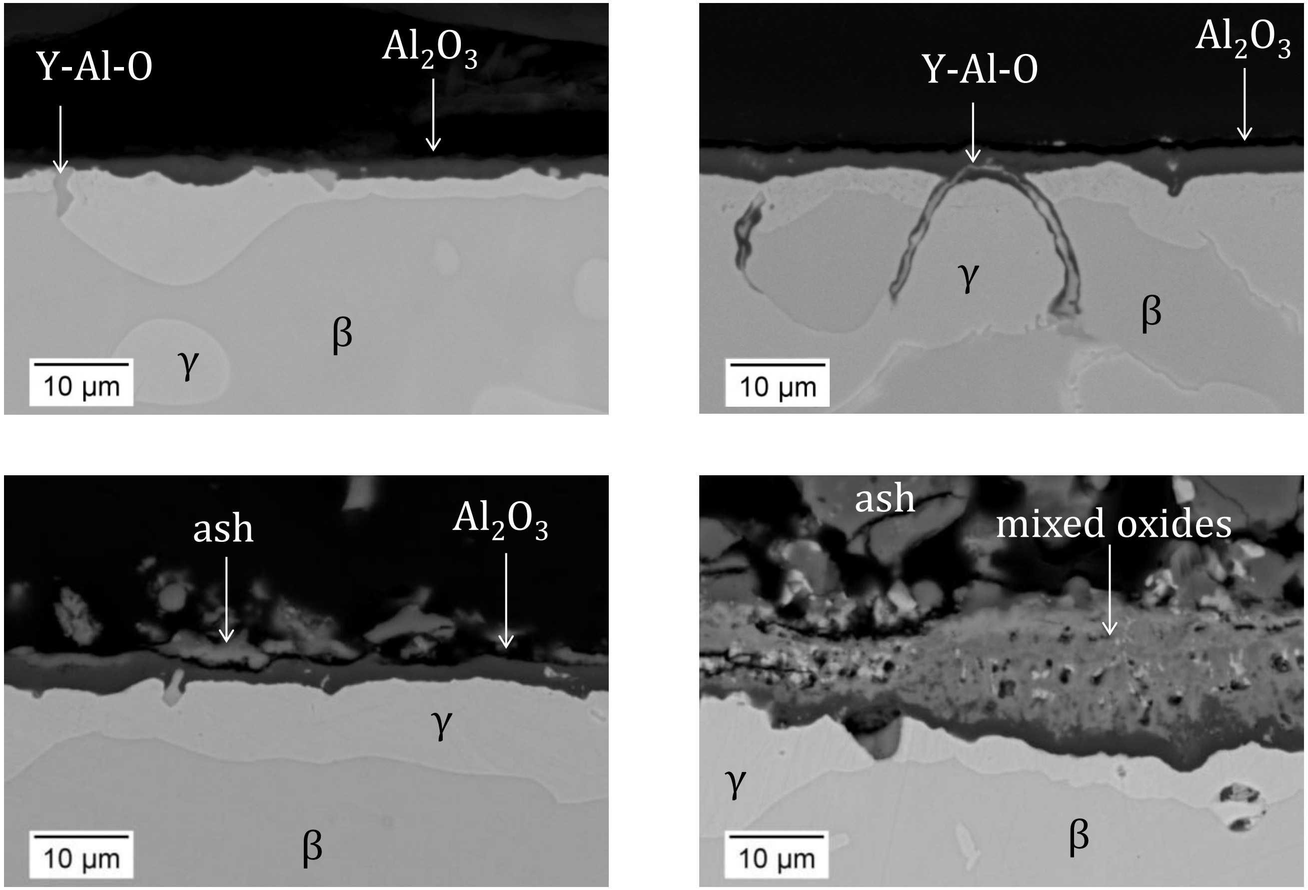

Number and size of Y-Al oxide pegs very sensitive to Y content.
Significant degradation of “overdoped” alloy in the presence of ash deposit.

Factors Considered in the Study

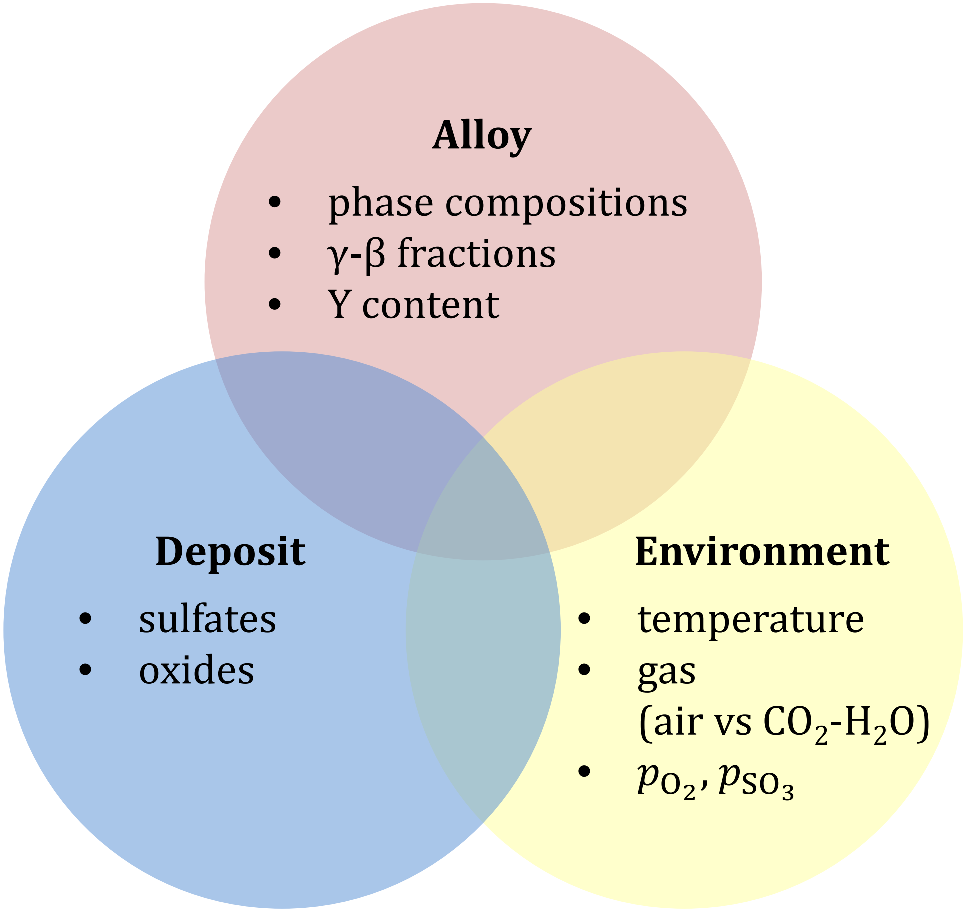

Alloy

- phase compositions
- γ-β fractions
- Y content

Deposit

- sulfates
- oxides

Environment

- temperature
- gas (air vs CO_2-H_2O)
- p_{O_2}, p_{SO_3}

Factors affecting fly-ash corrosion

1. Experimental protocol
2. Reactivity of class C ash, effect of alloy composition
3. **Reactivity of individual oxides**: CaO
4. Interactions between oxide and sulfate constituents, and gas p_{SO_3} and temperature

Exposure to Individual Oxides

Ni-19Co-16Cr-23Al-0.1Y
(γ-65β)

1100 °C, 50 h
dry air

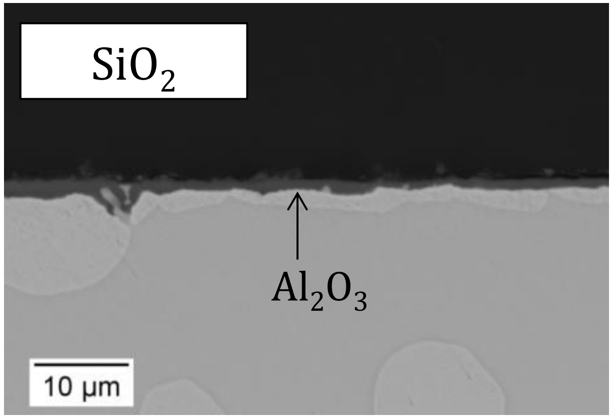

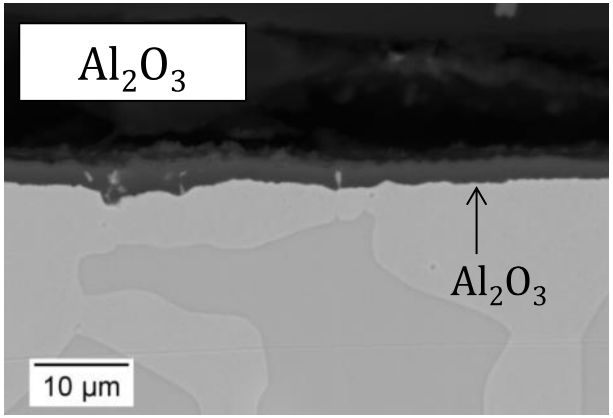

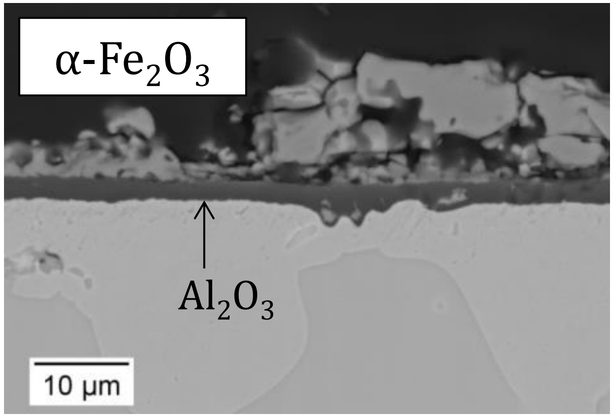

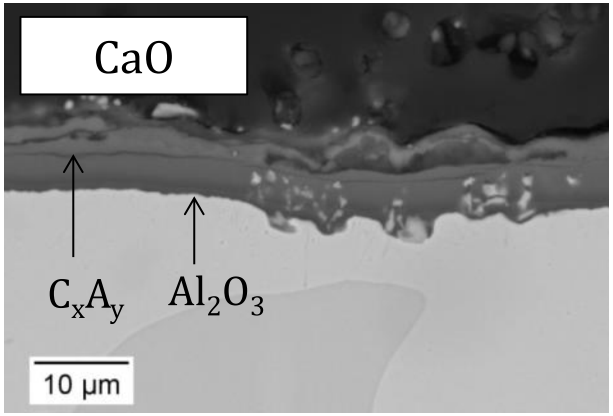

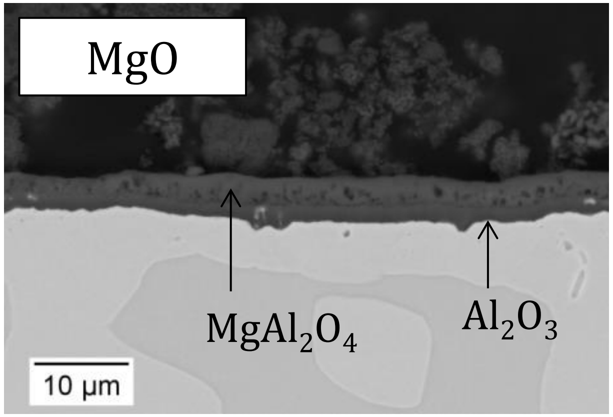

Thermally grown Al_2O_3 reacts at a significant rate with CaO and MgO

Exposure to CaO in Dry Air

Reaction with CaO: two distinct processes

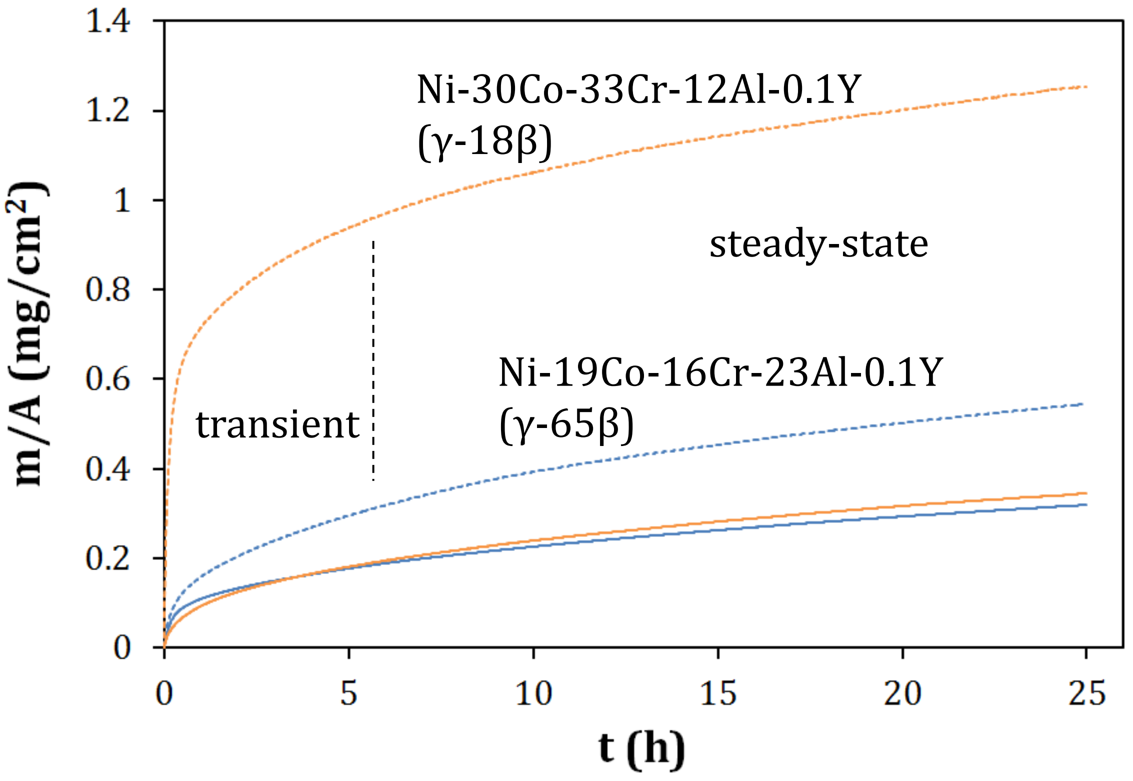

Transient stage: reaction rate much higher for low β fraction.

Steady-state: reaction rate similar for both alloys, higher than in the absence of CaO deposit.

Exposure to CaO in dry air

Reaction with CaO: two distinct processes

1100 °C, 50 h

Low β alloys

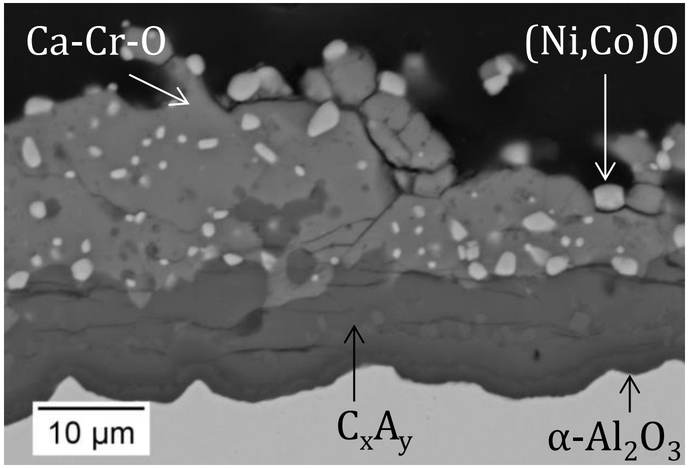

Ni-30Co-33Cr-12Al-0.1Y (γ-18β)

Reaction rate decreases when alloy passivates.

High β alloys

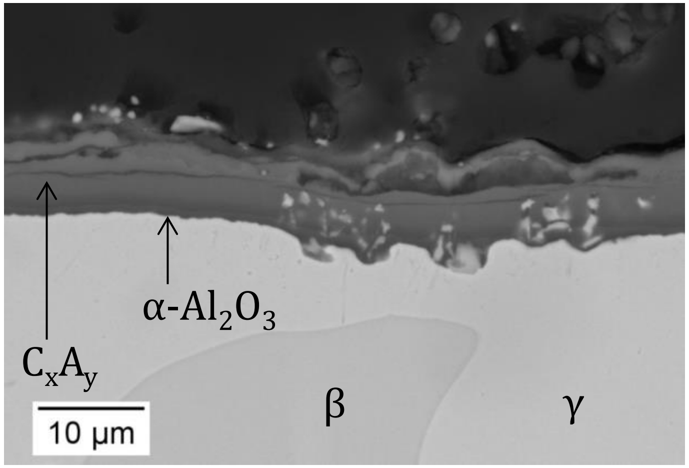

Ni-19Co-16Cr-23Al-0.1Y (γ-65β)

Steady-state reaction of CaO with TGO to form xCaO-yAl_2O_3 layers; minimal alloy consumption.

Exposure to CaO in Dry Air

Ni-30Co-33Cr-12Al-0.1Y (γ-18β) 1100 °C

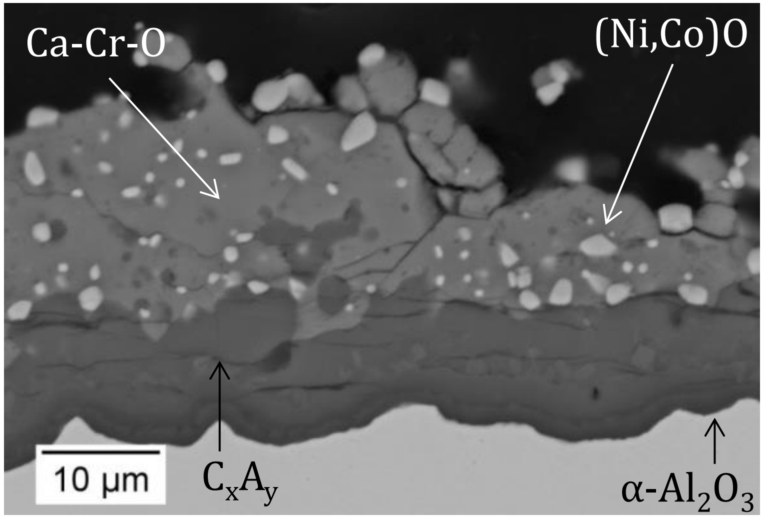

γ composition (at. %):	Ni	Co	Cr	Al
	23	32	37	8.2

CaO-Cr_2O_3 phase diagram

eutectic at 1061 °C

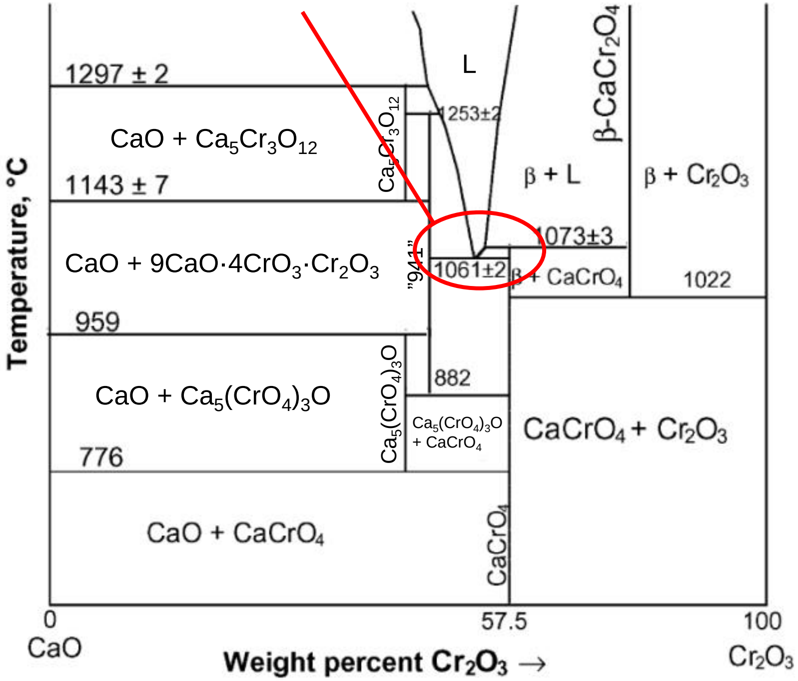

adapted from Kaiser et al, J. Am. Ceram. Soc. 1992

Reaction CaO-Cr_2O_3 to form a liquid

(*K.T. Chiang, G.H. Meier, R.A. Perkins, J. Materials for Energy Systems, 1984*)

Exposure to CaO in Dry Air

Ni-30Co-33Cr-12Al-0.1Y
(γ-18β)

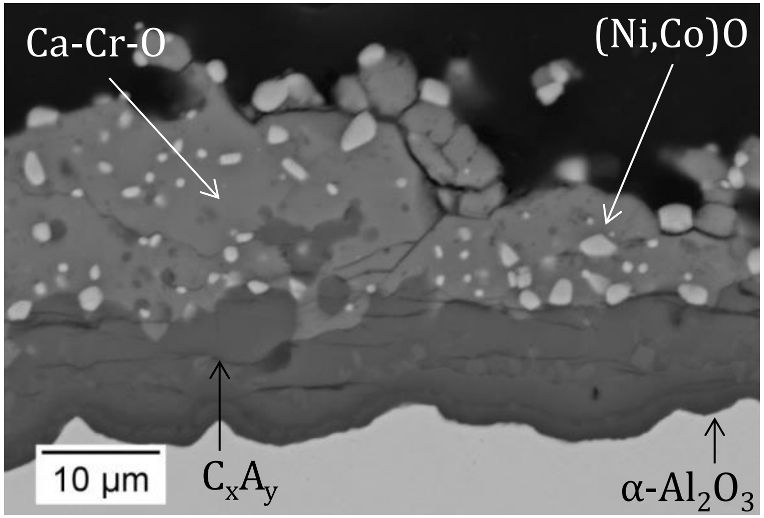

γ composition (at. %):	Ni	Co	Cr	Al
	23	32	37	8.2

Metastable
phase diagram

1100 °C

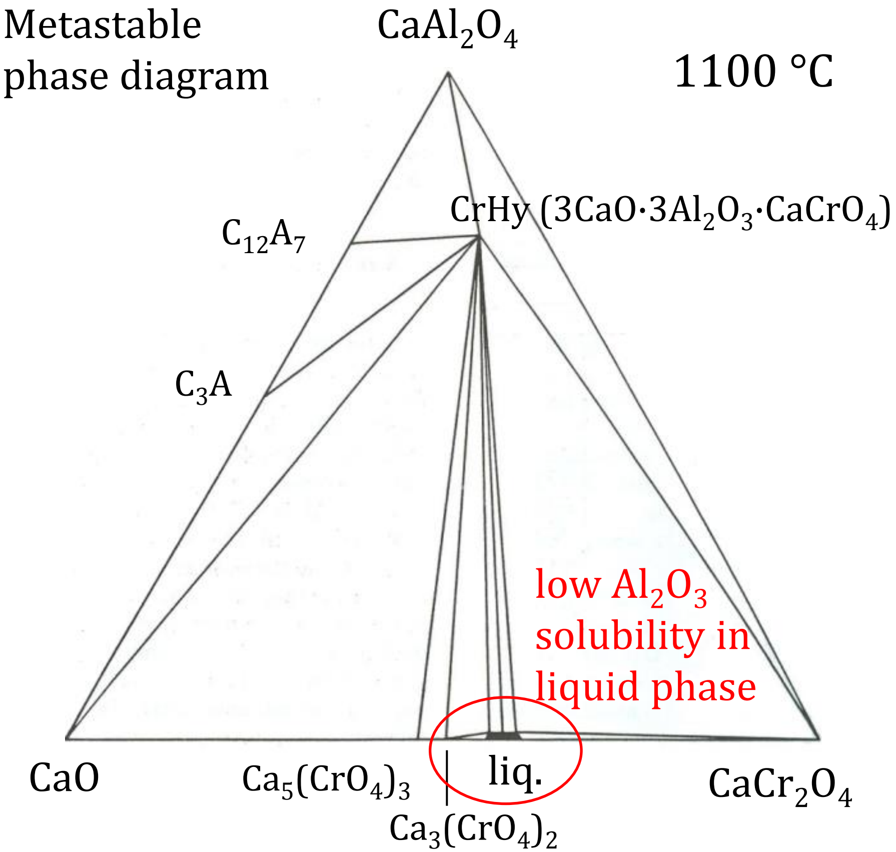

adapted from Kaiser et al, J. Am. Ceram. Soc. 1992

→ as γ is consumed, Al is rejected until Al_2O_3 can form

Exposure to CaO in dry air

Susceptibility to transient attack determined by distribution of Cr-rich γ phase in alloy

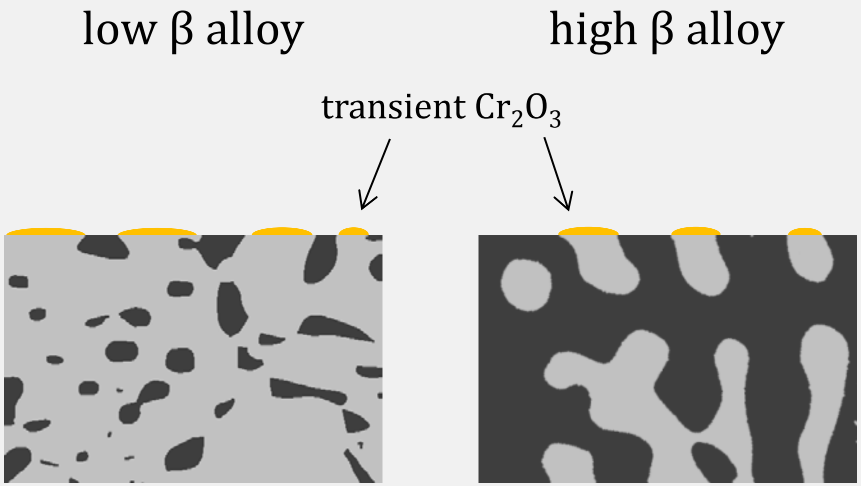

γ connected
highly susceptible to
transient attack

γ isolated
non-susceptible to
transient attack

Transient attack extremely severe for 100 % γ alloy

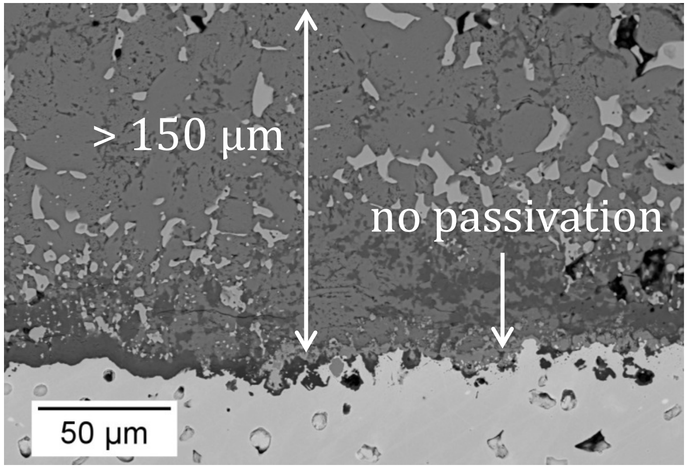

Ni-33Co-35Cr-7Al-0.1Y,
50 h at 1100 °C

In service conditions (thermal cycles), reaction product spallation will cause transient stage to be repeated.

Exposure to CaO in Dry Air

Ni-19Co-16Cr-23Al-0.1Y
(γ-65β)

50 h, 1100 °C

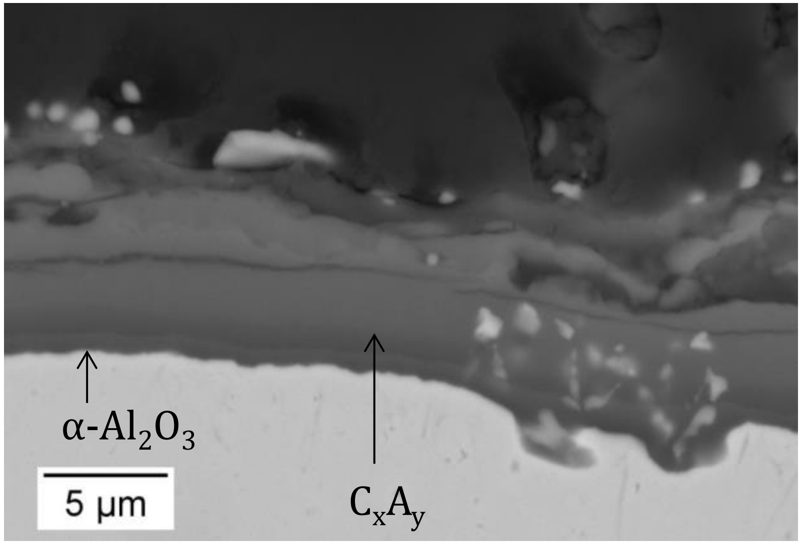

How does Al_2O_3 reaction to form $xCaO$-yAl_2O_3 affect Al consumption ?

Kinetics of Al_2O_3 formation-destruction

Al_2O_3 growth rate equation: $$\frac{dX}{dt} = \frac{p}{2X} - \alpha\frac{q}{2\sqrt{qt}}$$

Analytical solution: $$\begin{cases} X^2 = kt \\ k = \frac{1}{2}\left[2p + \alpha^2 q - \alpha\sqrt{q(4p + \alpha^2 q)}\right] \end{cases}$$

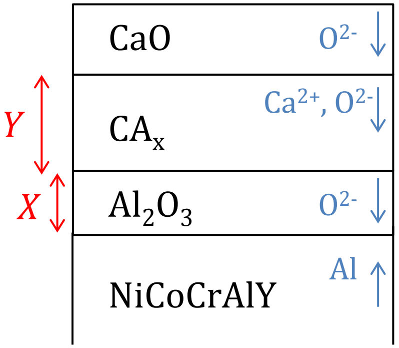

CaO O^{2-}

CA_x Ca^{2+}, O^{2-}

Al_2O_3 O^{2-}

NiCoCrAlY Al

Y

X

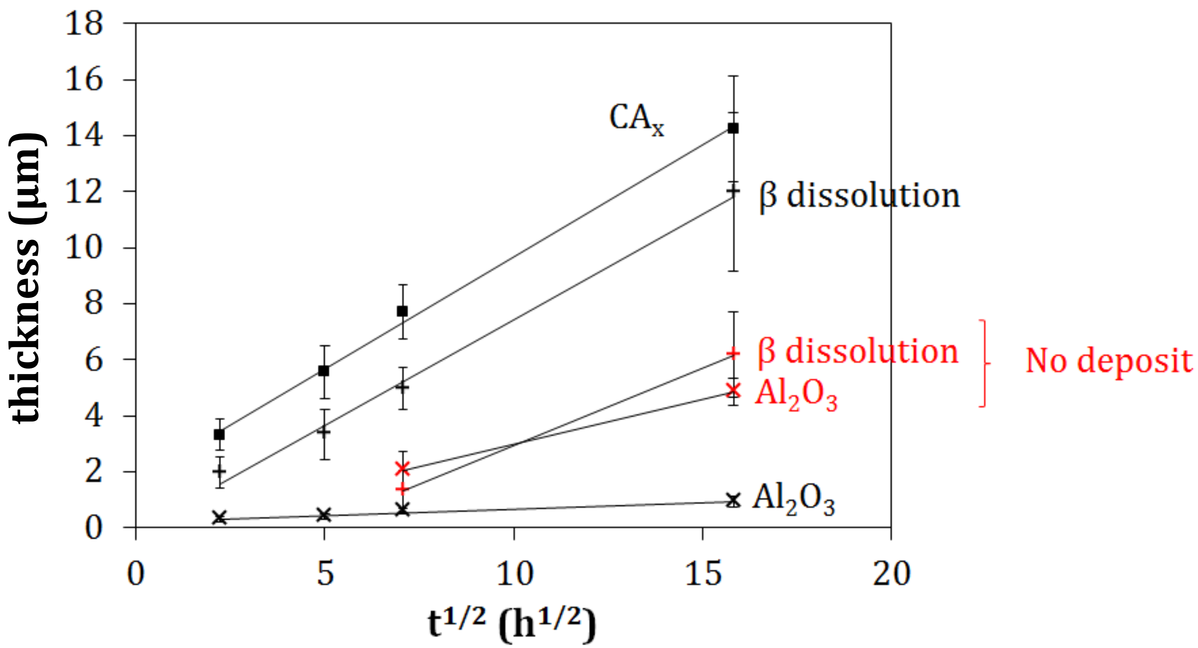

CaO deposit: enhanced Al consumption
→ decreased lifetime

Example:
190 µm bondcoat

Time for β depletion through half-thickness

No deposit: 31,000 h
CaO: 16,000 h

i.e., 48 % reduction

Factors Considered in the Study

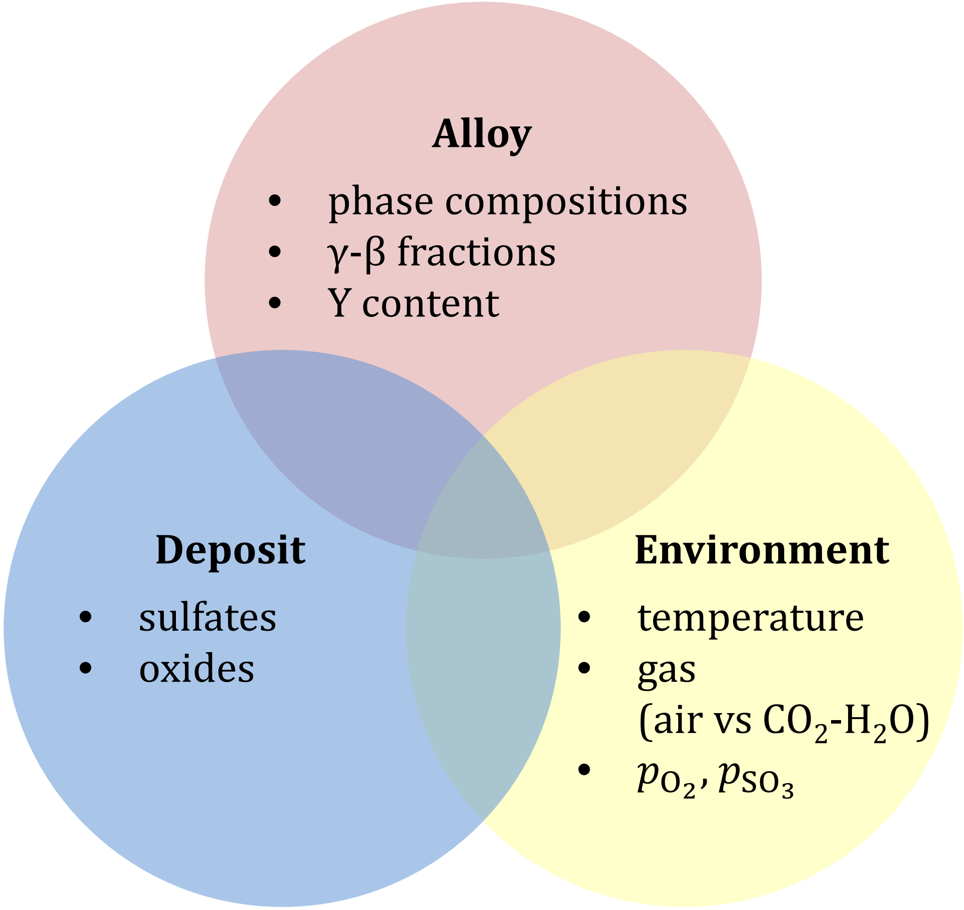

Alloy

- phase compositions
- γ-β fractions
- Y content

Deposit

- sulfates
- oxides

Environment

- temperature
- gas (air vs CO_2-H_2O)
- p_{O_2}, p_{SO_3}

Factors affecting fly-ash corrosion

1. Experimental protocol
2. Reactivity of class C ash, effect of alloy composition
3. Reactivity of individual oxides: CaO
4. **Interactions between oxide and sulfate constituents, and gas p_{SO_3} and temperature**

Role of Ash Oxide and Sulfate Contents

1100 °C

Class C ash (wt. %)

SiO_2	Al_2O_3	CaO	Fe_2O_3	MgO	Na_2SO_4	K_2SO_4
26	20	33	6	8	5	1

Synthetic C-ash

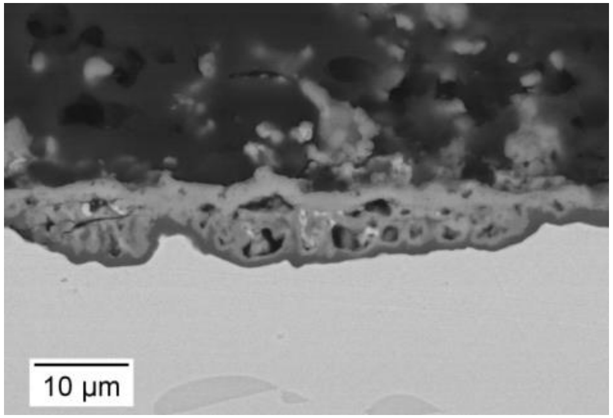

Ni-30Co-30Cr-12Al-0.1Y
CO_2-20%H_2O

C-ash with no sulfates

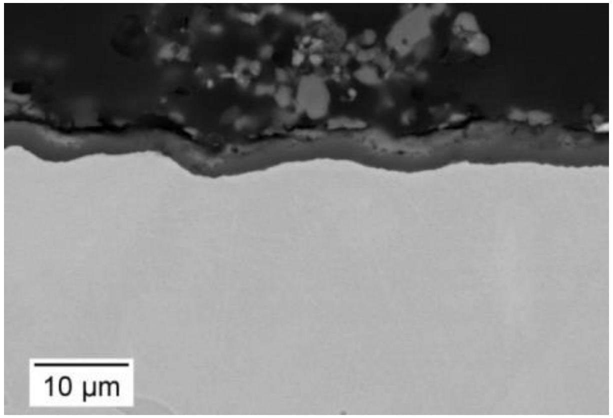

Ni-30Co-30Cr-12Al-0.1Y
dry air

Sulfates only (Na_2SO_4)

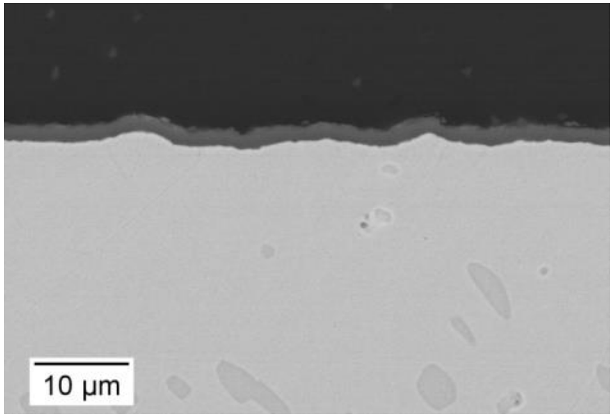

Ni-30Co-27Cr-12Al-0.1Y
dry air

Combination of sulfates and oxides is needed to cause alloy degradation.

Deposit reactivity at 1100 °C

1100 °C
CO_2-$20H_2O$-$1.6O_2$
Ni-30Co-27Cr-12Al-0.1Y

Al_2O_3-30%CaO

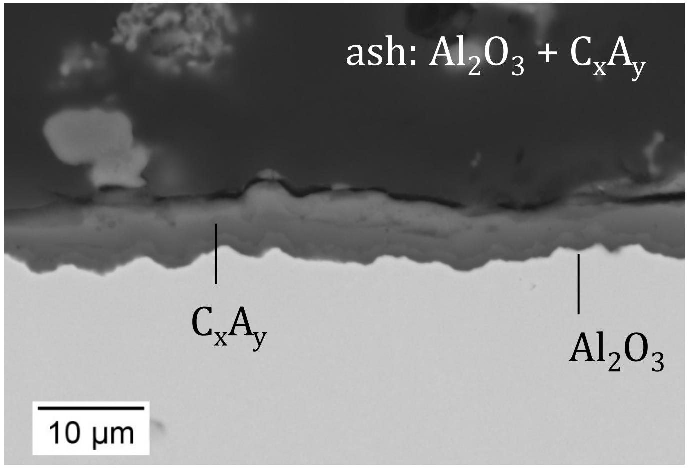

Formation of $xCaO$-yAl_2O_3 layers

Al_2O_3-30%CaO-10%SiO_2-10%Na_2SO_4

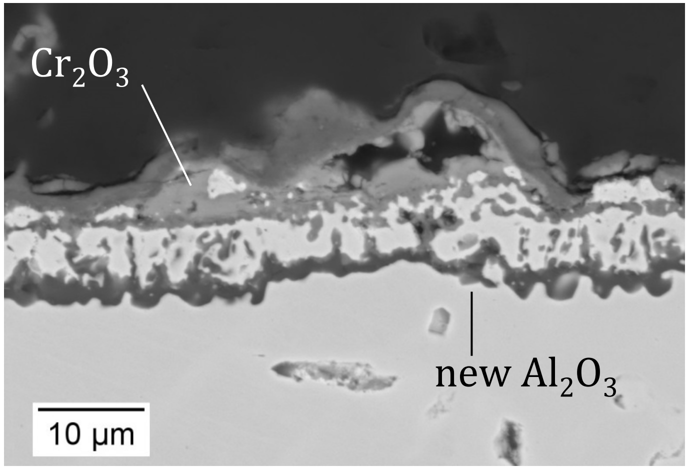

Breakaway and repassivation; similar to class C ash reaction

Acidification of Na_2SO_4 melt by SiO_2 probable cause of Al_2O_3 failure

Effect of p_{SO_3} at 1100 °C

1100 °C
Al_2O_3-CaO

CO_2-H_2O-O_2 → O_2-$0.1SO_2$

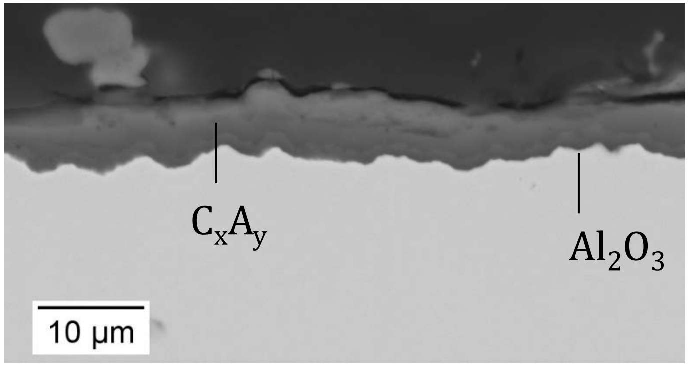

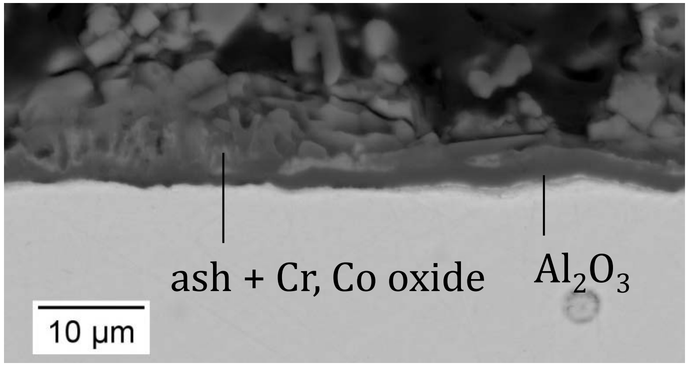

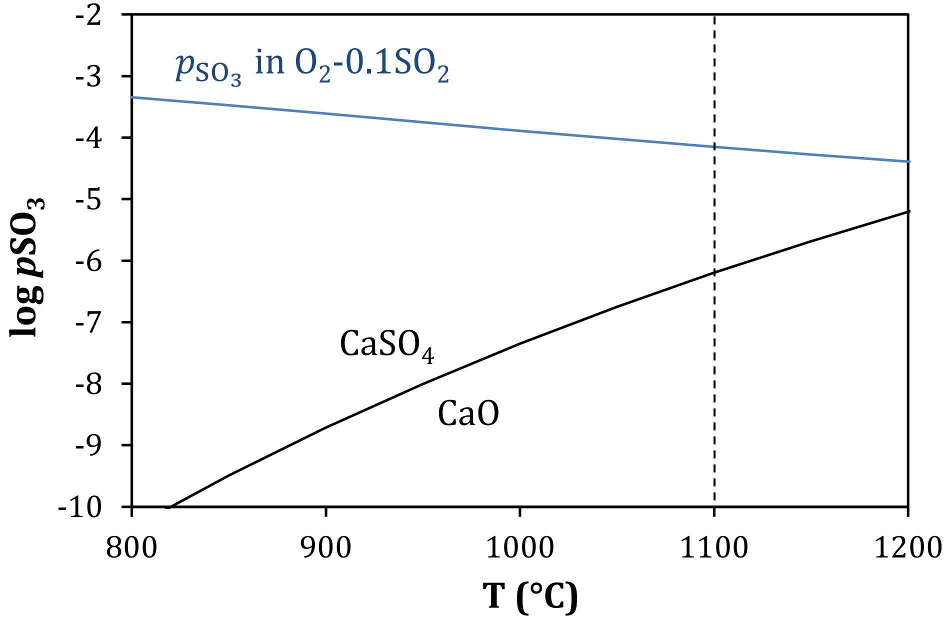

Consumption of Al_2O_3:
$xAl_2O_3 + yCaO = C_xA_y$

$CaSO_4 = CaO + SO_3$

→ CaO is not stable in O_2-$0.1SO_2$

Effect of p_{SO_3} at 1100 °C

1100 °C
Al_2O_3-CaO

CO_2-H_2O-O_2 → O_2-0.1SO_2

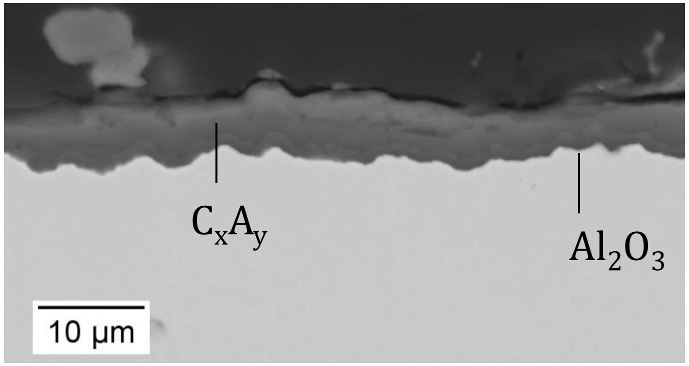

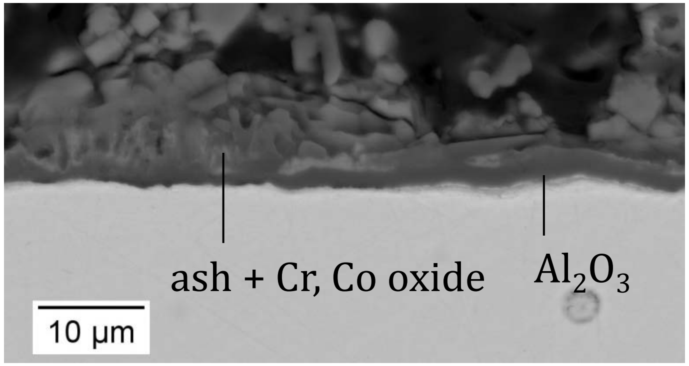

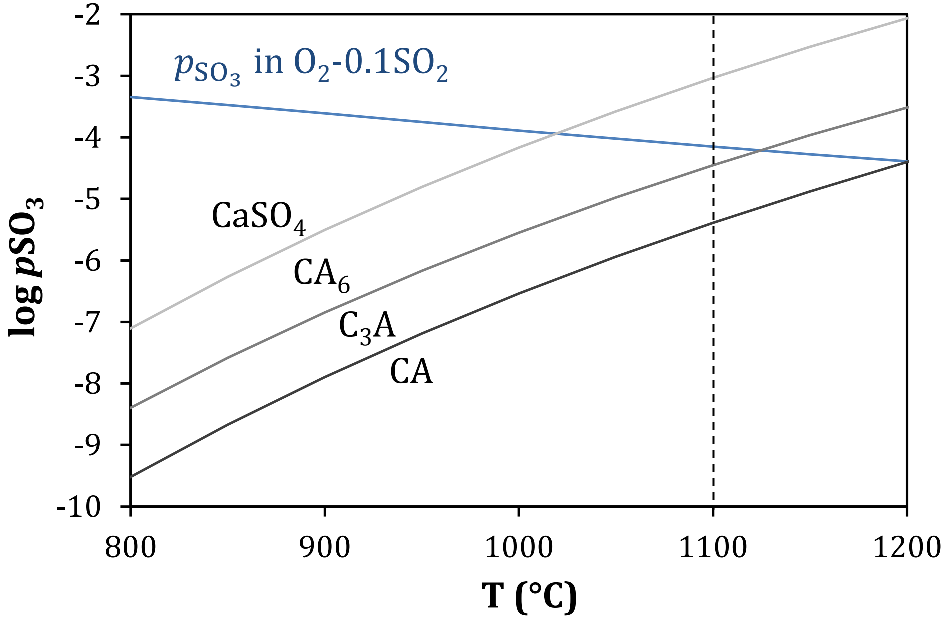

$CaSO_4 + 6Al_2O_3 = CA_6 + SO_3$

$3CaSO_4 + Al_2O_3 = C_3A + 3SO_3$

$CaSO_4 + Al_2O_3 = CA + SO_3$

→ $CaSO_4$ is more stable than the aluminates (*i.e.*, CaO is neutralized)

Effect of Temperature on CaO Reactivity

CO_2-$20H_2O$-$1.6O_2$
Al_2O_3-CaO
Ni-30Co-27Cr-12Al-0.1Y

1100 °C ⟶ 900 °C

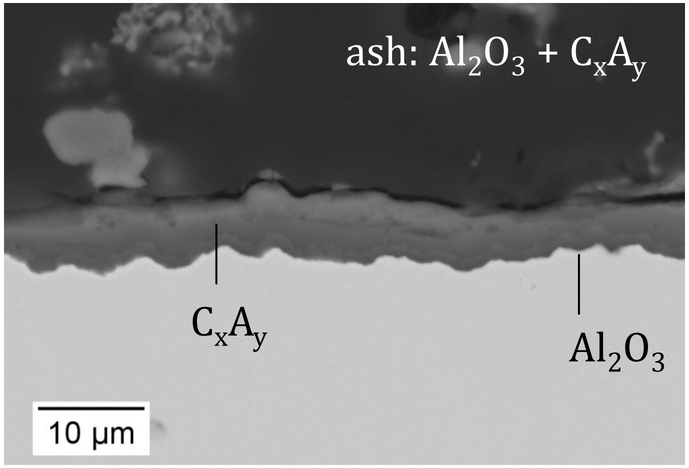

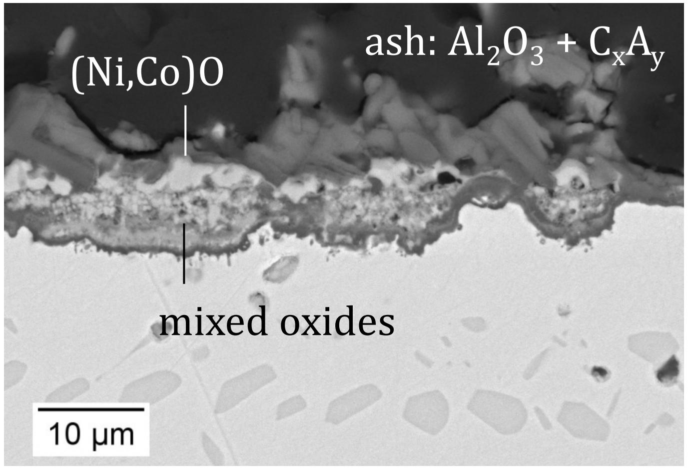

C_xA_y layers + continuous Al_2O_3
→ alloy passivated

Mixed oxides + Al_2O_3 protrusions
→ no passivation

Kinetics of Al_2O_3–CaO Reaction

Net growth rate of Al_2O_3

$$\frac{\mathrm{d}X}{\mathrm{d}t} = \frac{p}{2X} - \alpha\frac{q}{2\sqrt{qt}} \longrightarrow \left\{ \begin{array}{l} X^2 = kt \\ k = \frac{1}{2}\left[2p + \alpha^2 q - \alpha\sqrt{q(4p + \alpha^2 q)}\right] \end{array}\right.$$

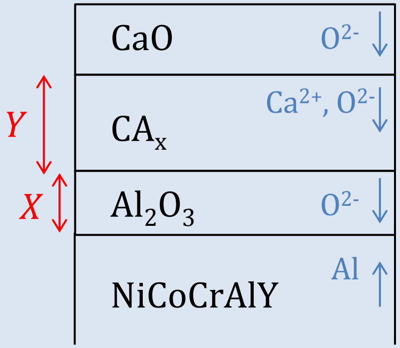

p: parabolic constant for pure oxidation, from TGA with no deposit

q: parabolic growth rate of C_xA_y, from thickness measurements

Minimum Al concentration to sustain Al_2O_3 growth (Wagner's analysis)

$$\left.\begin{array}{l} j_{\mathrm{Al}}^{\mathrm{alloy}} = \frac{N_{\mathrm{Al}}^{0} - N_{\mathrm{Al}}^{i}}{V_{\mathrm{alloy}}}\sqrt{\frac{\tilde{D}_{\mathrm{Al}}^{\mathrm{Ni}}}{\pi t}} \\ j_{\mathrm{Al}}^{\mathrm{oxide}} = \frac{1}{V_{\mathrm{oxide}}}\sqrt{\frac{k}{2t}} \end{array}\right\}$$

$$j_{\mathrm{Al}}^{\mathrm{alloy}} = j_{\mathrm{Al}}^{\mathrm{oxide}}$$

$$\longrightarrow N_{\mathrm{Al}}^{0} = \frac{2V_{alloy}}{V_{oxide}}\sqrt{\frac{\pi k}{2\tilde{D}_{\mathrm{Al}}^{\mathrm{Ni}}}}$$

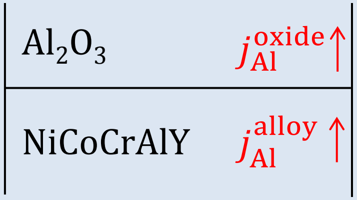

limiting case $N_{Al}^{i} = 0$

Kinetics of Al_2O_3–CaO Reaction

CO_2-H_2O-O_2
Al_2O_3-30%CaO

1100 °C → 900 °C

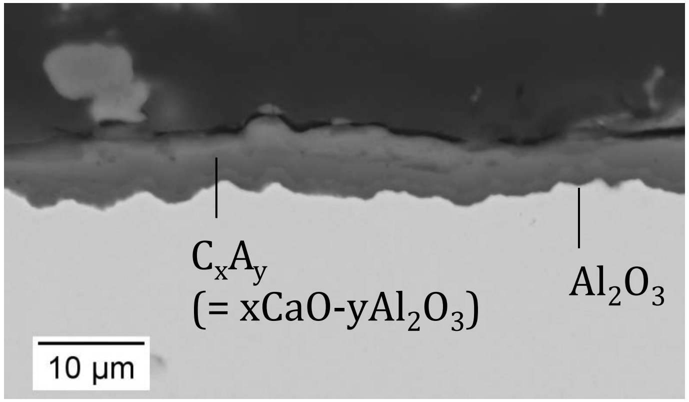

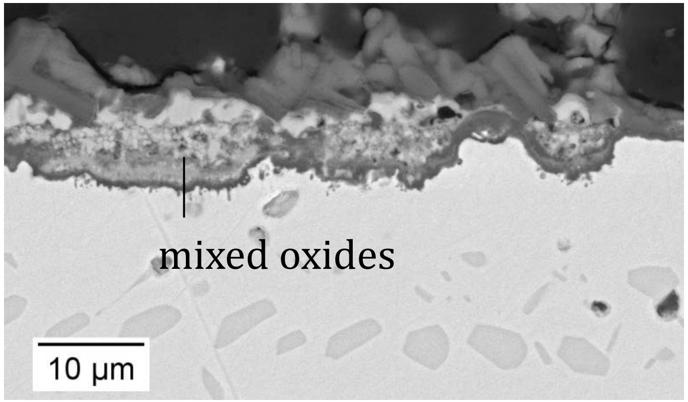

Alloy composition: Ni-30Co-27Cr-12Al-0.1Y

(at. %)	1100 °C	900 °C (extrapolated)	
	α-Al_2O_3	α-Al_2O_3	θ-Al_2O_3
min N_{Al}^0	1.4	0.3	11.1
N_{Al}^0 in γ	9.9	6.3	

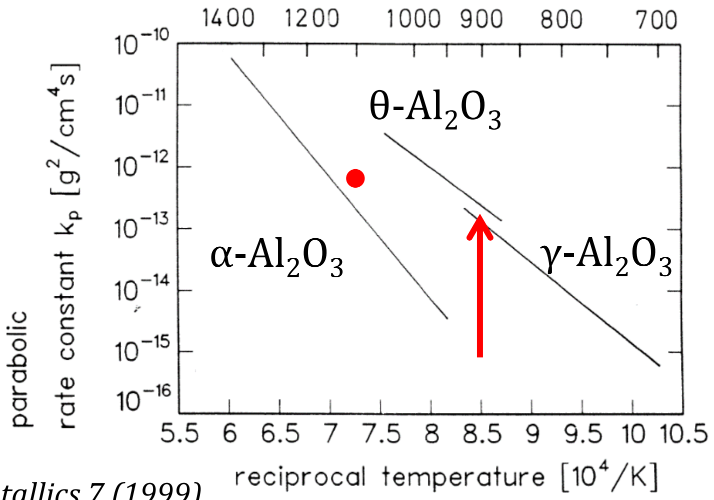

graph adapted from H.J. Grabke, Intermetallics 7 (1999)

Deposit Reactivity at 900 °C

900 °C
O_2-0.1SO_2
Ni-30Co-27Cr-12Al-0.1Y

Al_2O_3-30%CaO

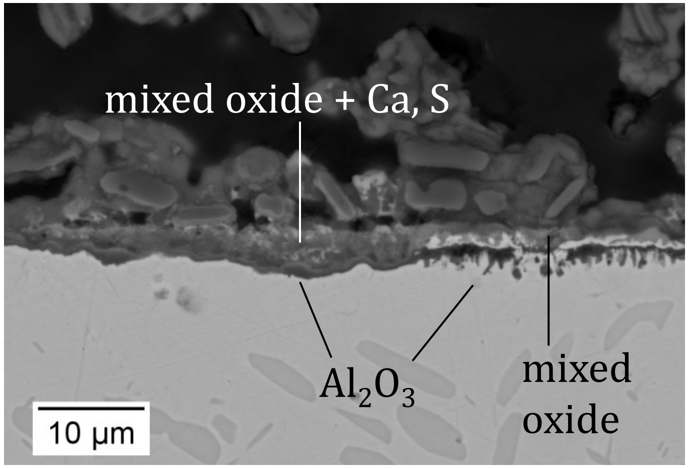

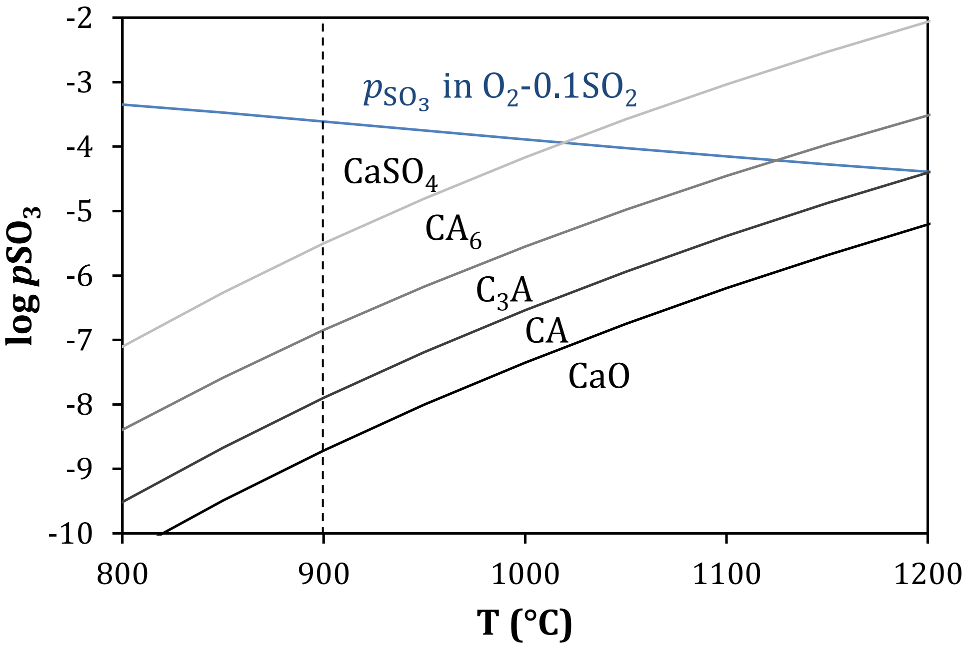

$CaSO_4$ is more stable than all aluminates
→ Al_2O_3 consumed via different reaction path (sulfate-induced but solid-state)
Calcium sulfo-aluminate involved ?

Summary and Conclusions

- Reaction with CaO at 1100 °C
  - transient stage: formation of liquid Ca-Cr-O causes significant alloy degradation; extent of attack reduced with increasing β fraction;
  - steady-state: consumption of Al_2O_3 sustains high Al depletion rate.

- Reaction with oxide-sulfate mixtures at 1100 °C
  - presence of SiO_2 or SO_3 (g) favor formation of very stable $CaSiO_3$ or $CaSO_4$, which effectively neutralizes CaO;
  - mixtures associating Na_2SO_4 with high levels of SiO_2 and CaO (like class C fly ash) cause breakaway oxidation; extent of attack reduced with increasing β fraction.

- Reaction with oxide-sulfate mixtures at 900 °C
  - Both CaO (S-free gas) and $CaSO_4$ (S-containing gas) cause significant alloy degradation, although via different routes;
  - $CaSO_4$-induced attack resembles Na_2SO_4-induced attack (hot corrosion).

Summary and conclusions

- Different modes of degradation may involve conflicting alloy requirements; compromise is needed depending on application of interest;
- It is critical to fine tune the amount of reactive elements like Y.

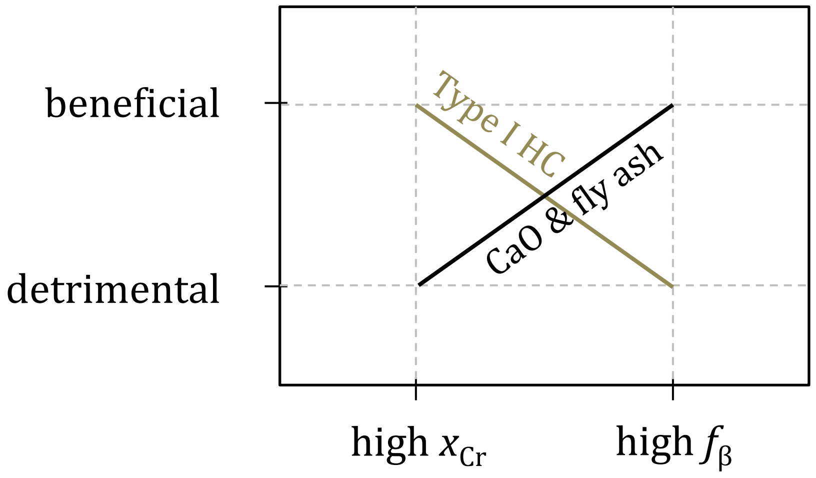

Thank you for your attention

Additional slides (bondcoat work)

Effect of Y content

1100 °C, 50 h
Ni-19Co-15Cr-24Al

0.3Y version

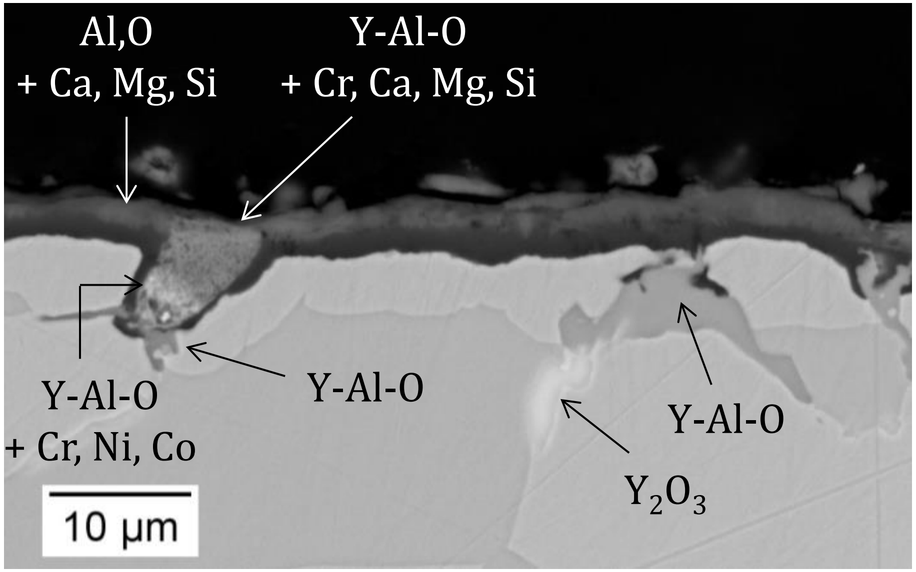

Yttrium-rich pegs are involved in severe alloy attack.

Situation similar to type II hot corrosion*.

**M. Task, PhD thesis, University of Pittsburgh (2012)*

Corrosion testing

CaO deposit in lab air, 50h, 1100 °C

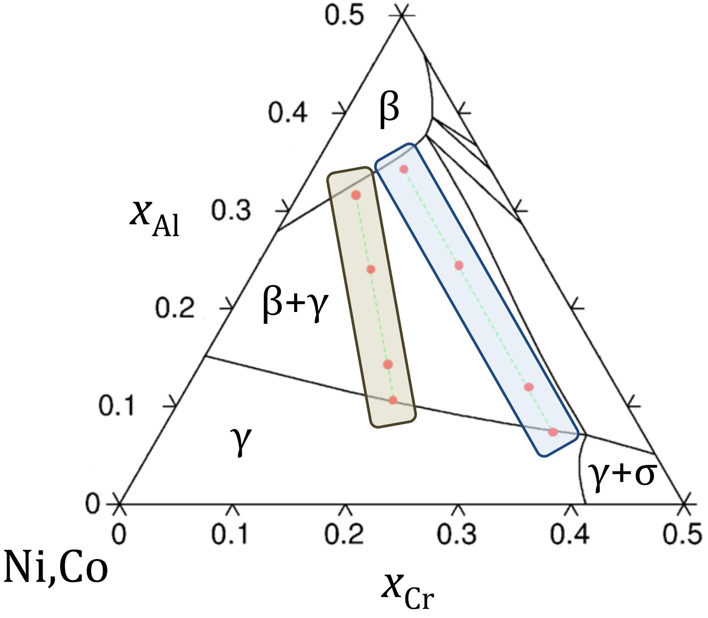

Better resistance with
- low x_{Cr}
- high f_{β}

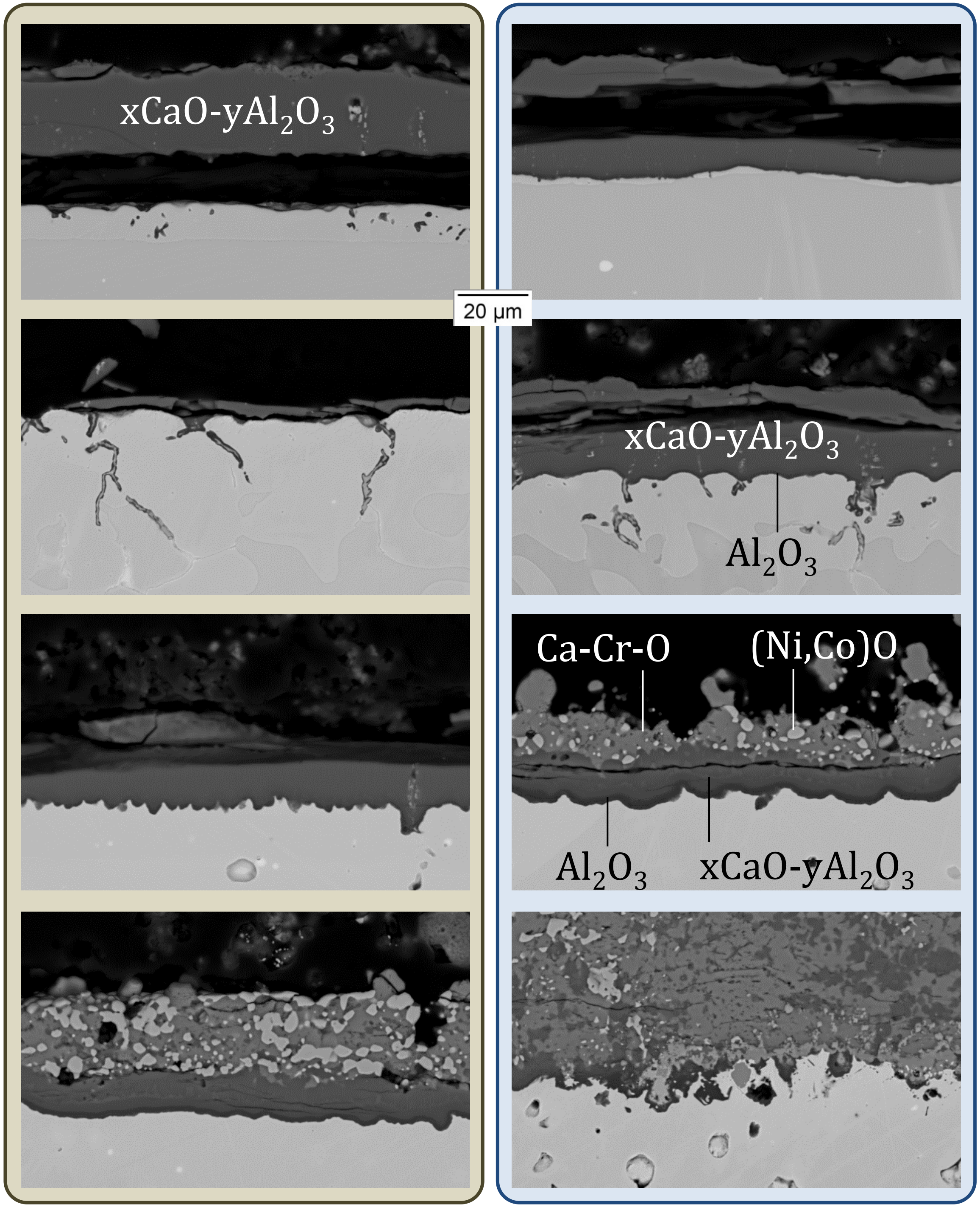

Corrosion testing

type I hot corrosion: Na_2SO_4, O_2-1000 ppm SO_2, 20 h
900 °C

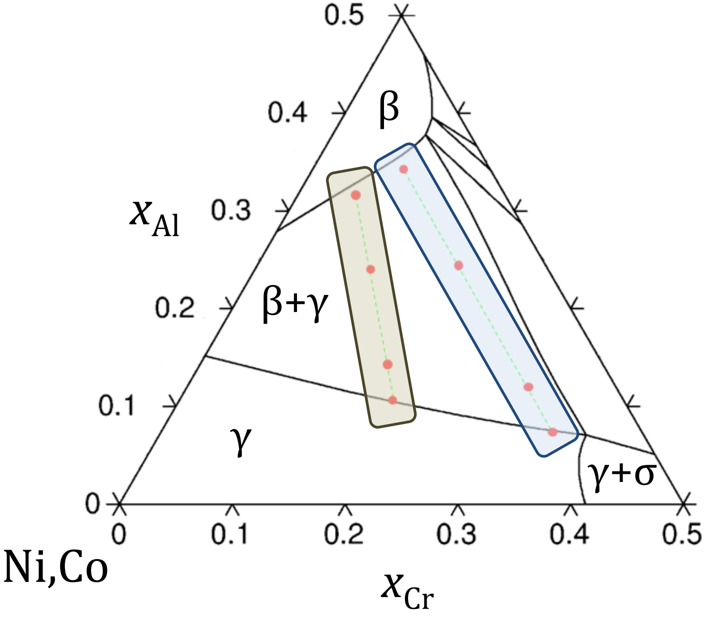

Better resistance with
- high x_{Cr}
- low f_β

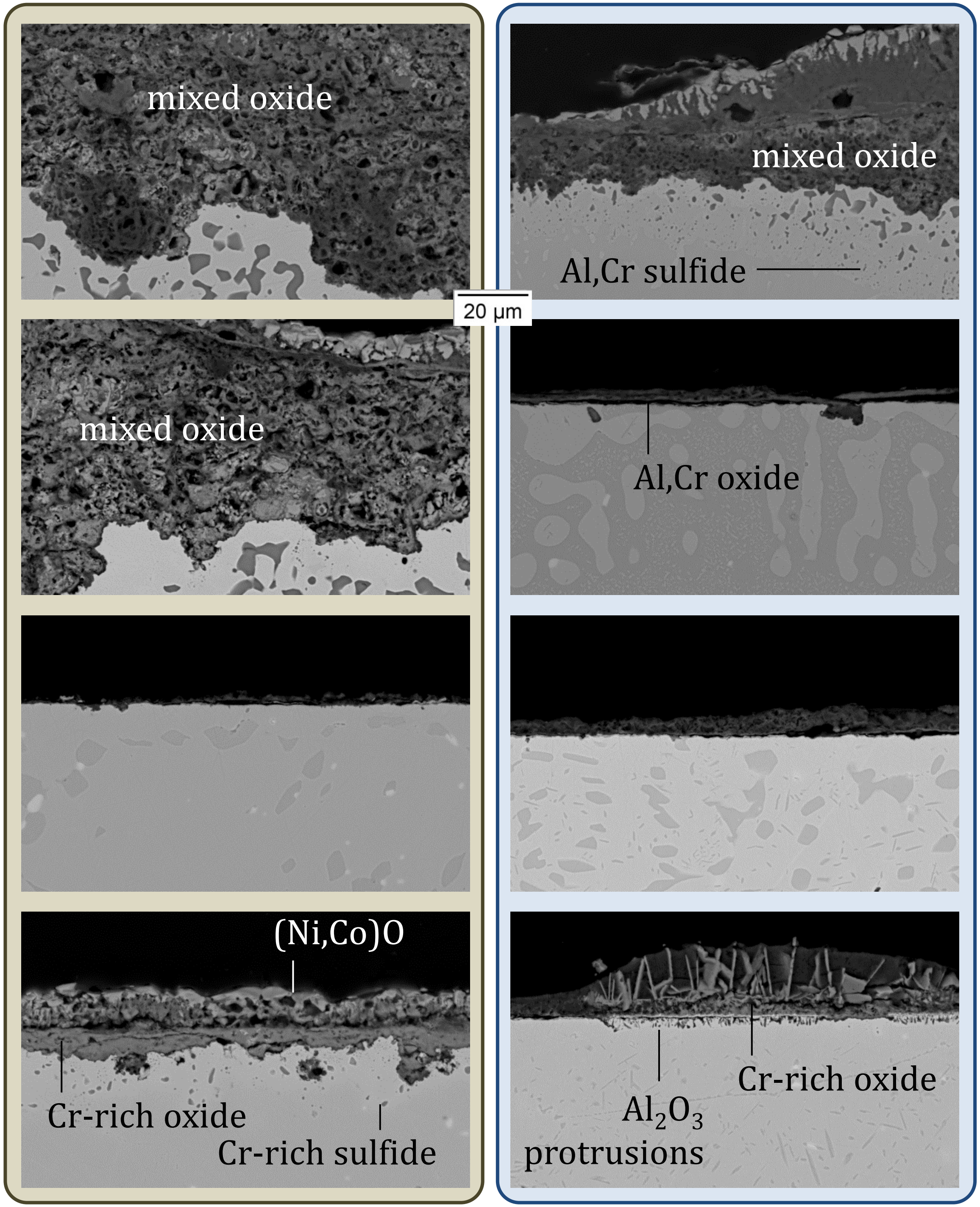

Moving forward:

- Study of alloy and thermally grown Al_2O_3 reaction with sulfates; relation with type I hot corrosion.
- Use of computational thermodynamics to design alloys which allow systematic investigation of effect of phase fraction vs phase composition; application to various types of degradation. Examples included here: CaO corrosion at 1100 °C, Na_2SO_4 corrosion at 900 °C (type I hot corrosion)

Deposit Reactivity at 900 °C

900 °C
O_2-0.1SO_2
Ni-30Co-27Cr-12Al-0.1Y

Al_2O_3-CaO

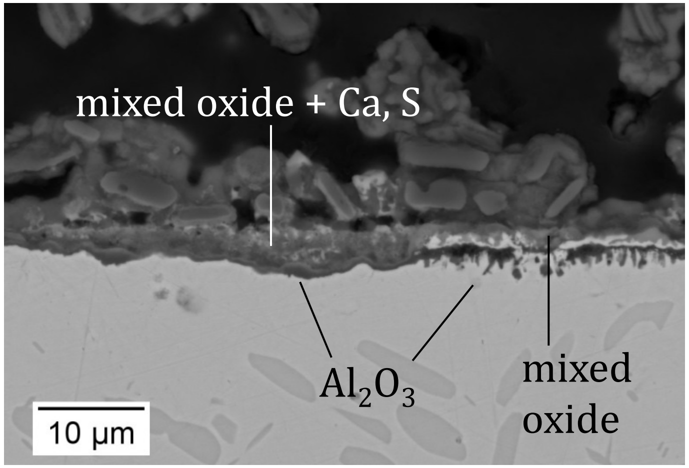

Al_2O_3-CaO-SiO_2-Na_2SO_4

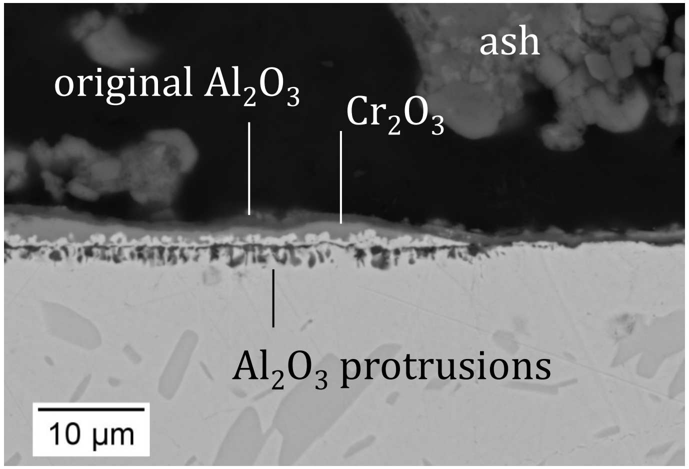

Local Al_2O_3 failure due to reaction with $CaSO_4$ or Na_2SO_4

CMAS Failure

Common Modes of TBC Failure

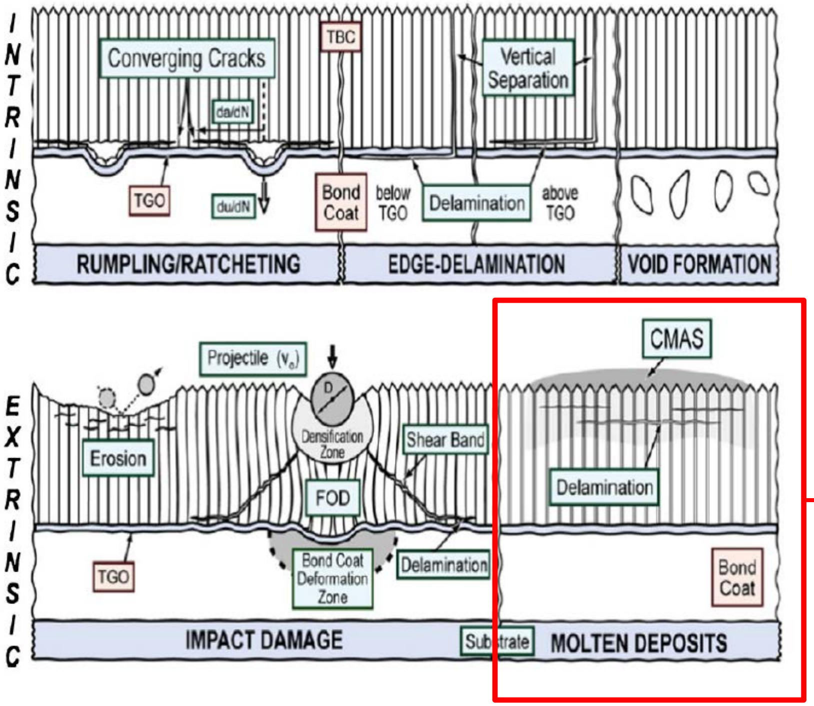

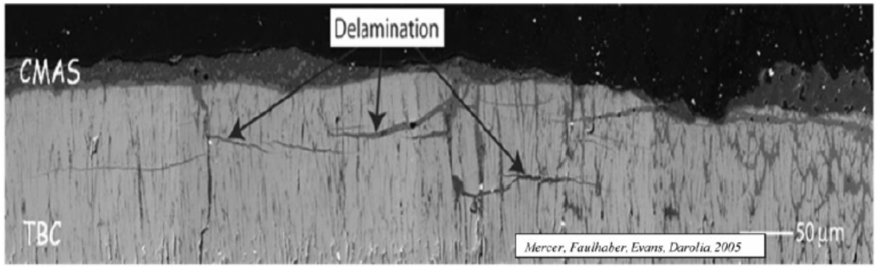

<u>Calcium Magnesium Alumino Silicate (CMAS):</u>

- Deposits contain CaO-MgO-Al_2O_3-SiO_2
- Melting at high temperatures ≥1250°C
- Molten deposit infiltrates top coat
- Thermo-chemical interactions with YSZ
- Thermo-mechanical interactions

A. G. Evans, D. R. Clarke and C. G. Levi: J. Eur. Ceram. Soci., 2008, 28, (7), 1405–1419.

CMAS

Thermo-Chemical Effects

Dissolution of YSZ into CMAS melt

Re-precipitation of ZrO_2 with different microstructure and composition

YSZ+CMAS, 1300°C, 4h

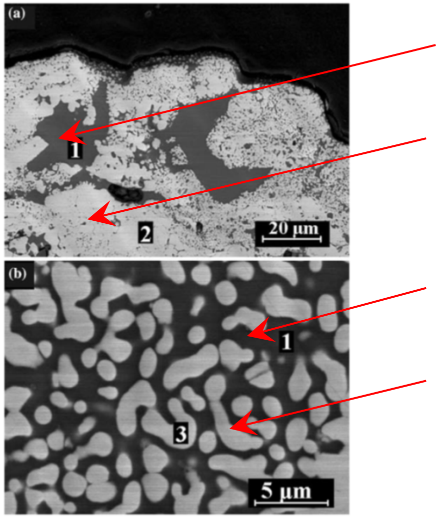

CMAS

Unaffected YSZ

CMAS

Reprecipitated ZrO_2 grains

Thermo-Mechanical Effects

Surface above melting point of CMAS

Cooling: delamination of TBC in infiltrated regions as a result of ΔE and ΔCTE

YSZ+CMAS, 1300°C, 4h

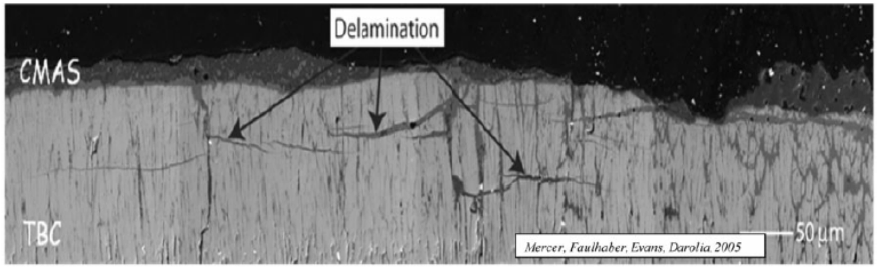

P. Mohan, T. Patterson, B. Yao, Y. Sohn, J. Thermal Spray Tech., 19(1-2) pp. 156-167, 2010

C. Mercer, S. Faulhaber, A. G. Evans and R. Darolia, *Acta Materialia,* vol. 53, pp. 1029-1039, 2005

Kinetics of Al_2O_3 formation-destruction

Reaction

Transport

Kinetics

$CaO = Ca^{2+} + O^{2-}$

$xCa^{2+} + xO^{2-} + yAl_2O_3 = C_xA_y$

$2Al^{3+} + 3O^{2-} = Al_2O_3$

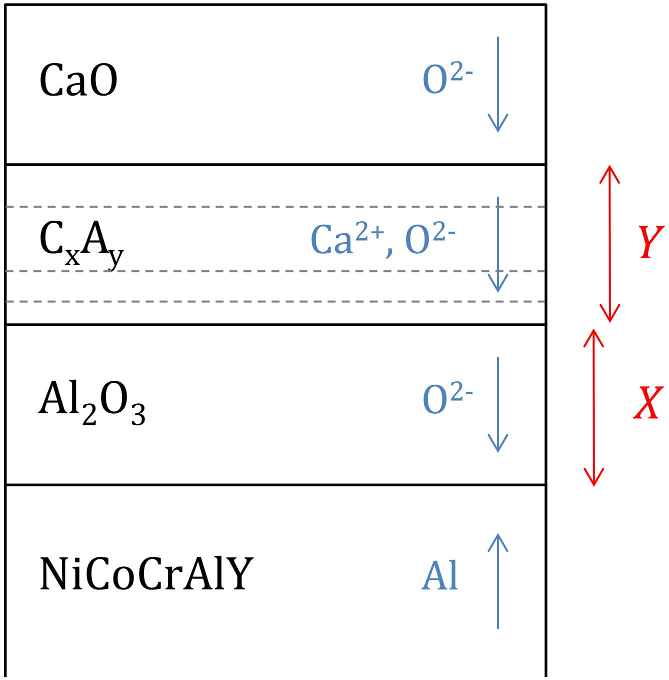

C_xA_y growth = Al_2O_3 destruction

$$\frac{\mathrm{d}Y}{\mathrm{d}t} = \frac{q}{2Y} \quad = -\frac{V_{C_xA_y}}{yV_{Al_2O_3}}\frac{(\mathrm{d}X)_\mathrm{d}}{\mathrm{d}t}$$

Al_2O_3 formation

$$\frac{(\mathrm{d}X)_\mathrm{f}}{\mathrm{d}t} = \frac{p}{2X}$$

→ Al_2O_3 net growth: $$\frac{\mathrm{d}X}{\mathrm{d}t} = \frac{(\mathrm{d}X)_\mathrm{f}}{\mathrm{d}t} + \frac{(\mathrm{d}X)_\mathrm{d}}{\mathrm{d}t} = \frac{p}{2X} - \alpha\frac{q}{2Y}$$

$$\left.\begin{array}{c}\dfrac{\mathrm{d}Y}{\mathrm{d}t} = \dfrac{q}{2Y} \\ \text{Y(0) neglected}\end{array}\right\} \quad Y^2 = qt$$

i.e. $$\left\{\begin{array}{l}\dfrac{\mathrm{d}X}{\mathrm{d}t} = \dfrac{p}{2X} - \alpha\dfrac{q}{2\sqrt{qt}} \\ \alpha = \dfrac{yV_{Al_2O_3}}{V_{C_xA_y}}\end{array}\right.$$

Alloy compositions

NiCoCrAl system, at. %
$x_{Co} = 0.3$
T = 1100 °C

ThermoCalc
NIST superalloy (2000) database
X. Liu, Penn State University

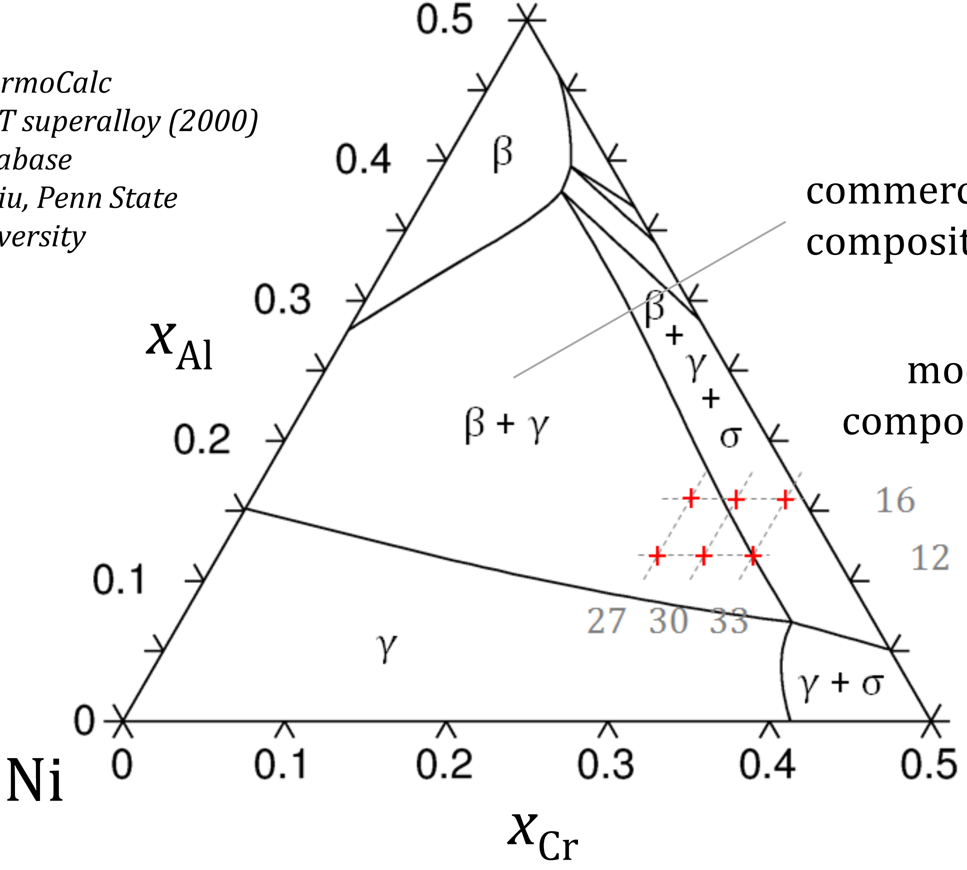

Samples: bulk, cast alloys

at. %, balance = Ni

	Co	Cr	Al	Y	f_β (%)
commercial composition	19	15	24	0.3	65
	19	15	24	0.1	
model compositions	30	33	16	0.1	42
	30	30	16	0.1	40
	30	27	16	0.1	34
	30	33	12	0.1	18
	30	30	12	0.1	16
	30	27	12	0.1	13

Testing at 1100 °C

Appendix

Low magnification micrographs

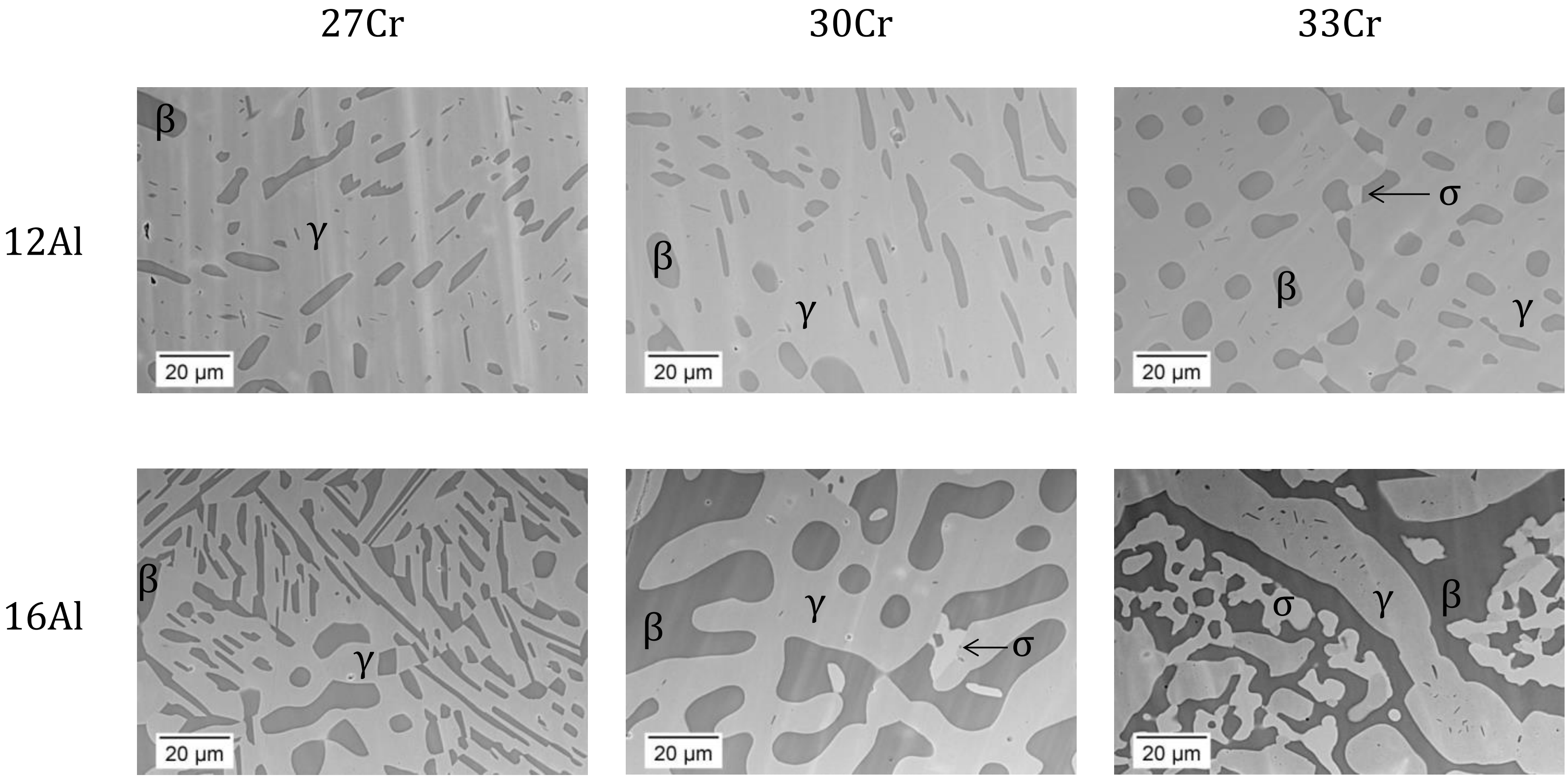

Appendix

Phase volume fractions

Determined by image analysis from SEM micrographs (cross-section)

#	γ	β	σ
3	87	13	
4	84	16	
5	81	18	1.0
6	66	34	
7	59	40	1.6
8	36	42	22

Phase compositions

Determined by SEM-EDS
at. %, balance = Ni

	γ			β			σ		
#	Co	Cr	Al	Co	Cr	Al	Co	Cr	Al
3	32	29	10	17	10	33			
4	32	33	8.5	18	11	32			
5	32	37	8.2	19	14	33	28	58	3.3
6	34	35	8.4	21	12	33			
7	35	37	7.8	22	14	32	30	57	3.3
8	37	37	7.6	23	14	32	31	57	3.3

Oxidation (no deposit)

Weight changes

1100 °C, 50 h

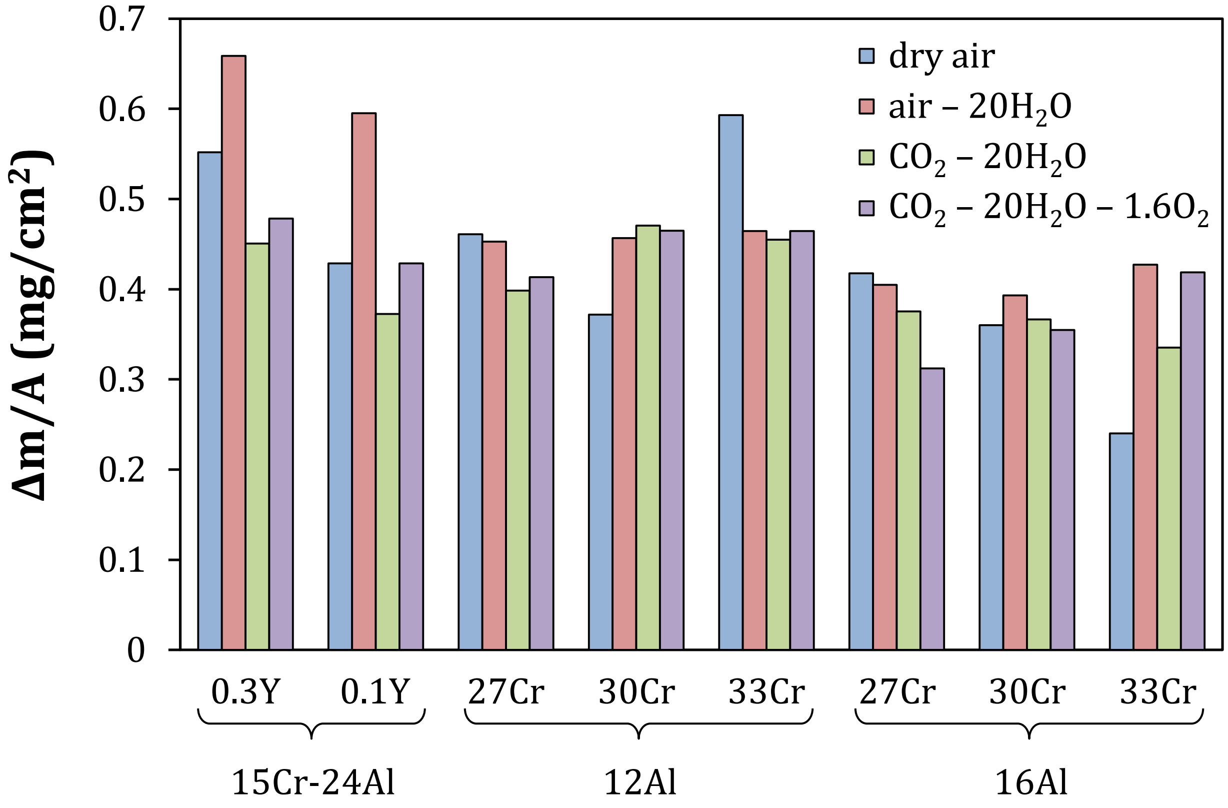

Δm/A (t = 10 h, 50 h)

→ $k_p \sim 8 \times 10^{-13}$ $g^2cm^{-4}s^{-1}$

typical of α-Al_2O_3 at 1100 °C

All alloys form Al_2O_3 in all atmospheres

Oxidation (no deposit)

1100 °C, 50 h

Scale thickness (µm)

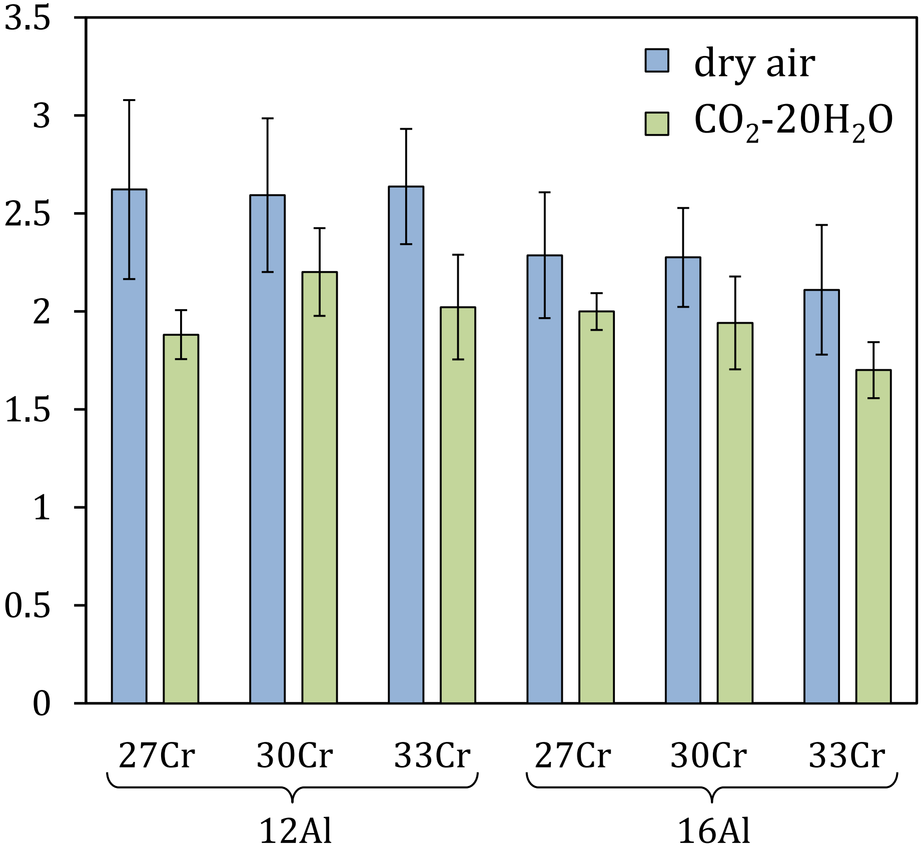

Weight gain (mg/cm^2)

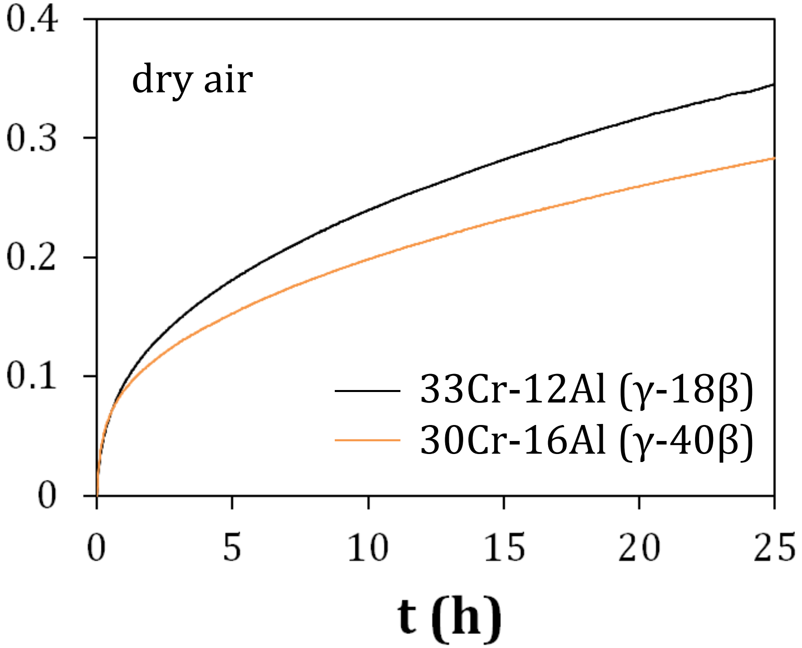

- Thinner Al_2O_3 scales in CO_2-H_2O
- In air, less transient oxidation with higher β fraction

Oxidation (no deposit)

1100 °C, 50 h

dry air

CO_2-20H_2O

27Cr-12Al
(γ-13β)

33Cr-12Al
(γ-18β)

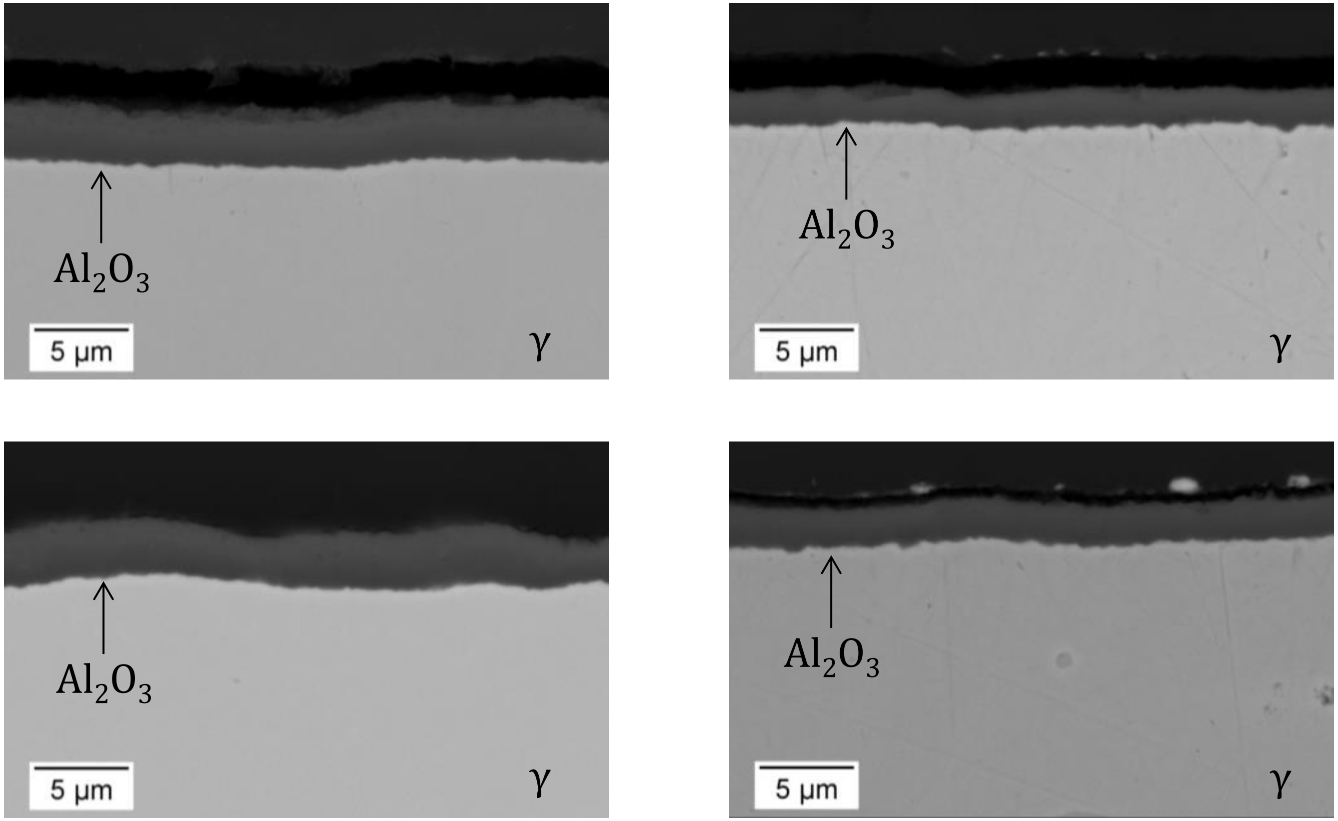

All alloys form Al_2O_3 in all atmospheres
(high Cr and Al contents, Al_2O_3 does not form volatile compound, good barrier to carbon)

Thinner scales in CO_2-H_2O than in air.

Experimental protocol

Ni-30Co-30Cr-12Al-0.1Y
1100 °C, 50 h
CO_2-H_2O

Class C ash (wt. %)

SiO_2	Al_2O_3	CaO	Fe_2O_3	MgO	Na_2SO_4	K_2SO_4
26	20	33	6	8	5	1

Commercial ash

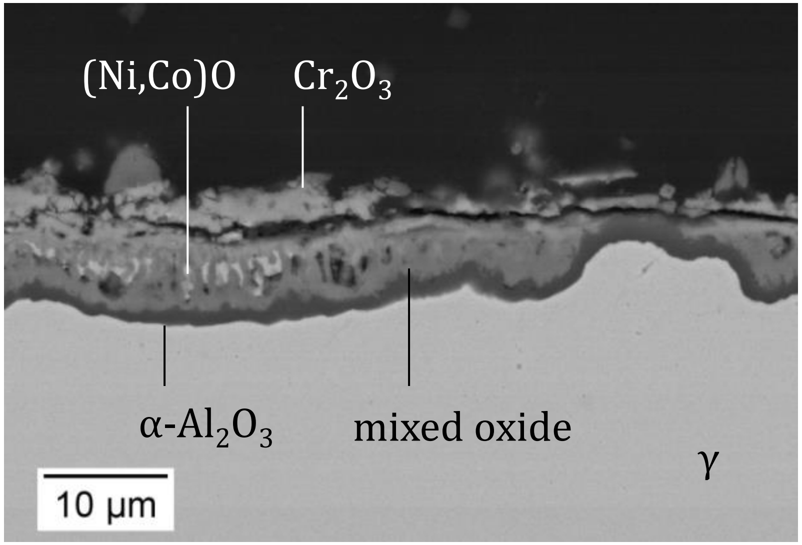

Synthetic mixture

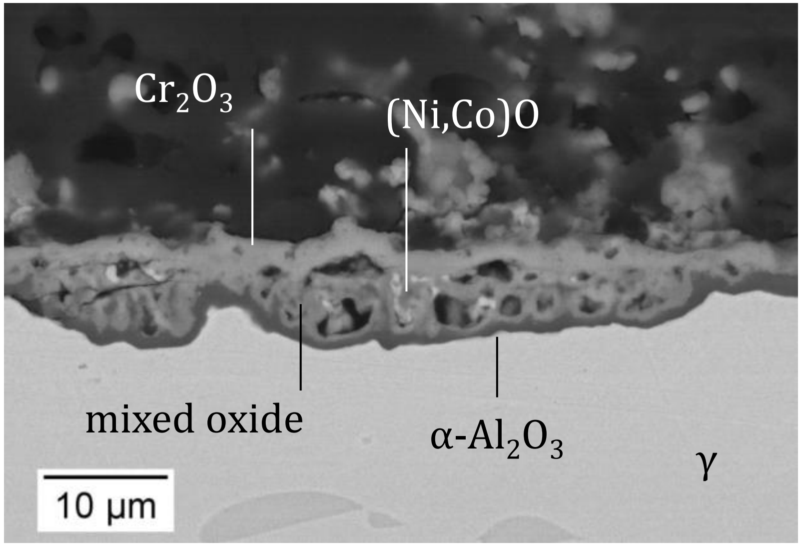

Complex reaction morphology induced by reaction with commercial fly ash is reproduced using a synthetic mixture
→ ability to test various deposit compositions

Exposure to C-ash in CO_2-H_2O

33Cr-12Al (γ-**18β**)

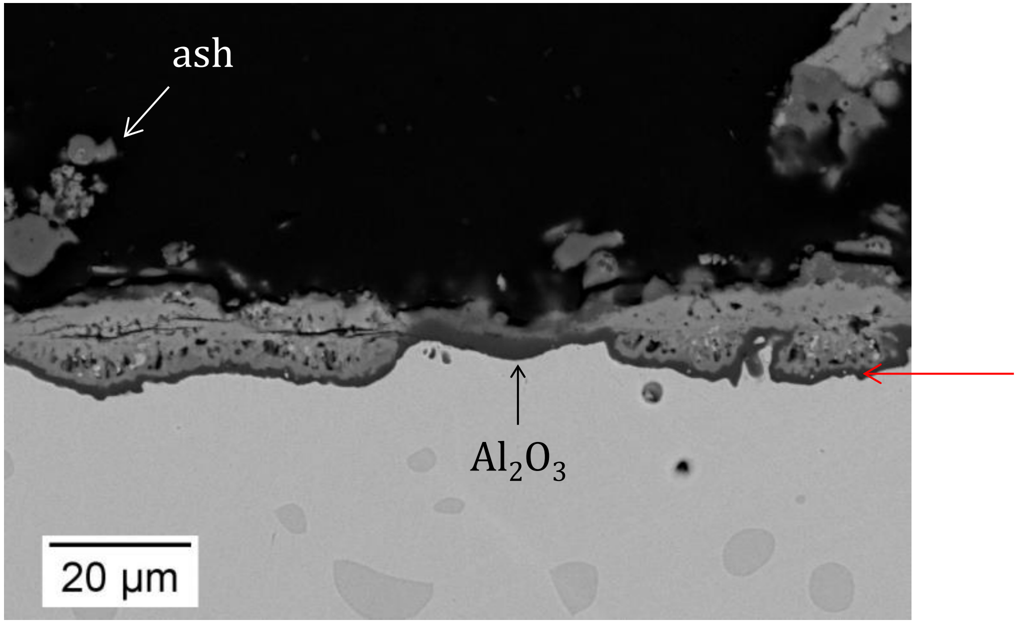

Photo-stimulated luminescence spectroscopy

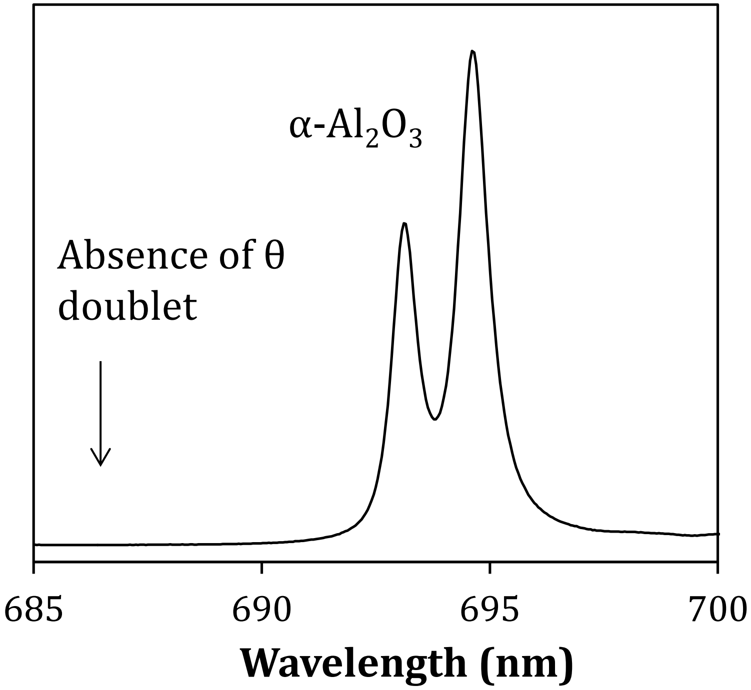

Non-uniform degradation.

Locally thick reaction product, contains large amounts of alloy constituents.

Effect of gas composition

1100 °C

Ni-30Co-27Cr-12Al-0.1Y

Class C ash

1 h exposures

No particular effect of CO_2, H_2O or low p_{O_2}

Nitridation due to N_2 in air

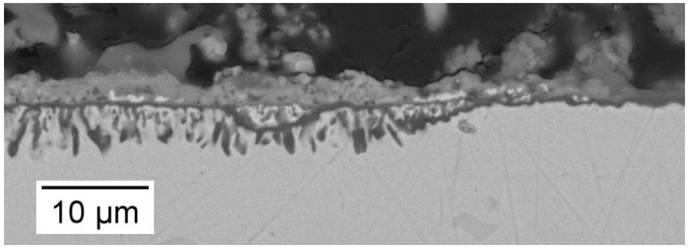

CO_2-20H_2O (eq. pO_2 40 ppm)

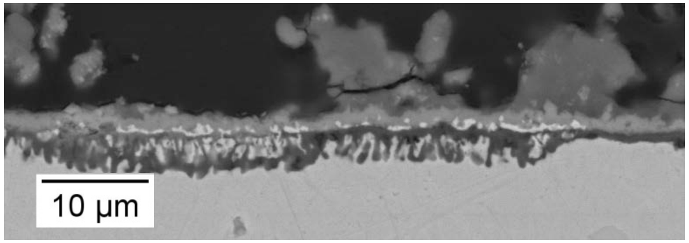

CO_2-20H_2O-1.6O_2

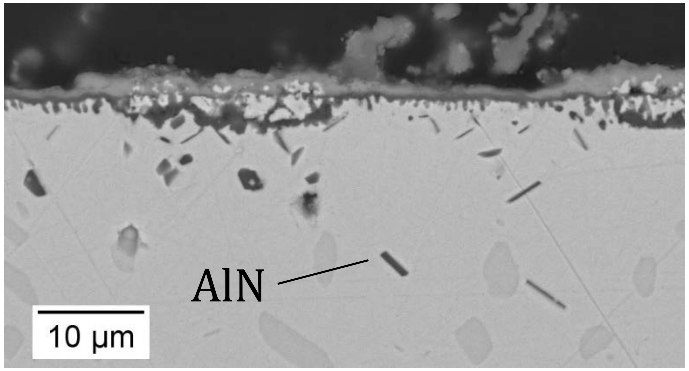

N_2-21O_2

CO_2-H_2O, no deposit, 50 h

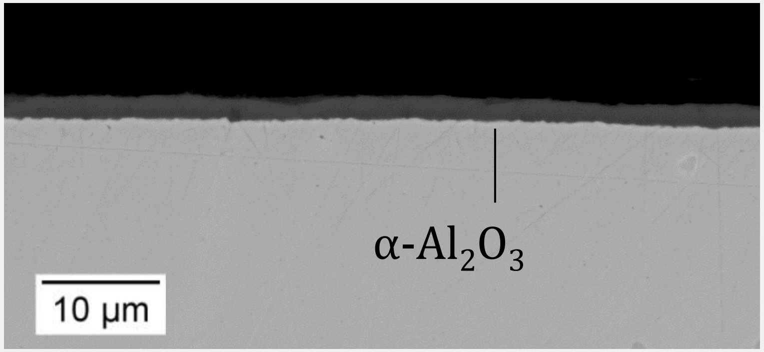

Absent a deposit, all alloys studied formed external Al_2O_3 scales in all atmospheres

Exposure to CaO in dry air

Ni-19Co-16Cr-23Al-0.1Y
(γ-65β)

1100 °C, 50 h

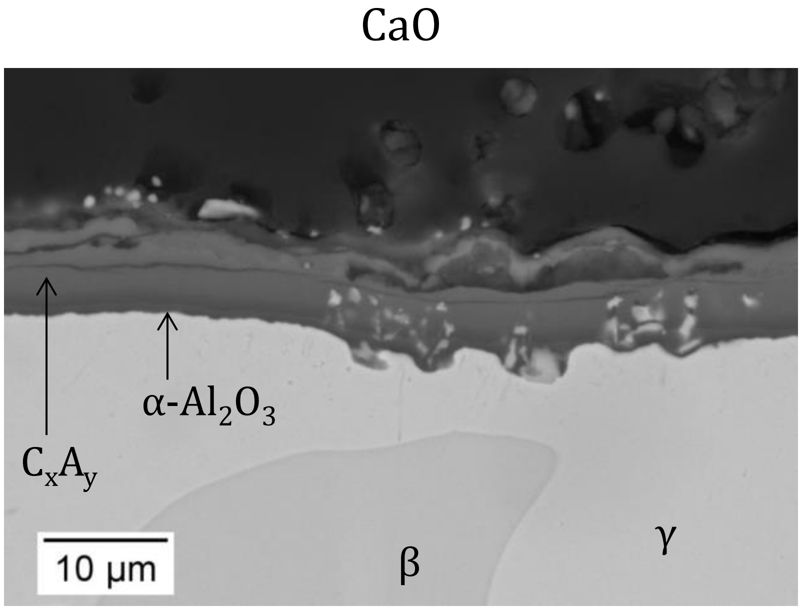

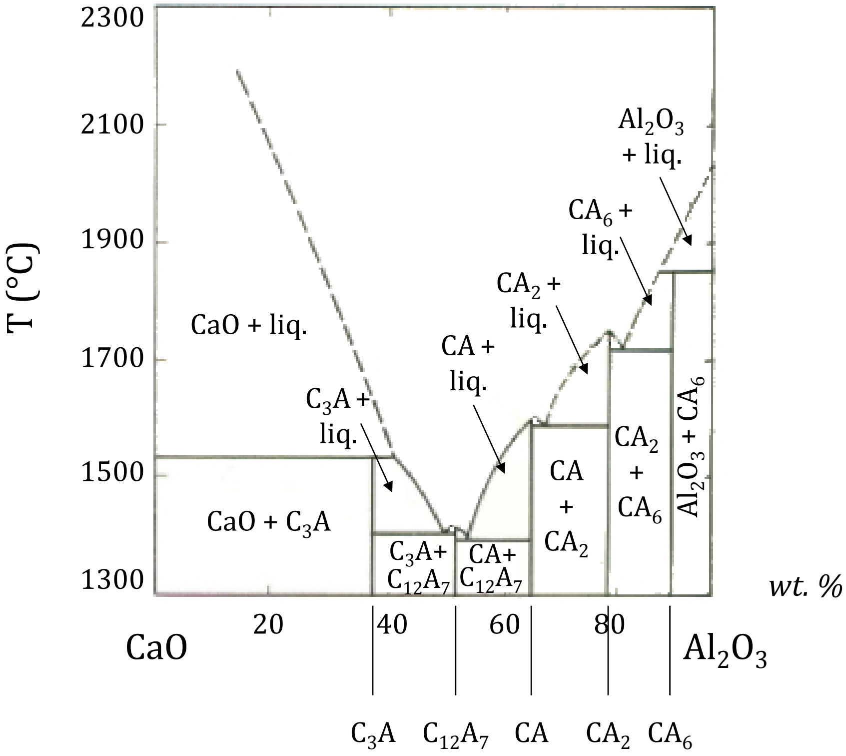

from Phase diagrams for ceramists, vol. 1, Levin et al, eds (1964)

Interaction deposited oxide-TGO with consumption of Al_2O_3, but no significant loss of alloy constituents.

Exposure to CaO in dry air

Ni-30Co-33Cr-12Al-0.1Y
(γ-18β)

1100 °C

5 h

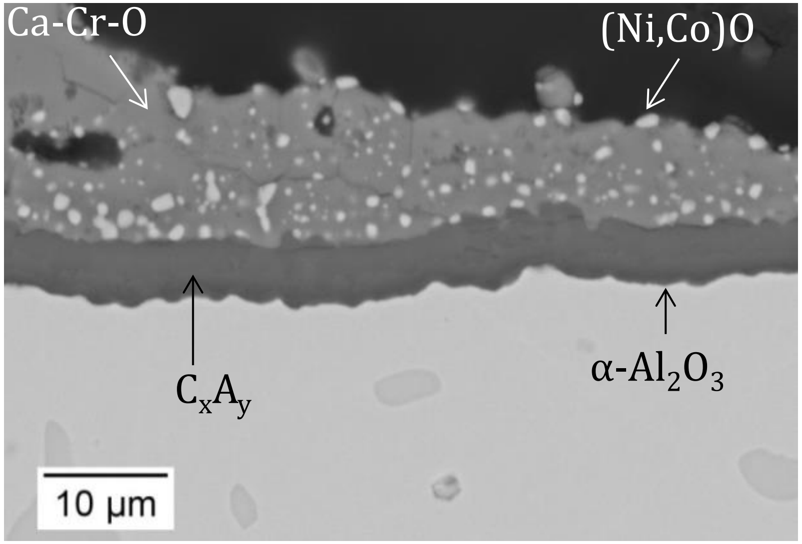

50 h

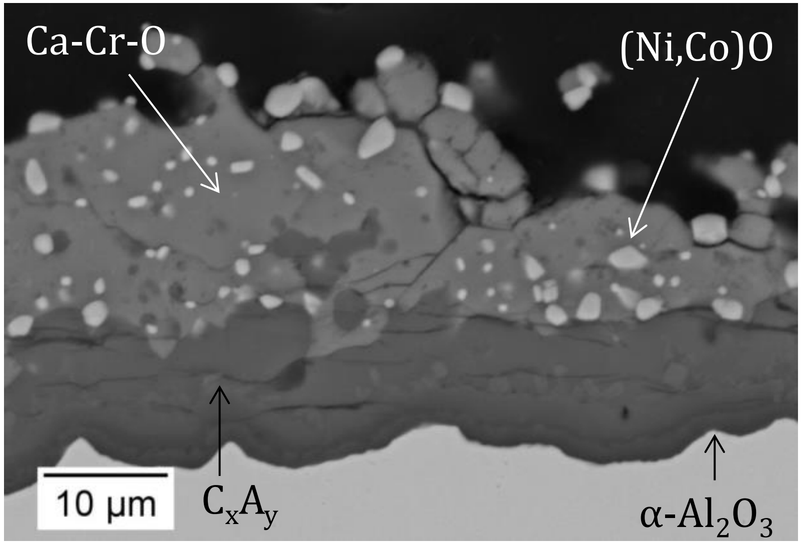

t < 5 h thick top layer, α-Al_2O_3 established

5 < t < 50 h only xCaO-yAl_2O_3 layers grow

→ top layer formation is rapid, then stops (i.e., transient)

Exposure to CaO in dry air

Ni-30Co-33Cr-12Al-0.1Y
(γ-18β)

1100 °C

10 h preoxidation, 40 h CaO

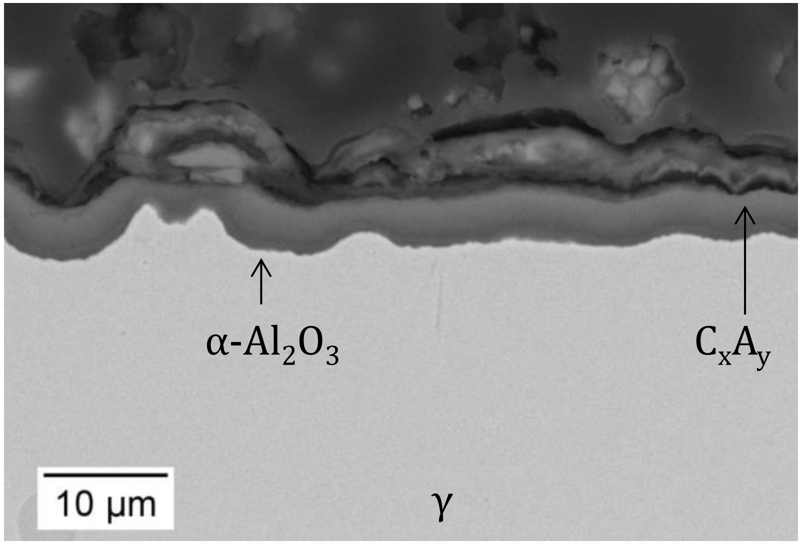

no preoxidation, 50 h CaO

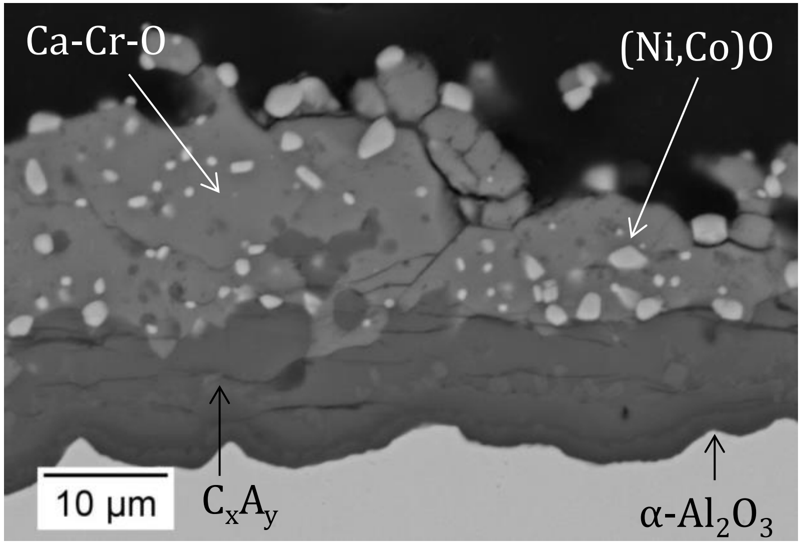

Preoxidation prevents rapid transient attack

Exposure to CaO in dry air

5h, 1100 °C

Ni-30Co-33Cr-12Al-0.1Y
(γ-18β)

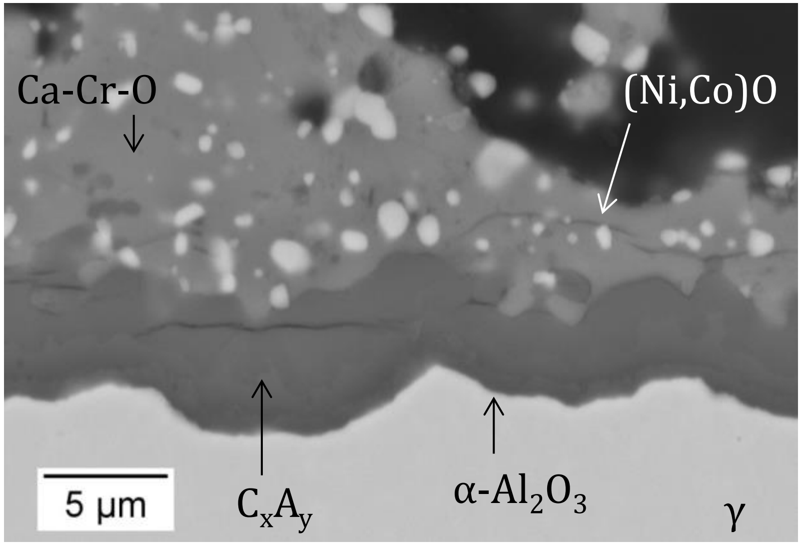

Ni-19Co-16Cr-23Al-0.1Y
(γ-65β)

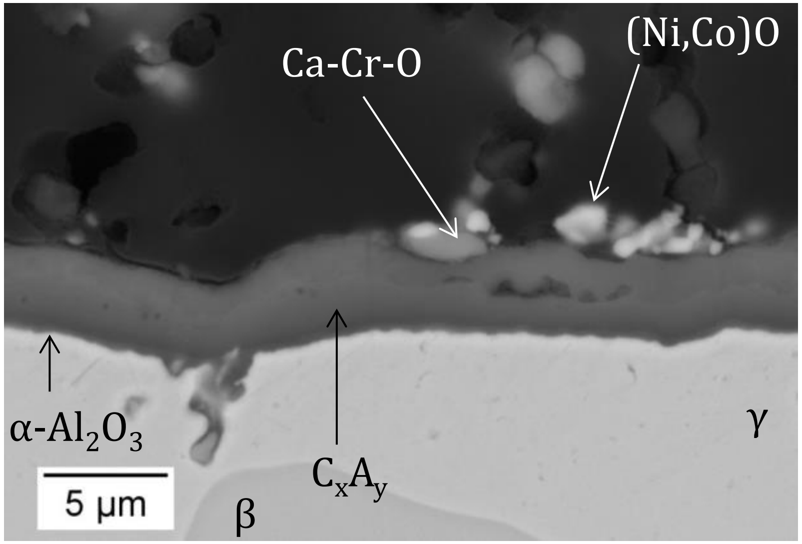

Large β fraction
→ same mechanism occurs to a lower extent (alloy degradation is more rapidly undercut by Al_2O_3).

Ash-induced degradation: reaction mechanism

Case of dry air

Evolution of the reaction morphology with reaction time

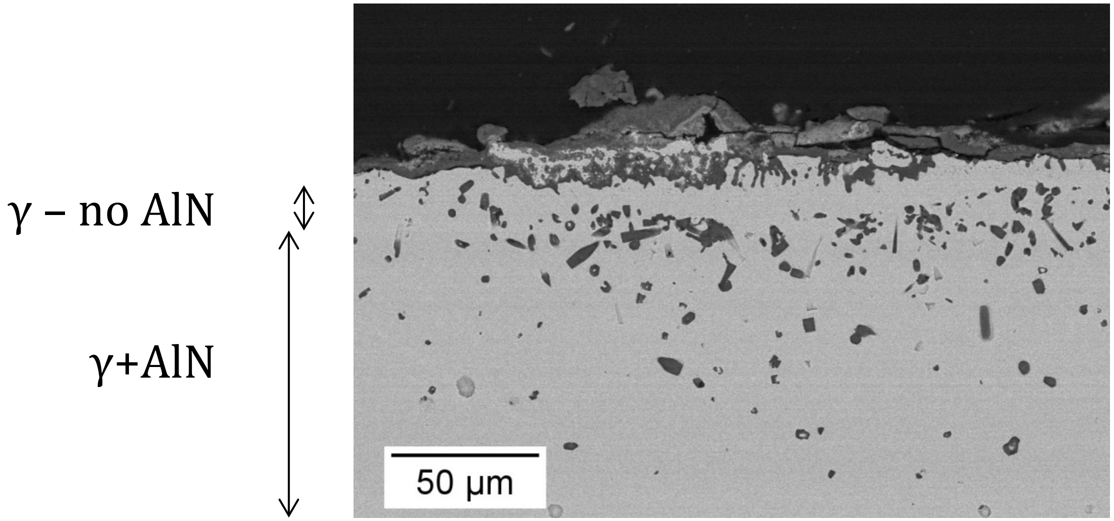

1 h

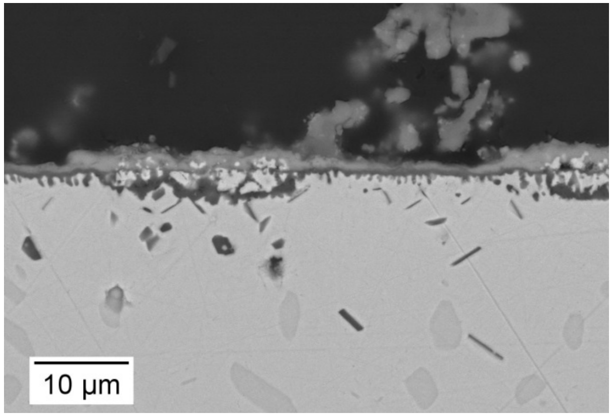

50 h

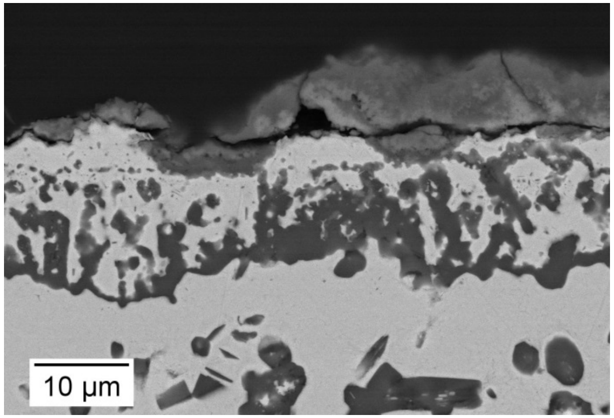

250 h

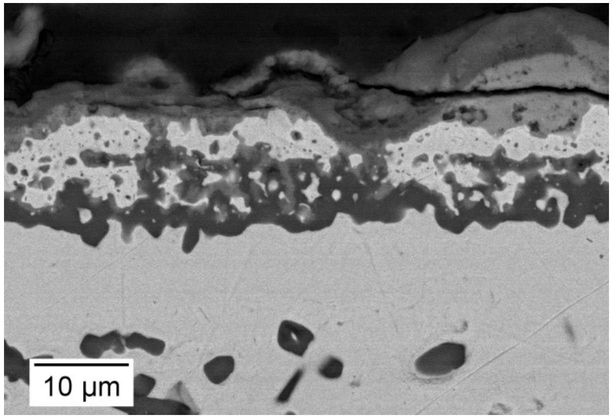

Deposit reactivity at 1100 °C

1100 °C
CO_2-H_2O-O_2
Ni-30Co-27Cr-12Al-0.1Y

Al_2O_3-CaO

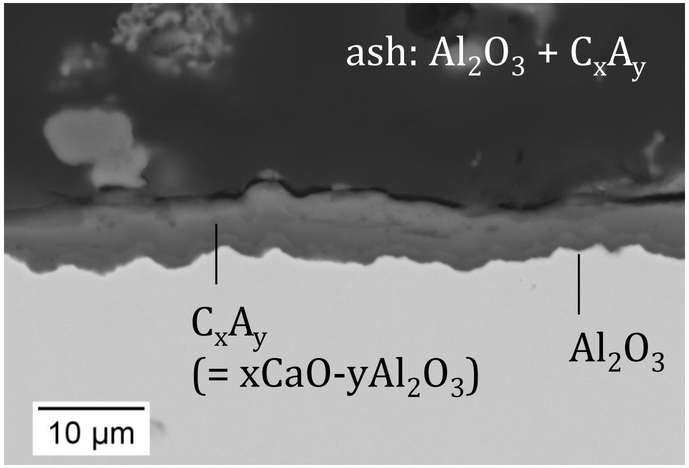

+ SiO_2

Al_2O_3-SiO_2-CaO

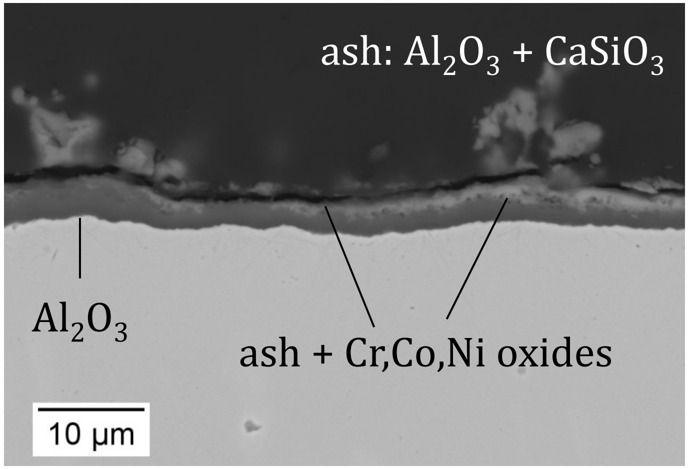

+ Na_2SO_4

Al_2O_3-SiO_2-CaO-Na_2SO_4

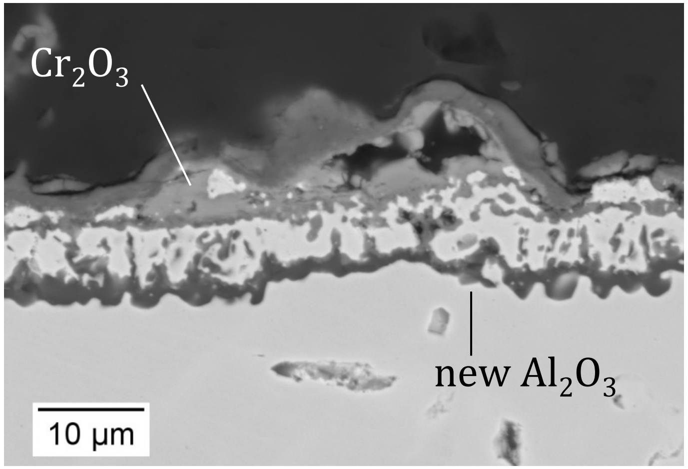

acidification of Na_2SO_4 melt by SiO_2 ?

Deposit reactivity at 900 °C

900 °C
O_2-SO_2
Ni-30Co-27Cr-12Al-0.1Y

Al_2O_3-CaO

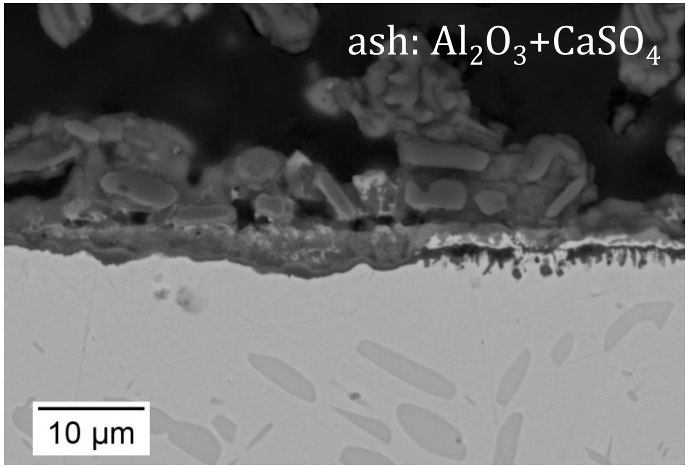

$CaSO_4$

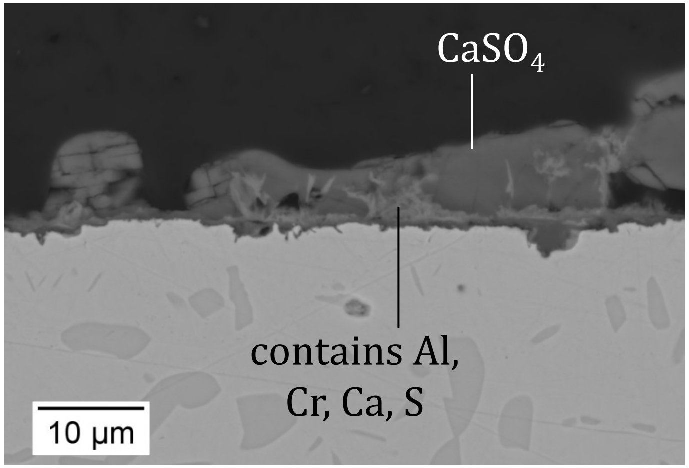

Reaction product yet to be identified but significant amounts of Al and Cr have reacted with $CaSO_4$

Deposit reactivity at 900 °C

900 °C
O_2-SO_2
Ni-30Co-27Cr-12Al-0.1Y

Al_2O_3-CaO

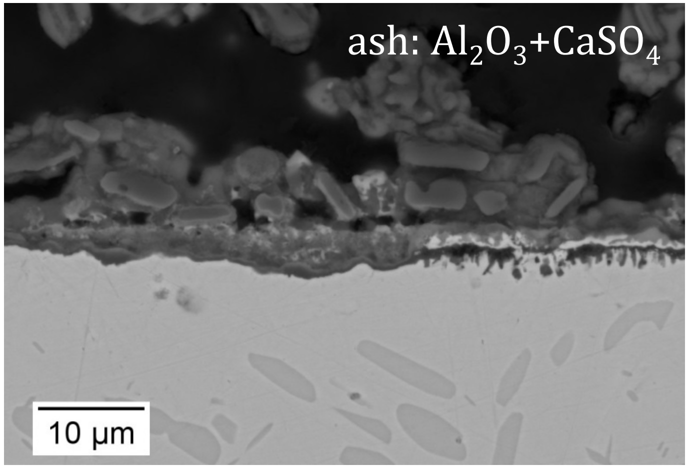

$\xcancel{Al_2O_3}$
+ SiO_2
$\longrightarrow$

SiO_2-CaO

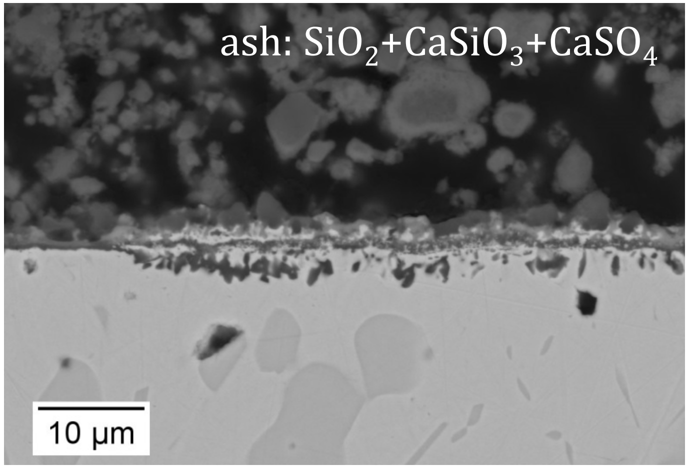

$CaSO_4$ more stable than $CaSiO_3$ → neutralization not effective

TBCs Provided by PST

dSpecimen Group #	Substrate Alloy	Bond Coat Type	Bond Coat Thickness (mils)	TBC Powder	TBC Density (%T.D.)	TBC Thickness (mils)	Quantity
1a	René N5	Dual Layer NiCoCrAlY	7-8	High Purity YSZ	85	15	10
1b	PWA 1484	Dual Layer NiCoCrAlY	7-8	High Purity YSZ	85	15	13
2a	René N5	Dual Layer NiCoCrAlY	7-8	High Purity YSZ	92	15	10
2b	PWA 1484	Dual Layer NiCoCrAlY	7-8	High Purity YSZ	92	15	13

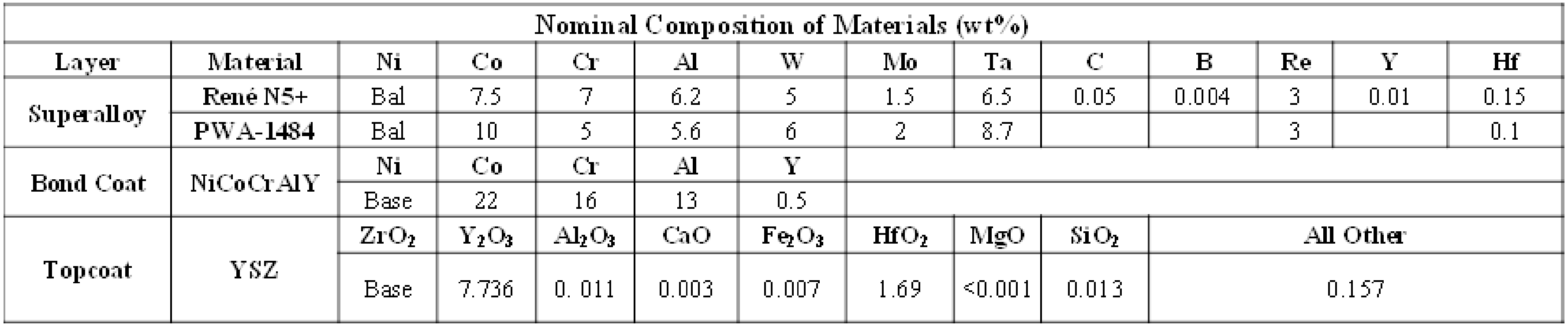

Nominal Composition of Materials (wt%)

Layer	Material	Ni	Co	Cr	Al	W	Mo	Ta	C	B	Re	Y	Hf
Superalloy	**René N5+**	Bal	7.5	7	6.2	5	1.5	6.5	0.05	0.004	3	0.01	0.15
	PWA-1484	Bal	10	5	5.6	6	2	8.7			3		0.1
Bond Coat	NiCoCrAlY	**Ni**	**Co**	**Cr**	**Al**	**Y**							
		Base	22	16	13	0.5							
Topcoat	YSZ	**ZrO_2**	**Y_2O_3**	**Al_2O_3**	**CaO**	**Fe_2O_3**	**HfO_2**	**MgO**	**SiO_2**	**All Other**			
		Base	7.736	0. 011	0.003	0.007	1.69	<0.001	0.013	0.157			

Thermal Barrier Coatings (TBCs)

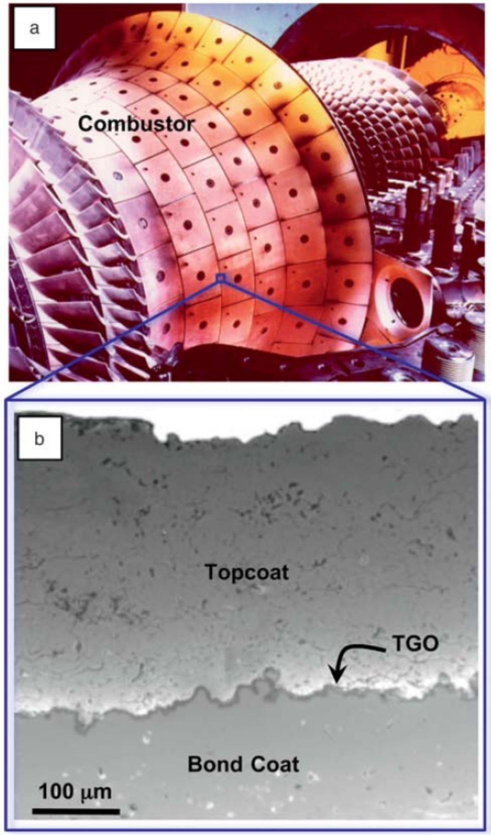

Multi-Layered TBC System

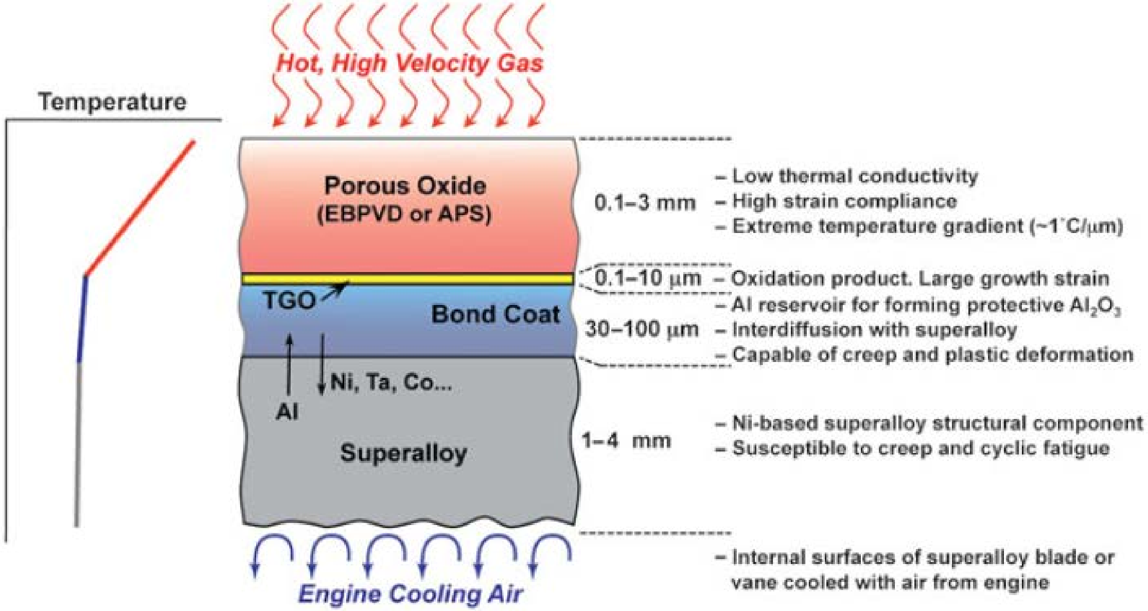

Clarke, Oechsner, Padture, *MRS Bulletin*, **37** (2012)

Thermal Barrier Coatings (TBCs)

Yttria Stabilized Zirconia (YSZ) Top Coat

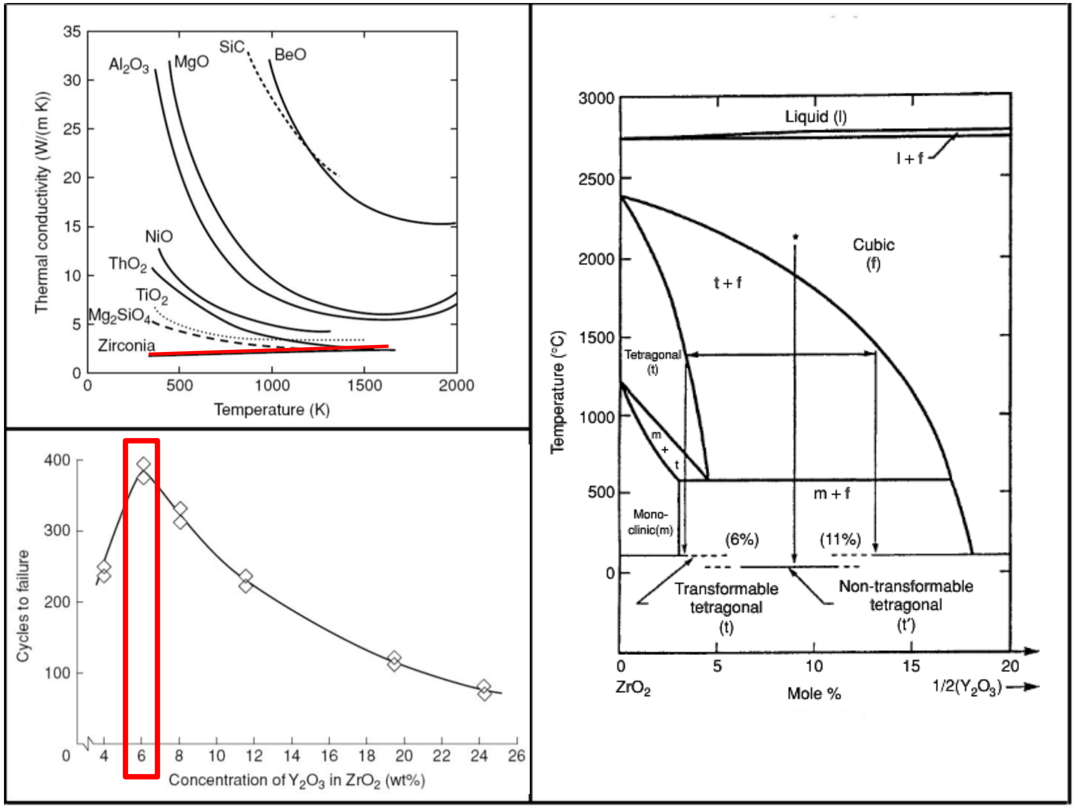

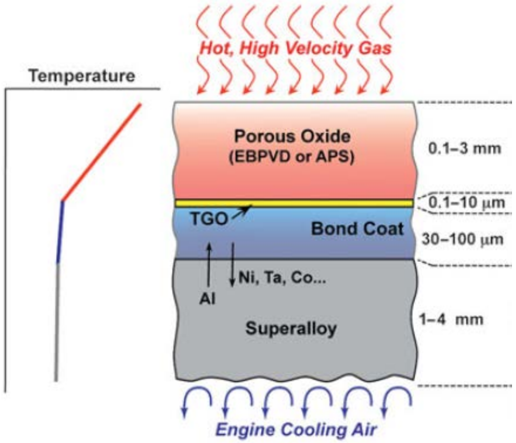

Clarke, Oechsner, Padture, *MRS Bulletin*, **37** (2012)

- ZrO_2: low thermal conductivity
- High resistance to thermal cycling
- ~7wt% Y_2O_3: t' phase

R.C. Reed, The Superalloys: Fundametals and Applications, Cambridge (2006).

Cyclic TBC Exposure to High-SiO_2 Ash

Early Failure of HPLD TBCs with **“high-SiO_2”** ash with K_2SO_4

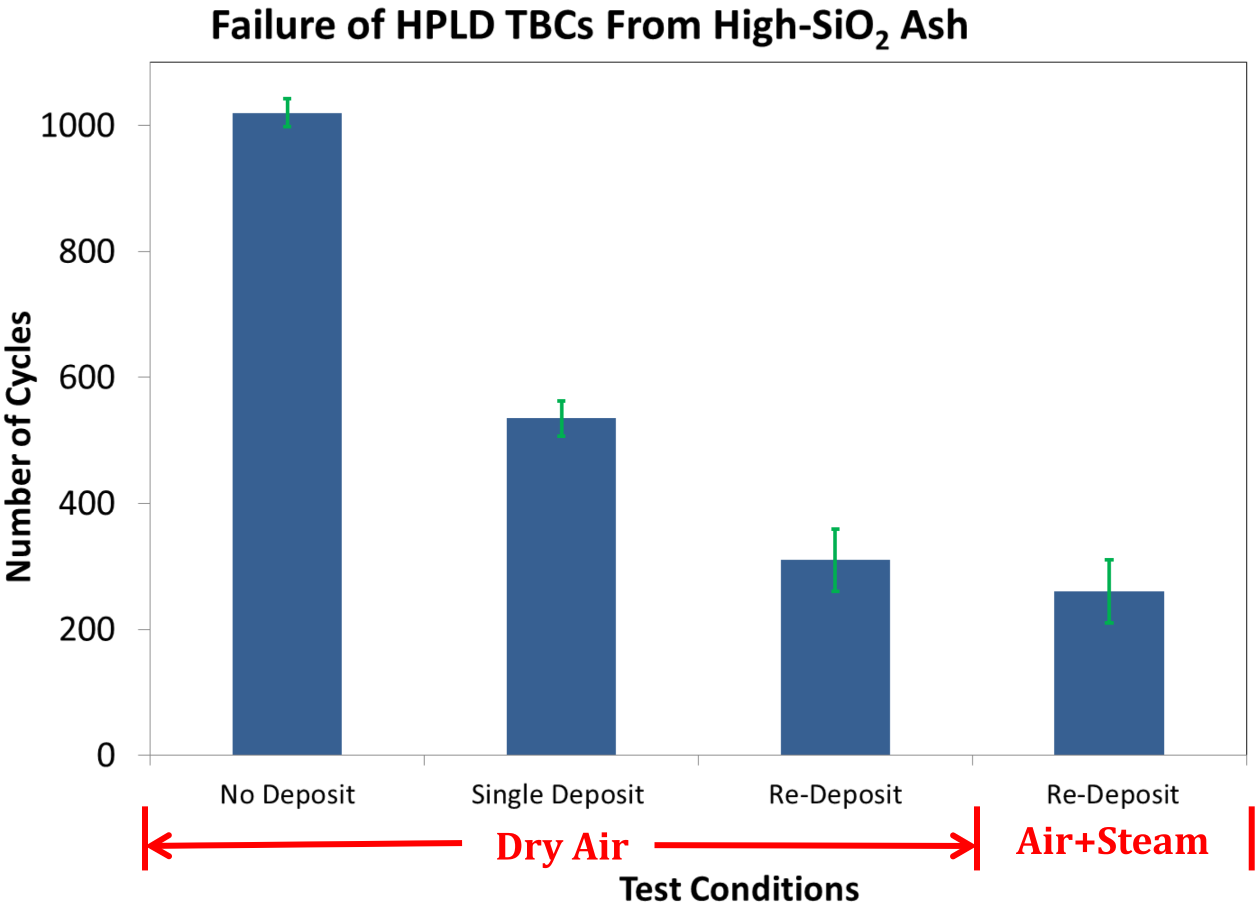

“High-SiO_2”
Ash+.1K_2SO_4

	Wt%
SiO_2	**45**
Al_2O_3	22.5
CaO	9
Fe_2O_3	9
MgO	4.5
K_2SO_4	10

- Failure determined by complete delamination of top coat
- Significant damage to YSZ before complete failure

CaO Dependence on Reaction

Synthetic ash mixtures

Ash #	1	2	3	4	5
SiO_2	50	30	24	18	10
Al_2O_3	25	15	12	9	5
Fe_2O_3	10	6	4	2	2
MgO	5	3	2	1	1
CaO	**10**	**46**	**58**	**70**	**82**

72h Exposures, Dry Air 1100°C

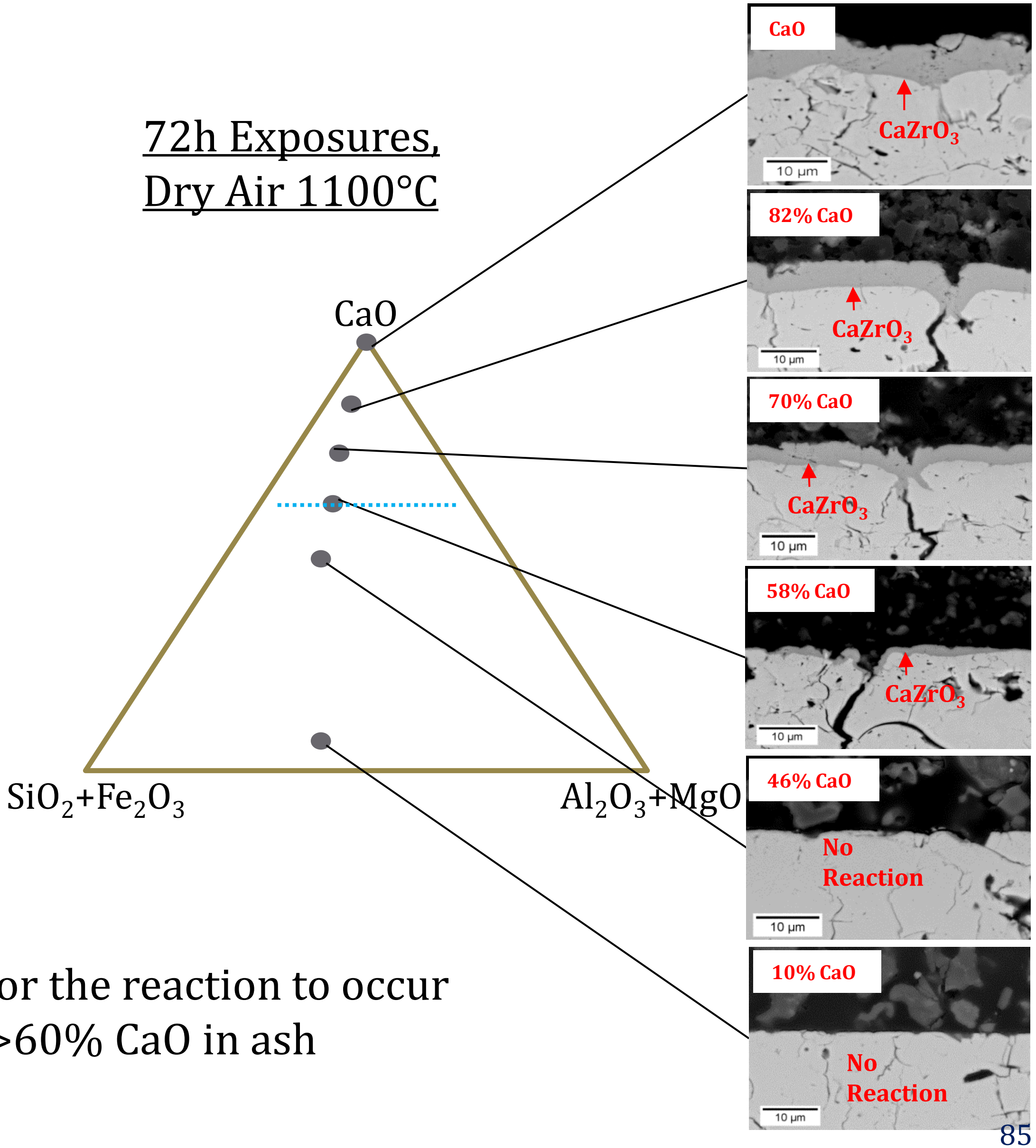

- There is a clear boundary for the reaction to occur
- Continuous reaction layer >60% CaO in ash

TBC Failure After Cyclic Exposure

Comparison of failure: High-CaO Ash+5%FeS+5%K_2SO_4

HPLD Top Coat Failure

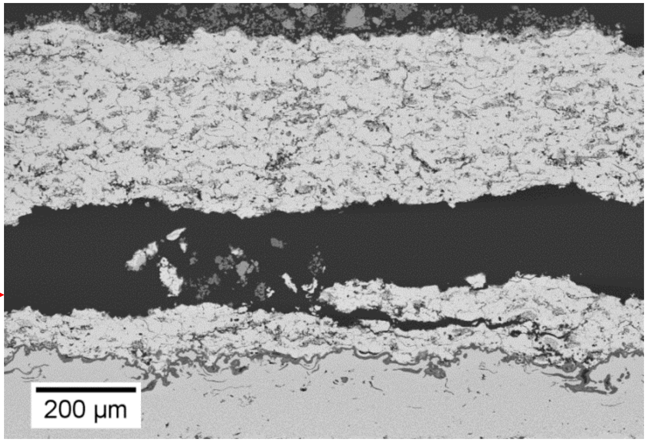

Failure in YSZ far from TGO

DVF Top Coat Failure

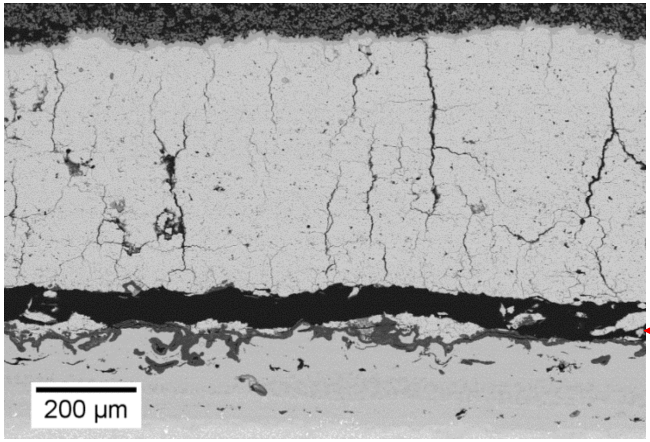

Failure along TGO/BC Interface

Location of TBC spallation is different.

TBC Failure After Cyclic Exposure

TBC Failure after 444 Cycles at 1100°C

Synthetic Ash (70%CaO) + 5%FeS + 5%K_2SO_4

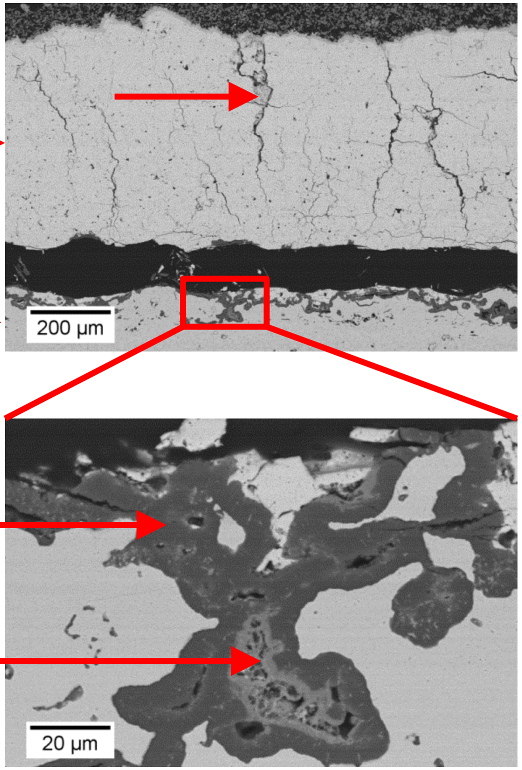

YSZ

Bond Coat

TGO

Mixed Ni-Co-Cr-Al-Y Oxides

TBC Failure after 1200 Cycles at 1100°C
<u>without deposit</u>

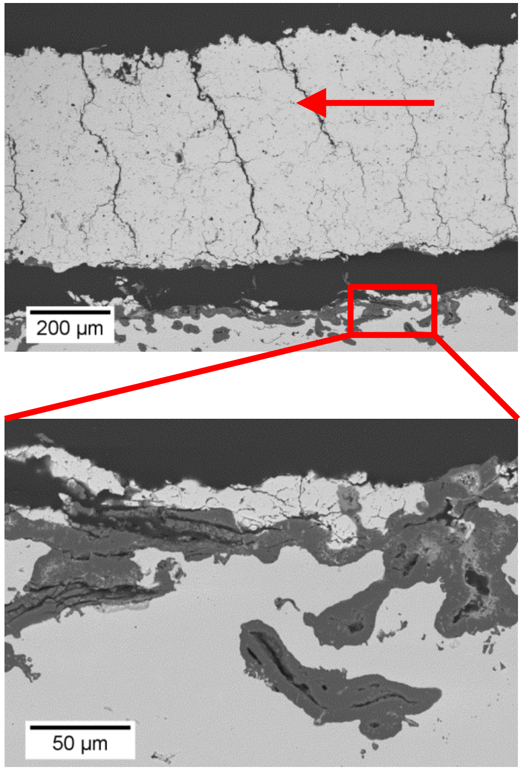

Similar failure, but ash causes failure to occur **early**.

Cyclic Exposure to High-SiO_2 Ash

HPLD TBC high-SiO_2 Ash + $0.10K_2SO_4$ Dry Air

260 Cycles: Re-apply every 20 cycles

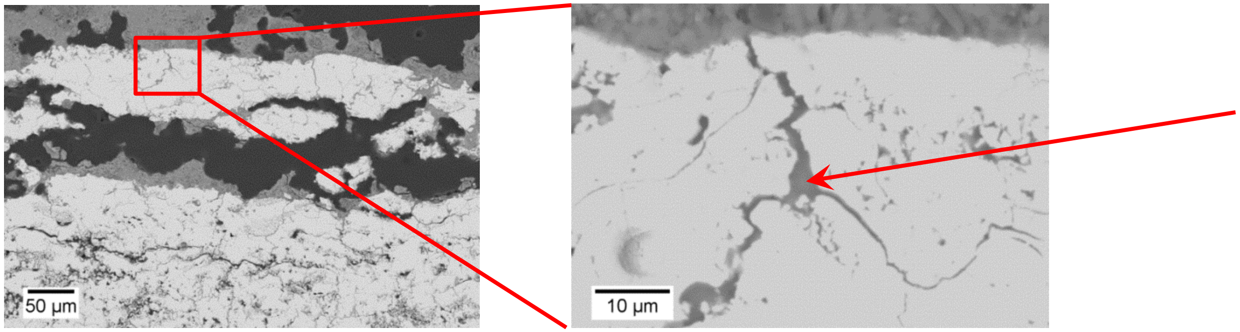

Si, K, O

HPLD TBC high-SiO_2 Ash + $0.10K_2SO_4$ Air+20%H_2O

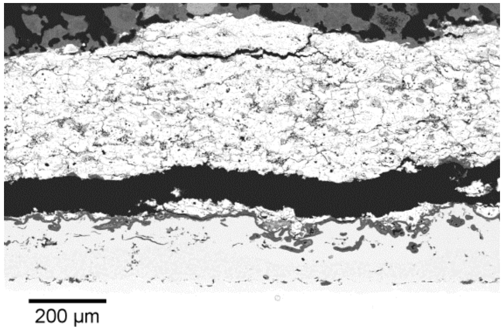

Reactions of Fly Ash with YSZ

Free-standing YSZ isothermal exposure to C-Ash in dry air 1300°C.

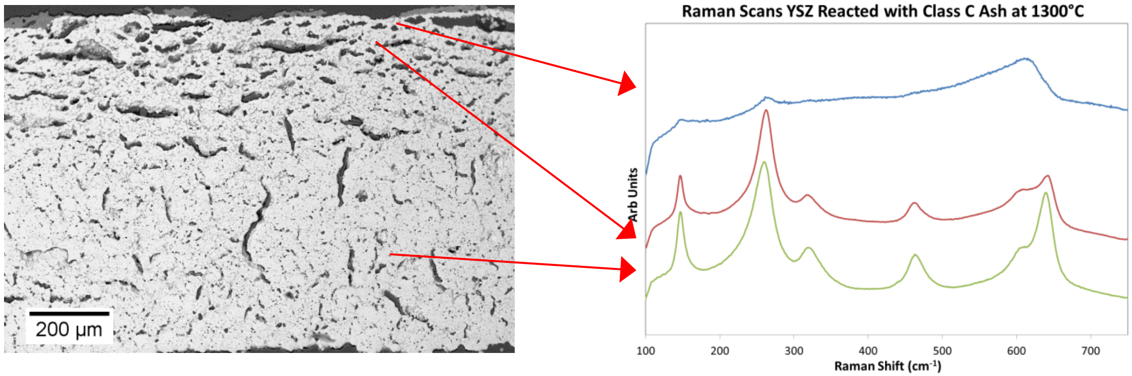

Destabilization of t’ phase from liquid fly-ash interaction with YSZ.

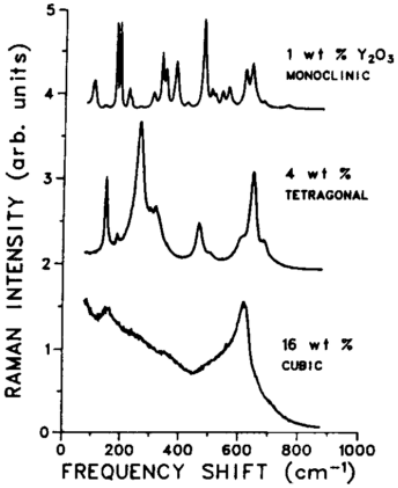

Raman spectra used to identify change from t’ phase

Hamilton; Nagelberg, Journal of the American Ceramic Society, 67[10], pp. 686-690 (1984).

Temperature Dependence of Reaction

Different ratios of oxides can result in different melting point.

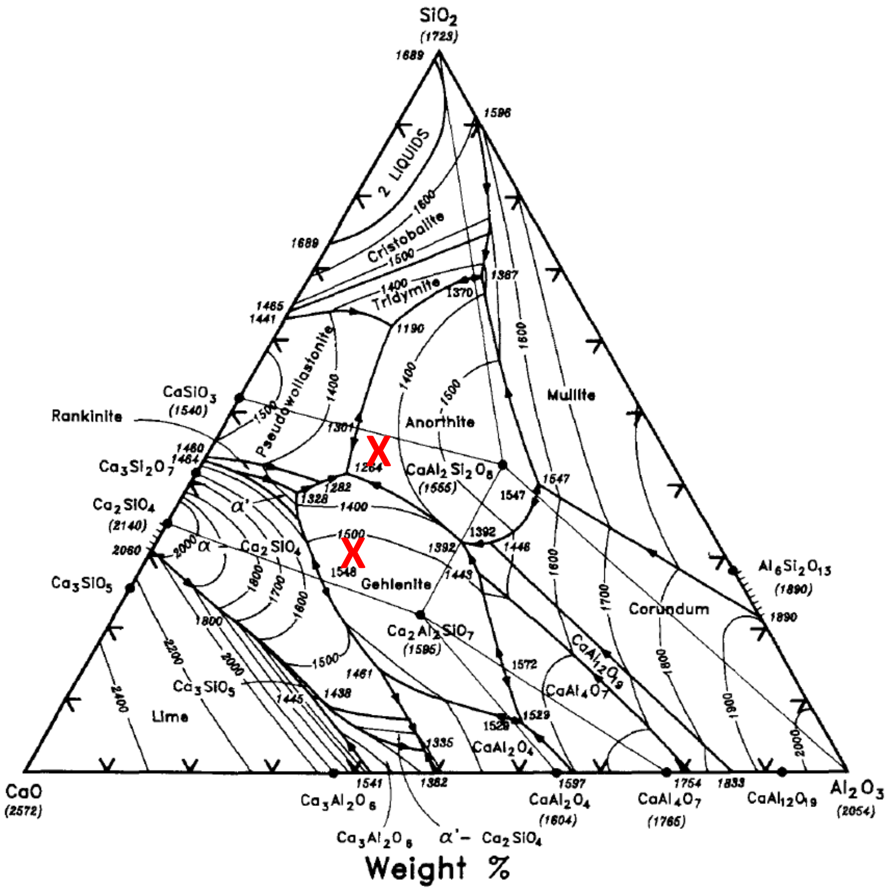

Class C Ash 1200 °C, 24h in Dry Air

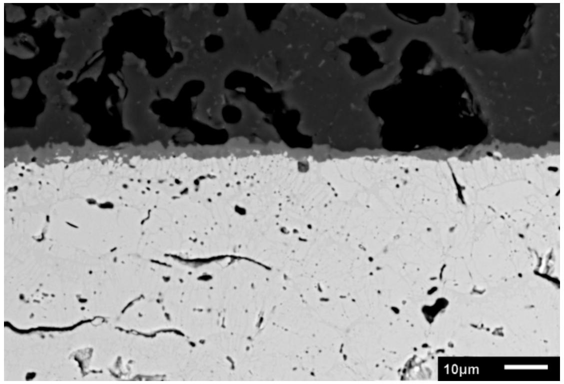

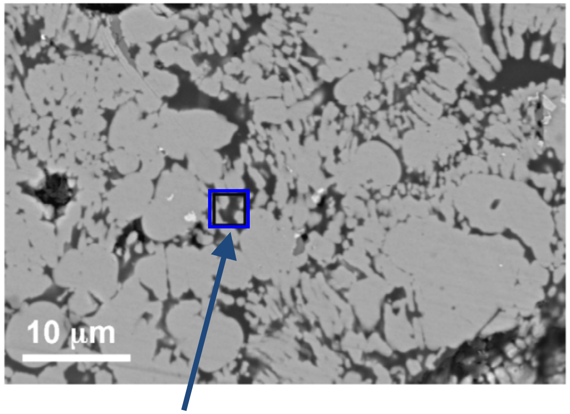

Melted ash penetrated into YSZ

Adapted from Eriksson, et al, Metallurgical Transactions B, 24B (1993) 807-816.